AD-A122 188 OPTIMUM ARRAY PROCESSING FOR DETECTING BINARY SIGNALS CORRUPTED BY DIRECT.. (U) OHIO STATE UNIV COLUMBUS ELECTROSCIENCE LAB C CHIU DEC 72 ESL-3433-2 1/2

UNCLASSIFIED N00019-72-C-0184 F/G 9/2 NL

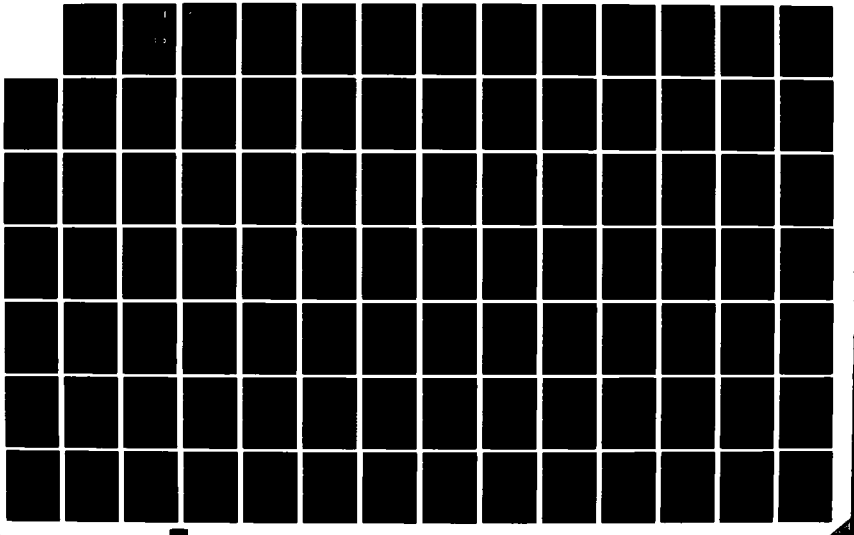

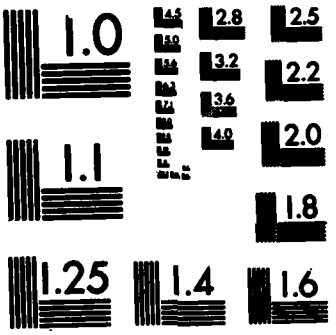

PHOTOGRAPH THIS SHEET

AD A122188

DTIC ACCESSION NUMBER

II

LEVEL

I

INVENTORY

Rept. No. ESL-TR-3433-2

DOCUMENT IDENTIFICATION

Dec. 72

Chiu, Chen-Shu

Contract N00019-72-C-0184

DISTRIBUTION STATEMENT A
Approved for public release;
Distribution Unlimited

DISTRIBUTION STATEMENT

ACCESSION FOR	
NTIS	GRA&I
DTIC	TAB
UNANNOUNCED	
JUSTIFICATION	
Acq#: 82-2348, dtd. 22 Nov 82	
BY	
DISTRIBUTION /	
AVAILABILITY CODES	
DIST	AVAIL AND/OR SPECIAL
A	

DISTRIBUTION STAMP

DTIC COPY INSPECTED 2

DTIC ELECTE S DEC 8 1982 D

D

DATE ACCESSIONED

82 12 08 055

DATE RECEIVED IN DTIC

PHOTOGRAPH THIS SHEET AND RETURN TO DTIC-DDA-2

DTIC FORM OCT 79 70A

DOCUMENT PROCESSING SHEET

OPTIMUM ARRAY PROCESSING FOR DETECTING BINARY SIGNALS CORRUPTED BY DIRECTIONAL INTERFERENCE

Chen-Shu Chiu

The Ohio State University

ElectroScience Laboratory

Department of Electrical Engineering
Columbus, Ohio 43212

TECHNICAL REPORT 3433-2

December 1972

Contract N00019-72-C-0184

Department of the Navy
Naval Air Systems Command
Washington, D.C. 20360

NOTICES

When Government drawings, specifications, or other data are used for any purpose other than in connection with a definitely related Government procurement operation, the United States Government thereby incurs no responsibility nor any obligation whatsoever, and the fact that the Government may have formulated, furnsihed, or in any way supplied the said drawings, specifications, or other data, is not to be regarded by implication or otherwise as in any manner licensing the holder or any other person or corporation, or conveying any rights or permission to manufacture, use, or sell any patented invention that may in any way be related thereto.

OPTIMUM ARRAY PROCESSING FOR DETECTING BINARY SIGNALS CORRUPTED BY DIRECTIONAL INTERFERENCE

Chen-Shu Chiu

TECHNICAL REPORT 3433-2

December 1972

Contract N00019-72-C-0184

Department of the Navy
Naval Air Systems Command
Washington, D.C. 20360

ACKNOWLEDGMENTS

The author wishes to express his sincere gratitude to all those persons who aided in the completion of this dissertation. Special acknowledgment is given to Professor R.T. Compton, Jr., his graduate adviser, for his guidance and suggestions. A debt of gratitude is also owed to Professors C.H. Walter and A.A. Ksienski for their encouragement and their critical reading of the manuscript.

The material contained in this report is also used as a dissertation submitted to the Department of Electrical Engineering, The Ohio State University as partial fulfillment for the degree Doctor of Philosophy.

ABSTRACT

This report examines optimum array processing for bit detection of a binary communication signal in the presence of a directional interfering signal. The binary communication signal is assumed to be either completely known or to have random parameters (Rayleigh amplitude and uniform phase). The interfering signal is a wide-sense stationary Gaussian process. The receiving antenna is a linear array of equally spaced isotropic point elements. Statistically independent white noise is added to the signal at each element.

An analytical expression for the inverse of the covariance matrix is obtained, and the general structure for the optimum detector is derived. The optimum processor is a correlation receiver whose detailed structure is dependent in general on the power spectrum of the interference, as well as the other antenna and signal parameters.

The detection error is calculated for several cases. It is found that the detection error is minimized if the array elements have an optimum spacing, determined by the array size and the incidence angles of the desired signal and the interference. When the optimum spacing is used, the structure of the detection system is not dependent on the power spectrum of the interfering signal.

CONTENTS

Chapter		Page
I	INTRODUCTION	1
II	THE COVARIANCE MATRIX AND ITS INVERSE	3
	A. Introduction	3
	B. The Covariance Matrix	6
	C. Broadside Interference	12
	D. Interference from Arbitrary Angles	14
III	THE OPTIMUM DETECTOR FOR DETECTING COMPLETELY KNOWN BINARY SIGNALS	19
	A. The Likelihood Ratio Test	19
	B. Receiver Operating Characteristic	25
IV	THE DIRECTIONAL CHARACTERISTICS AND THE ERROR RATE PERFORMANCE	29
	A. Introduction	29
	B. The Mean of L(R)	31
	C. The Directional Characteristics	33
	D. The Probability of Error	43
	E. The Optimum Spacing	51
	F. Arbitrary Power Spectrum	53
V	THE DETECTOR FOR BINARY SIGNALS HAVING A RANDOM PHASE AND AMPLITUDE	60
	A. The Optimum Processor	60
	B. The Distribution Function	66
	C. The Probability Equations: ASK	70
	D. On Parameters α_k, β_k and γ_k	73
	E. Numerical Results, ASK Signals	79

VI ON SYSTEMS DESIGNED FOR THE OPTIMUM SPACING..... 101

A. The Interference-Free Spacing 101
B. FSK Binary Detector 103
C. On General Random Phase and Random Amplitude Detector 106

VII CONCLUSIONS..... 109

Appendix

A A PROOF OF EQ. (2-36)..... 111

B THE STATISTICS OF L(R), $L_{ku}(r)$ and $L_{kv}(r)$..... 114

BIBLIOGRAPHY..... 123

CHAPTER I
INTRODUCTION

Statistical decision theory has been applied for some time to the problem of determining the optimum structure of a receiver. The basic concept of optimal detection for completely known signals or known signal with unknown parameters corrupted by additive Gaussian noise has been discussed extensively in [1-5]. During the past decade this theory has been extended to analyze a communication system which includes an antenna array. The philosophy is to seek an optimum performance of the entire system based on statistical decision theory, rather than to consider the performance of the array or the receiver separately.

Basically, a decision theory receiver processes the received signals and makes one of several possible decisions, based on an optimum decision rule. Peterson et al [6] showed that the receiver which forms the likelihood ratio from the received signal and compares it with a threshold is an optimal receiver regardless of which criterion is used (e.g., Bayes, minimax, Neyman-Pearson, etc.). The various criteria affect the receiver only in the value of the threshold setting. A paper by Stocklin [7] formally showed that optimal space-time signal processing also called for likelihood ratio detection. Bryn [8] applied Rice's Fourier series representation to a vector representation of the signals to obtain a likelihood ratio detection good for wide-sense stationary processes. The problem of spacing a finite number of point detectors in a plane to detect spatially isotropic signals corrupted by spatially isotropic and covariance-separable noise was studied extensively by Gaerder [9]. Capon [10], Young [11-13], Gallop [14] have also treated various problems in this area.

The goal of this research is to find and examine the behavior of an optimum detector for detecting binary signals received by a linear array of equally spaced isotropic point elements. The novelty of the problem treated here is that the signal is assumed to be corrupted by an external directional interfering signal. The interfering signal is modeled as a wide-sense stationary process. In addition, the processing unit behind each antenna is assumed to contribute white noise, statistically independent from one element to the next.

The research discussed here is motivated by the adaptive antenna array research currently being conducted at the ElectroScience Laboratory[24-26]. The purpose of this research is to determine the performance of the optimum detection system so that this

performance may be taken as a base for evaluating the performance of the adaptive antenna array.

A similar problem has been treated by Urkowitz [15]. However, his approach requires the solution of a matrix integral equation, and his results, which are carried out only in general terms, do not include a detailed examination of specific cases.

Two different series representations of a vector random process are discussed in Van Trees [3]. These two methods both require the solution to a matrix integral equation, which is tedious and difficult. The method used here is the scalar Karhunen-Loève representation. The advantage of this choice is that only one integral equation needs to be solved. The material will be presented in the following manner.

Chapter II is devoted to formulating a workable expression for the covariance matrix and its inverse. First, the inverse of the covariance matrix associated with broadside interference is obtained by generalizing the results for a two-element array, a three-element array, etc. Then an expression for the inverse valid for an arbitrary arrival angle is obtained by employing a transformation. This transformation relates the original observation space to a modified space associated with delayed versions of the signals.

In Chapter III, the structure of the optimum processor for detecting completely known binary signals is found from the likelihood ratio test. Also, the equations for the receiver operating characteristics are given. To make the results more specific, some numerical results for the case when the desired communication signals are biphase modulated are given in Chapter IV. The discussion concentrates on the directional characteristics of the optimum detector and its error rate performance.

The optimum system for detecting the signal which has a random amplitude and phase is investigated in Chapter V. We assume that the amplitude is a Rayleigh random variable and the phase is uniformly distributed between $-\pi$ and π. Some numerical results for the case when the desired signals are on-off keying signals are discussed in detail in the last section of this Chapter.

In Chapter VI, we briefly discuss the general optimum system for detecting binary signals with phase and amplitude distributed arbitrarily. Also, we prove that the processing outputs are free from interference when an optimum-spaced array is used in the detection system.

CHAPTER II
THE COVARIANCE MATRIX AND ITS INVERSE

A. Introduction

The mathematical model of a general array detection system is shown in Fig. 2-1. The antenna array which is linear, and consists of m equally spaced isotropic point elements, is designed to receive the signal $x'(t)$ from a remote station. The signal $x'(t)$ may be either one of two waveforms,

$$x'(t) = \begin{cases} a'(t) \text{ under hypothesis } H_a \\ b'(t) \text{ under hypothesis } H_b \end{cases}$$

and the task of the receiver is to decide which waveform was sent. The signal transmitted by the source is corrupted by an additive directional interference $n'(t)$. The output at each antenna terminal will be the sum of the desired communication signal and the interfering random noise component. Those two components are temporal and spatial functions.

Suppose the incident angles for the desired and interfering signals measured from the array axis are θ and ϕ, respectively. Then the signals received by two adjacent antennas will be out of phase due to differences in the arrival times. The time delays τ and ν, given by

$$(2\text{-}1) \qquad \tau = \frac{d}{c} \cdot \cos\theta$$

$$(2\text{-}2) \qquad \nu = \frac{d}{c} \cos\phi \ ,$$

are the arrival time differences between adjacent elements for the desired signal and the interference, respectively. d is the spacing between antennas, and c is the speed of light.

Often, the received signal is amplified to a certain level before being processed. We assume that the gain and phase shift for each of the m ideal, linear amplifiers are identical. For simplicity, but without losing generality, the phase shift of each amplifier is assumed to be zero. Let $x_i(t)$ and $n_i(t)$ be the outputs of the ith amplifier when the inputs are $x_i'(t)$ and $n_i'(t)$, respectively. Since

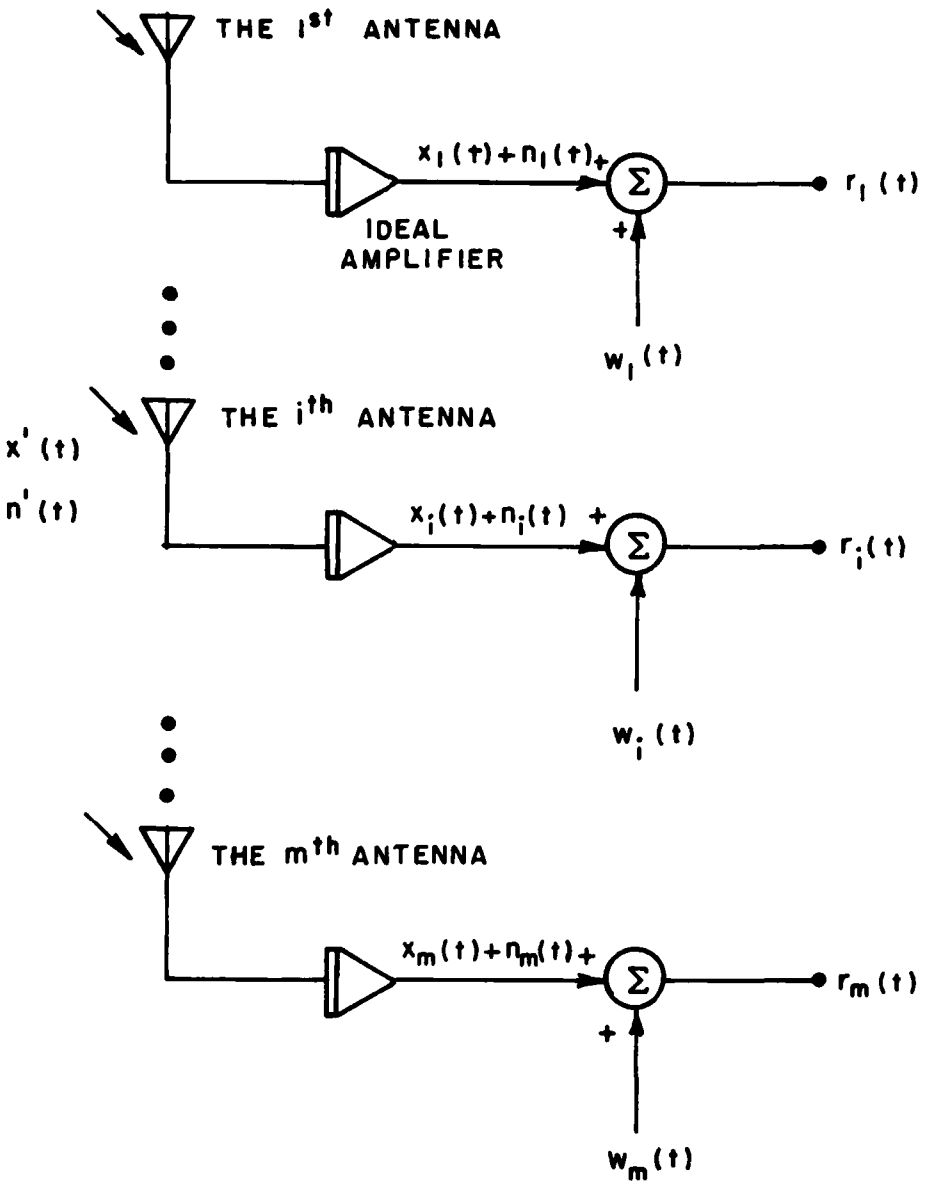

Fig. 2-1--Model of general array detection system.

the amplifiers are ideal and do not introduce phase shift, we have

$$(2\text{-}3) \qquad \begin{aligned} x_i(t) &= x[t-(i-1)\tau] \\ n_i(t) &= n[t-(i-1)\nu], \quad 1 \leq i \leq m. \end{aligned}$$

The interfering signal n(t) is assumed to be a wide-sense stationary Gaussian process of zero-mean,* i.e.,

$$(2\text{-}4) \qquad E\{n(t)\} = E\{n_i(t)\} = 0$$

$$(2\text{-}5) \qquad E\{n(t) \cdot n(z)\} \triangleq R(t-z) = R(z-t)$$

where R(t-z) is the autocorrelation function of the signal n(t). The functions $w_i(t)$, $1 \leq i \leq m$, in Fig. 2-1 represent internal noises, generated by the amplifiers and other electronic components (e.g., mixers) in each processing unit (not shown in the figure). We further assume that the interference and the internal noises are statistically independent, and $w_i(t)$ is a Gaussian white noise process with zero-mean and spectral height h_w for all i. Since the noise sources in each channel are statistically independent, we have

$$(2\text{-}6) \qquad E\{w_i(t) \cdot w_j(z)\} = \delta_{ij} \cdot h_w \cdot \delta(t-z)$$

where δ_{ij} is the Kronecker delta and $\delta(\cdot)$ is the Dirac delta function.

The goal of this research is to find an optimum processor for detecting the signal x(t) in the presence of interference. We treat here the binary detection problem. That is, the signal to be processed in the ith channel, $r_i(t)$, is of one of two forms, as follows:

$$(2\text{-}7) \qquad \text{hypothesis } H_a: \quad r_i(t) = a_i(t) + n_i(t) + w_i(t)$$

$$(2\text{-}8) \qquad \text{hypothesis } H_b: \quad r_i(t) = b_i(t) + n_i(t) + w_i(t)$$

---

*$E\{\cdot\}$ is the expectation operator.

B. The Covariance Matrix

There are many ways of characterizing waveforms and random processes. The method adopted here uses an orthogonal series Karhunen-Loéve representation [17]. That is, we express the waveform as a series expansion on the orthonormal basis function $\{\phi_\ell(t)\}$ given by the eigenfunctions of the integral equation [18]

$$(2\text{-}9) \qquad \lambda_\ell \, \phi_\ell(t) = \int_{-T}^{T} c(t,u) \cdot \phi_\ell(u) \cdot du, \quad 1 \leq \ell < \infty$$

where the bounds specify the observation interval, from t = -T to t=T, and the kernel of the integral equation is given by,

$$(2\text{-}10) \qquad c(t,u) = E\{[n_i(t) + w_i(t)][n_i(u) + w_i(u)]\}$$

$$= R(t-u) + h_w \cdot \delta(t-u), \quad 1 \leq i \leq m \ .$$

We have made use of Eqs. (2-5) and (2-6), and the assumption that $n_i(t)$ and $w_i(t)$ are uncorrelated, to get Eq. (2-10). The integral equation may then be written

$$(2\text{-}11) \qquad (\lambda_\ell - h_w) \cdot \phi_\ell(t) = \int_{-T}^{T} R(t-u) \cdot \phi_\ell(u) \cdot du$$

For a Gaussian random process, the coefficients in the expansion are statistically independent Gaussian random variables [19]. It is in this case that the expansion becomes attractive.

We approximate the signal $r_i(t)$ for the ith channel by an N-term expansion

$$(2\text{-}12) \qquad r_i(t) = \sum_{\ell=1}^{N} r_{i\ell} \, \phi_\ell(t)$$

$$= \sum_{\ell=1}^{N} (a_{i\ell} + n_{i\ell} + w_{i\ell}) \cdot \phi_\ell(t), \quad 1 \leq i \leq m$$

under hypothesis H_a, or

$$(2\text{-}13) \qquad r_i(t) = \sum_{\ell=1}^{N} (b_{i\ell} + n_{i\ell} + w_{i\ell}) \cdot \phi_\ell(t), \quad 1 \leq i \leq m$$

under hypothesis H_b, where

$$(2\text{-}14)\qquad \begin{bmatrix} r_{i\ell} \\ a_{i\ell} \\ b_{i\ell} \\ n_{i\ell} \\ w_{i\ell} \end{bmatrix} \triangleq \int_{-T}^{T} \begin{bmatrix} r_i(t) \\ a_i(t) \\ b_i(t) \\ n_i(t) \\ w_i(t) \end{bmatrix} \cdot \phi_\ell(t) \cdot dt$$

We define the observation vector R for the detection system as

$$(2\text{-}15)\qquad R \triangleq \begin{bmatrix} R_1 \\ R_2 \\ \vdots \\ R_i \\ \vdots \\ R_m \end{bmatrix}$$

where R_i, associated with the ith channel, is itself a column vector, i.e.,

$$(2\text{-}16)\qquad R_i \triangleq \begin{bmatrix} r_{i1} \\ r_{i2} \\ \vdots \\ r_{i\ell} \\ \vdots \\ r_{iN} \end{bmatrix}$$

The dimension for the Gaussian random vector R is mN. We define*

(2-17)

$$M = E\{R|H_k\} = E \left\{ \begin{bmatrix} R_1|H_k \\ R_2|H_k \\ \vdots \\ R_i|H_k \\ \vdots \\ R_m|H_k \end{bmatrix} \right\} \triangleq \begin{bmatrix} M_1 \\ M_2 \\ \vdots \\ M_i \\ \vdots \\ M_m \end{bmatrix}$$

$$= \begin{cases} A & \text{under hypothesis } H_a \\ B & \text{under hypothesis } H_b \end{cases}$$

and the covariance matrix

(2-18) $$K = E\{(R-M)(R-M)^T\} \triangleq Q^{-1}$$

If K is nonsingular,** the probability density function of R for an m-channel, N-term expansion is [20]

(2-19) $$p(R|H_k) = \frac{1}{\sqrt{(2\pi)^{mN}|K|}} \cdot e^{-\frac{1}{2}(R-M)^T Q (R-M)}$$

where $|K|$ is the determinant of K

---

* We use H_k to represent either hypothesis.

**If K is singular, we have a singular detection problem. K becomes singular if the spectral height h_w is zero. We will not examine this case here.

The following several pages will be devoted to finding a workable expression for the covariance matrix. Symbolically, we may write

$$K = E\left\{\begin{bmatrix} (R_1-M_1)(R_1-M_1)^T & (R_1-M_1)(R_2-M_2)^T & \cdots & (R_1-M_1)(R_m-M_m)^T \\ (R_2-M_2)(R_1-M_1)^T & (R_2-M_2)(R_2-M_2)^T & \cdots & (R_2-M_2)(R_m-M_m)^T \\ \vdots & \vdots & & \vdots \\ (R_m-M_m)(R_1-M_1)^T & (R_m-M_m)(R_2-M_2)^T & \cdots & (R_m-M_m)(R_m-M_m)^T \end{bmatrix}\right\} \tag{2-20}$$

where

$$M_i \triangleq \begin{bmatrix} m_{i1} \\ m_{i2} \\ \vdots \\ m_{i\ell} \\ \vdots \\ m_{iN} \end{bmatrix} \triangleq E\left\{\begin{bmatrix} r_{i1}|H_k \\ r_{i2}|H_k \\ \vdots \\ r_{i\ell}|H_k \\ \vdots \\ r_{iN}|H_k \end{bmatrix}\right\} \tag{2-21}$$

It is apparent that $m_{i\ell} = a_{i\ell}$ under hypothesis H_a and $m_{i\ell} = b_{i\ell}$ under hypothesis H_b. For an m-element array, the m^2 submatrices may be classified into two types: the one associated with the ith channel, namely, the autocovariance submatrix

$$K_{ii} \triangleq E\{(R_i - M_i)(R_i-M_i)^T\} \tag{2-22}$$

and the crossvariance submatrix

$$K_{ij} \triangleq E\{(R_i-M_i)(R_j-M_j)^T\} \quad , \quad i \neq j, \tag{2-23}$$

which is associated with the ith and jth channels, respectively. These submatrices may also be expressed in terms of the elements of R_i in Eq. (2-15), as follows,

(2-24)

$$K_{ij}=E\left\{\begin{bmatrix} (r_{i1}-m_{i1})(r_{j1}-m_{j1}) & (r_{i1}-m_{i1})(r_{j2}-m_{j2}) & \cdots & (r_{i1}-m_{i1})(r_{jN}-m_{jN}) \\ (r_{i2}-m_{i2})(r_{j1}-m_{j1}) & (r_{i2}-m_{i2})(r_{j2}-m_{j2}) & \cdots & (r_{i2}-m_{i2})(r_{jN}-m_{jN}) \\ \vdots & \vdots & & \vdots \\ (r_{iN}-m_{iN})(r_{j1}-m_{j1}) & (r_{iN}-m_{iN})(r_{j2}-m_{j2}) & \cdots & (r_{iN}-m_{iN})(r_{jN}-m_{jN}) \end{bmatrix}\right\} .$$

We proceed to examine the elements of K_{ij} under both hypotheses. Since $r_{i\ell}$ and r_{jn} are statistically independent Gaussian random variables, and processes $n_i(t)$ and $w_i(t)$ are uncorrelated, we have under H_a

(2-25)
$$\begin{aligned} & E\{(r_{i\ell}-m_{i\ell})(r_{jn}-m_{jn})|H_a)\} \\ & = E\{(r_{i\ell}r_{jn})|H_a\} - a_{i\ell}a_{jn} \\ & = \iint_{-T}^{T} R[t-u+(j-i)\nu] \cdot \phi_\ell(t)\phi_n(u) \cdot dudt + \delta_{ij}\,\delta_{\ell n} \cdot h_w \\ & = \delta_{ij}\delta_{\ell n} \cdot h_w + (\lambda_n - h_w) \cdot \int_{-T}^{T} \phi_\ell(t) \cdot \phi_n[t+(j-i)\nu] \cdot dt \end{aligned}$$

The elements of K_{ij} for $i \neq j$ hence become

(2-26)
$$E\{(r_{i\ell}-m_{i\ell})(r_{jn}-m_{jn})|H_a\} = (\lambda_n - h_w) \cdot \int_{-T}^{T} \phi_\ell(t) \cdot \phi_n[t+(j-i)\nu]dt$$

and the elements of K_{ii} become

(2-27) $$E\{(r_{i\ell}-m_{i\ell})(r_{in}-m_{in})|H_a\}$$

$$= (\lambda_n-h_w)\cdot\int_{-T}^{T}\phi_\ell(t)\,\phi_n(t)dt + \delta_{\ell n}\cdot h_w$$

$$=\begin{cases}0 & \text{if } \ell \neq n\\ \lambda_n & \text{if } \ell = n\end{cases}$$

The elements of K_{ii} and K_{ij} under hypothesis H_b may be derived in the same manner. It is found that they are identical to those under hypothesis H_a. Consequently, the covariance matrices under the hypotheses defined in Eqs. (2-7) and (2-8) are equal, and the hypothesis detection must rely on the difference in the mean M associated with each hypothesis. The autocovariance submatrix and the cross covariance submatrix have the following forms:

(2-28) $$K_{ii} = \begin{bmatrix}\lambda_1 & 0 & 0 & & 0\\ 0 & \lambda_2 & 0 & \cdots & 0\\ 0 & 0 & \lambda_3 & \cdots & 0\\ \vdots & \vdots & \vdots & & \vdots\\ 0 & 0 & 0 & \cdots & \lambda_N\end{bmatrix}$$

(2-29)

$$K_{\substack{ij\\ i\neq j}} = \begin{bmatrix}(\lambda_1-h_w)\int_{-T}^{T}\phi_1(t)\phi_1[t+(j-i)\nu]dt & (\lambda_2-h_w)\int_{-T}^{T}\phi_1(t)\phi_2[t+(j-i)\nu]dt & \cdots & (\lambda_N-h_w)\int_{-T}^{T}\phi_1(t)\phi_N[t+(j-i)\nu]dt\\ (\lambda_1-h_w)\int_{-T}^{T}\phi_2(t)\phi_1[t+(j-i)\nu]dt & (\lambda_2-h_w)\int_{-T}^{T}\phi_2(t)\phi_2[t+(j-i)\nu]dt & \cdots & (\lambda_N-h_w)\int_{-T}^{T}\phi_2(t)\phi_N[t+(j-i)\nu]dt\\ \vdots & \vdots & & \vdots\\ (\lambda_1-h_w)\int_{-T}^{T}\phi_N(t)\phi_1[t+(j-i)\nu]dt & (\lambda_2-h_w)\int_{-T}^{T}\phi_N(t)\phi_2[t+(j-i)\nu]dt & \cdots & (\lambda_N-h_w)\int_{-T}^{T}\phi_N(t)\phi_N[t+(j-i)\nu]dt\end{bmatrix}$$

The element of K_{ij} at the ℓn position, is equal to that of K_{ji} at the $n\ell$ position, because

$$(2\text{-}30)\qquad (\lambda_n - h_w)\int_{-T}^{T} \phi_\ell(t)\cdot\phi_n[t+(j-i)\nu]\cdot dt$$

$$= \int_{-T}^{T}\phi_n(u)\cdot\int_{-T}^{T} R[t+(j-i)\nu-u]\cdot\phi_\ell(t)\,.\,dt\,du$$

$$= (\lambda_\ell - h_w)\int_{-T}^{T}\phi_n(u)\cdot\phi_\ell[u+(i-j)\nu]\cdot du.$$

Hence, $K_{ij}=K_{ji}^T$ and consequently the covariance matrix K is symmetric. In terms of K_{ii} and K_{ij}, the covariance matrix K may be written

$$(2\text{-}31)\qquad K = \begin{bmatrix} K_{11} & K_{12} & \cdots & K_{1m} \\ K_{21} & K_{22} & \cdots & K_{2m} \\ \vdots & \vdots & & \vdots \\ K_{m1} & K_{m2} & \cdots & K_{mm} \end{bmatrix}$$

Since

$$(2\text{-}32)\qquad Q \triangleq K^{-1} = (K^T)^{-1} = Q^T$$

the Q matrix is also symmetric.

C. Broadside Interference

To compute the Q matrix, one has to go through a tedious process. First, the integral equation defined by Eq. (2-11) has to be solved. Afterwards, one has to compute many integrals in order to get K_{ij}. Finally, one must invert the covariance matrix K.

Referring to Eq. (2-29), we see that a much simpler expression for K is obtained if the external interference arrives from the broadside direction of the array, i.e., if $\nu = 0$. When this is the case, the orthogonality property of $\{\phi_\ell(t)\}$ ensures that all off-diagonal elements of K_{ij}, $i\neq j$, vanish. Furthermore, all cross-covariance submatrices become equal, as follows:

$$(2\text{-}33)\qquad K_{ij}(\nu=0) = \begin{bmatrix} \lambda_1-h_w & 0 & \cdots & 0 \\ 0 & \lambda_2-h_w & \cdots & 0 \\ \cdot & \cdot & & \cdot \\ \cdot & \cdot & & \cdot \\ \cdot & \cdot & & \cdot \\ 0 & 0 & \cdots & \lambda_N-h_w \end{bmatrix}$$

$$\triangleq K^*_{ij}$$

Let K^* be the covariance matrix for this special case. Then the expression for each element of Q^*, defined by $Q^* = K^{*-1}$, can be obtained by generalizing the results for the inverses of the covariance matrices associated with a two-element array, a three-element array, etc. It is found that all submatrices Q^*_{ii} are identical and diagonal. The nonvanishing elements

$$(q^*_{\ell\ell},\ q_{(N+\ell)(N+\ell)},\ q_{(2N+\ell)(2N+\ell)},\ \text{etc})$$

may be written as[+]

$$(2\text{-}34)\qquad q^*_{[(i-1)N+\ell][(i-1)N+\ell]} = \frac{\lambda_\ell + (m-2)(\lambda_\ell-h_w)}{\lambda_\ell^2+(m-2)\lambda_\ell \cdot (\lambda_\ell-h_w) - (m-1)(\lambda_\ell-h_w)^2}$$

$$= \frac{\lambda_\ell + (m-2)\cdot(\lambda_\ell-h_w)}{h_w \cdot [m\lambda_\ell - (m-1)h_w]}, \qquad \begin{matrix} 1 \le i \le m \\ 1 \le \ell \le N \end{matrix}$$

The submatrices Q^*_{ij}, $i\neq j$, are equal and diagonal as well. The diagonal elements may be expressed as

$$(2\text{-}35)\qquad q^*_{[(i-1)N+\ell][(j-1)N+\ell]} = \frac{-(\lambda_\ell - h_w)}{h_w[m\lambda_\ell - (m-1)h_w]}, \quad i\neq j$$

Combining Eqs. (2-34) and (2-35), we have

$$(2\text{-}36)\qquad q^*_{[(i-1)N+\ell][(j-1)N+\ell]} = \frac{\delta_{ij}}{h_w} - \frac{\lambda_\ell - h_w}{h_w[m\lambda_\ell - (m-1)h_w]}, \quad 1 \le i, j \le m$$

[+]A simple proof of Eq. (2-36) is shown in Appendix A. Notice that $Q^*_{ij} \neq K^{*-1}_{ij}$ for all i and j.

Although Eq. (2-36) is only good for $\nu = 0$, the result of this special case can be generalized.

D. Interference from Arbitrary Angles

Although the digital computer may be used to obtain the Q matrix numerically if the order of K is not too large, we hope to obtain a general analytical result. Thus we shall have to find another method for computing the Q matrix.

The simplicity for the case of broadside interference is due to the interfering signal having equal phase at each element. Suppose we consider the following delayed signal

$$(2\text{-}37)\quad r_i^*(t) \triangleq \{a_i(z) + n_i(z) + w_i(z)\}_{z=t-(m-i)\nu}$$

$$= a[t-(m-i)\nu-(i-1)\tau] + n[t-(m-1)\nu] + w_i[t-(m-i)\nu]$$

where Eq. (2-3) has been used to replace $a_i(z)$ and $n_i(z)$. The second term in Eq. (2-37) does not have the index i, becuase the interference has the same phase for all $r_i^*(t)$'s. We examine the covariance matrix associated with $r_i^*(t)$. Let

$$(2\text{-}38)\quad r_{i\ell}^* \triangleq \int_{-T}^{T} r_i^*(t)\, \phi_\ell(t) \cdot dt$$

$$(2\text{-}39)\quad m_{i\ell}^* \triangleq E\{r_i^* \mid H_k\} .$$

Then the element of the ijth submatrix at the ℓn position is

$$(2\text{-}40)\quad E\{(r_{i\ell}^* - m_{i\ell}^*)(r_{jn}^* - m_{jn}^*)\}$$

$$= \iint_{-T}^{T} E\{n[t-(m-1)\nu] \cdot n[u-(m-1)\nu]\} \cdot \phi_\ell(t)\phi_n(u) \cdot dt\, du$$

$$+ \iint_{-T}^{T} E\{w_i[t-(m-i)\nu] \cdot w_j[u-(m-j)\nu]\} \cdot \phi_\ell(t)\phi_n(u) \cdot dt\, du$$

$$= \delta_{\ell n}(\lambda_n - h_w) + h_w \cdot \delta_{ij} \iint_{-T}^{T} \delta[t-u+(i-j)\nu] \cdot \phi_\ell(t)\phi_n(u) \cdot du\, dt$$

$$= \begin{cases} \delta_{\ell n} \cdot (\lambda_n - h_w) & \text{if } i \neq j \\ \delta_{\ell n} \cdot \lambda_n & \text{if } i = j \end{cases}$$

Equation (2-40) indicates that the covariance matrix of $r_i^*(t)$ is identical to that for broadside interference. This is also true if $a_i(t)$ in Eq. (2-37) is replaced by $b_i(t)$, which is the signal under hypothesis H_b.

Physically, $r_i^*(t)$ is the signal obtained by delaying the signal $r_i(t)$ in the ith channel by $t-(m-i)\nu$ seconds. In general, such time shifting of the received signal could be done with a delay line behind each array element. Since the $w_i(t)$ are assumed to be wide-sense stationary processes, shifting on the time axis will not affect their statistics. We next examine how the $r_{i\ell}^*$'s are related to the $r_{i\ell}$'s. We know that

$$(2\text{-}41) \qquad r_i(t) = \lim_{N\to\infty} \sum_{\ell=1}^{N} r_{i\ell}\, \phi_\ell(t), \quad -T \le t \le T$$

It is also true that

$$(2\text{-}42) \qquad r_i[t-(m-i)\nu] = \lim_{N\to\infty} \sum_{\ell=1}^{N} r_{i\ell} \cdot \phi_\ell[t-(m-i)\nu], \; -T \le t-(m-i)\nu \le T$$

and

$$(2\text{-}43) \qquad r_i^*(t) \triangleq r_i[t-(m-i)\nu] = \lim_{N\to\infty} \sum_{\ell=1}^{N} r_{i\ell}^* \phi_\ell(t)$$

Equating Eqs. (2-42) and (2-43), we have

$$(2\text{-}44) \qquad \sum_{\ell=1}^{\infty} r_{i\ell}^*\, \phi_\ell(t) = \sum_{\ell=1}^{\infty} r_{i\ell}\, \phi_\ell[t-(m-i)\nu]$$

If both sides of Eq. (2-44) are multiplied by $\phi_n(t)$ and integrated between the limits -T and T, the result yields

$$(2\text{-}45) \qquad r_{in}^* = \sum_{\ell=1}^{\infty} r_{i\ell} \cdot \int_{-T}^{T} \phi_n(t) \cdot \phi_\ell[t-(m-i)\nu] \cdot dt$$

We define the vector R*

$$(2\text{-}46) \qquad R^* \triangleq \begin{bmatrix} R_1^* \\ R_2^* \\ \cdot \\ \cdot \\ \cdot \\ R_i^* \\ \cdot \\ \cdot \\ \cdot \\ R_m^* \end{bmatrix}$$

where R_i^* is itself a column matrix given by

$$(2\text{-}47) \qquad R_i \triangleq \begin{bmatrix} r_{i1}^* \\ r_{i2}^* \\ \cdot \\ r_{i\ell}^* \\ \cdot \\ \cdot \\ \cdot \\ r_{iN}^* \end{bmatrix}$$

We also define a matrix C

$$(2\text{-}48) \qquad C \triangleq \begin{bmatrix} C_1 & 0 & 0 & \cdots & 0 \\ 0 & C_2 & 0 & \cdots & 0 \\ 0 & 0 & C_3 & \cdots & 0 \\ \cdot & \cdot & \cdot & & \cdot \\ \cdot & \cdot & \cdot & & \cdot \\ \cdot & \cdot & \cdot & & \cdot \\ 0 & 0 & 0 & \cdots & C_m \end{bmatrix}$$

where 0 is a null matrix and the submatrix C_i is a square, unsymmetric matrix, defined by

(2-49)

$$C_i = \begin{bmatrix} \int_{-T}^{T} \phi_1(t)\cdot\phi_1[t-(m-i)\nu]dt & \int_{-T}^{T} \phi_1(t)\cdot\phi_2[t-(m-i)\nu]dt & \cdots & \int_{-T}^{T} \phi_1(t)\cdot\phi_N[t-(m-i)\nu]dt \\ \int_{-T}^{T} \phi_2(t)\cdot\phi_1[t-(m-i)\nu]dt & \int_{-T}^{T} \phi_2(t)\cdot\phi_2[t-(m-i)\nu]dt & \cdots & \int_{-T}^{T} \phi_2(t)\cdot\phi_N[t-(m-i)\nu]dt \\ \vdots & \vdots & & \vdots \\ \int_{-T}^{T} \phi_N(t)\cdot\phi_1[t-(m-i)\nu]dt & \int_{-T}^{T} \phi_N(t)\cdot\phi_2[t-(m-i)\nu]dt & \cdots & \int_{-T}^{T} \phi_N(t)\cdot\phi_N[t-(m-i)\nu]dt \end{bmatrix}$$

In matrix notation, Eq. (2-45) may be expressed as

(2-50) $$\lim_{N\to\infty} R^* = \lim_{N\to\infty} CR$$

We have pointed out earlier that if we compute $E\{(R^*-M^*)(R^*-M^*)^T\}$, where $M^* \triangleq E\{R^*|H\}$, we get the same covariance matrix as if the interferring source were at broadside. In other words,

(2-51) $$K^* = E\{(R^*-M^*)(R^*-M^*)^T\}$$

Substituting Eq. (2-50) into Eq. (2-51), yields,

(2-52) $$K^* = CKC^T$$

From Eq. (2-52), it can be shown that

(2-53) $$Q = C^T Q^* C$$

Eq. (2-53) provides us with a much easier way to compute the Q matrix. Since Eq. (2-42) is defined for $-T \leq t - (m-i)\nu \leq T$ and the series given by Eqs. (2-41) and (2-43) converge to $r_i(t)$ and $r_i^*(t)$ respectively if N approaches infinity, Eq. (2-53) is correct and exact if those two conditions hold. For a finite N, Eq. (2-53) is merely an approximation.

Now we use this transformation to find the elements of Q for an arbitrary ϕ. Performing the matrix multiplications indicated by Eq. (2-53), we find that the submatrix Q_{ij}, which is one of m^2 of its kind, is given by

$$(2\text{-}54) \qquad Q_{ij} = C_i^T \, Q_{ij}^* \, C_j, \quad i \le i, \, j \le m.$$

If the last term for the series expansion is denoted as N, then there are N^2 elements in the square matrix Q_{ij}. We use q, with proper subscripts, to denote elements of Q. From Eq. (2-54), we find the element of Q_{ij} at the ℓn position is equal to

(2-55)

$$q_{[(i-1)N+\ell][(j-1)N+n]} = \lim_{N\to\infty} \int\int_{-T}^{T} \phi_\ell[t-(m-i)\nu] \cdot \phi_n[u-(m-j)\nu] \cdot \cdot \sum_{k=1}^{N} q^*_{[(i-1)N+k][(j-1)N+k]} \cdot \phi_k(t)\phi_k(u) \cdot dt\,du$$

Substituting Eq. (2-36) into Eq. (2-55), yields

(2-56)

$$q_{[(i-1)N+\ell][(j-1)N+n]} = \frac{\delta_{ij}}{h_w} \int_{-T}^{T} \phi_\ell[t-(m-i)\nu] \cdot \phi_n[t-(m-j)\nu] \cdot dt - \frac{1}{h_w} \sum_{k=1}^{\infty} \frac{\lambda_k - h_w}{m\lambda_k - (m-1)h_w} \cdot \int\int_{-T}^{T} \phi_\ell[t-(m-i)\nu] \cdot \phi_n[u-(m-j)\nu] \cdot \cdot \phi_k(t)\, \phi_k(u) \cdot dt\, du$$

We have made use of

$$(2\text{-}57) \qquad \delta(t-u) = \sum_{\ell=1}^{\infty} \phi_\ell(t)\, \phi_\ell(u)$$

to get Eq. (2-56). This result will be used to formulate the analytical expression for the test statistics in the next chapter.

CHAPTER III
THE OPTIMUM DETECTOR FOR DETECTING COMPLETELY KNOWN BINARY SIGNALS

A. The Likelihood Ratio Test

In this chapter, the equations of the test statistic and those required for showing the receiver operating characteristic of the optimum processor are formulated. The results presented here optimize the performance of the entire detection system, rather than the antenna array or the receiver separately.

The binary signals a(t) and b(t) are assumed known exactly. Thus the uncertainty in the signal at the input of each channel arises solely from the additive random noise which is the sum of the interference and the internal noises. The detection system will have to make a choice between two hypotheses by processing the signal from each channel. The signal to be processed at the ith channel can have one of two different signals:

$$\text{Hypothesis } H_a: \quad r_i(t) = a_i(t) + n_i(t) + w_i(t)$$

$$\text{Hypothesis } H_b: \quad r_i(t) = b_i(t) + n_i(t) + w_i(t)$$

where $1 \leq i \leq m$.

Dual hypotheses testing relies on a decision rule for dividing the observation space into two parts. Various optimum decision rules (e.g., Bayes criterion, Neyman-Pearson criterion, etc.) can be used. These decision criteria for the optimal receiver all lead to a likelihood ratio test [21]:

$$\text{(3-1)} \qquad \text{L.R.T.} \triangleq \lim_{N\to\infty} \frac{p(R|H_b)}{p(R\,H_a)} \underset{H_a}{\overset{H_b}{\gtrless}} \text{threshold}$$

where N is the last term of the Karhunen-Loéve expansion. The structure of the optimum detector immediately follows once the result for the likelihood ratio test is obtained.

The probability density function of R under hypothesis H_a for a N-term Karhunen-Loeve expansion and an m-element array is equal to

$$(3\text{-}2) \qquad p(R|H_a) = \frac{1}{\sqrt{(2\pi)^{mN}|K|}} \; e^{-\frac{1}{2}(R-A)^T Q (R-A)}$$

The exponent may be written as

$$(3\text{-}3) \qquad -\frac{1}{2}(R-A)^T \cdot Q \cdot (R-A)$$

$$= -\frac{1}{2} \sum_{i=1}^{m} \sum_{j=1}^{m} \sum_{\ell=1}^{N} \sum_{n=1}^{N} (r_{i\ell}-a_{i\ell}) \cdot q_{[(i-1)N+\ell][(j-1)N+n]} \cdot (r_{jn}-a_{jn})$$

$$= -\frac{1}{2} \sum_{i,j=1}^{m} \iint_{-T}^{T} [r_i(t)-a_i(t)][r_j(z)-a_j(z)]$$

$$\cdot \sum_{\ell,} \sum_{n=1}^{N} q_{[(i-1)N+\ell][(j-1)N+n]} \, \phi_\ell(t) \, \phi_n(z) \cdot dt \, dz.$$

We may express Eq. (3-3) in a more compact form by defining

$$(3\text{-}4) \qquad H_{ij}^N(t,z) \triangleq \sum_{\ell,n=1}^{N} q_{[(i-1)N+\ell][(j-1)N+n]} \, \phi_\ell(t) \, \phi_n(z)$$

Since the Q matrix is symmetric, it can be shown that $H_{ij}(t,z) = H_{ji}(z,t)$ and thus

$$(3\text{-}5) \qquad \sum_{i,j=1}^{m} \iint_{-T}^{T} [r_i(t)a_j(z) + a_i(t) \, r_j(z)] \cdot H_{ij}^N(t,z) \cdot dt \, dz$$

$$= 2 \sum_{i,j=1}^{m} \iint_{-T}^{T} r_i(t)a_j(z) \cdot H_{ij}^N(t,z) \cdot dt \, dz$$

Hence, in terms of $H_{ij}^N(t,z)$, the exponent becomes

$$(3\text{-}6) \qquad -\frac{1}{2}(R-A)^T \cdot Q \cdot (R-A)$$

$$= -\frac{1}{2}\sum_{i,j=1}^{m}\sum \iint_{-T}^{T} r_i(t)r_j(z) \cdot H_{ij}^N(t,z)\cdot dtdz$$

$$-\frac{1}{2}\sum_{i,j=1}^{m}\sum \iint_{-T}^{T} a_i(t)\, a_j(z) \cdot H_{ij}^N(t,z) \cdot dt\, dz$$

$$+\sum_{i,j=1}^{m}\sum \iint_{-T}^{T} r_i(t)\, a_j(z) \cdot H_{ij}^N(t,z) \cdot dt\, dz$$

The probability density of R under H_b is readily obtained by changing a(t) in Eq. (3-6) to b(t). We compute the likelihood ratio

$$(3\text{-}7) \qquad \text{L.R.} = \lim_{N\to\infty} \frac{p(R|H_b)}{p(R|H_a)}$$

$$= \lim_{N\to\infty} \exp\left\{\sum_{i,j=1}^{m}\sum \iint_{-T}^{T} r_i(t) \cdot[b_j(z)-a_j(z)]\cdot H_{ij}^N(t,z)\cdot dt\, dz\right.$$

$$\left. -\frac{1}{2}\sum_{i,j=1}^{m}\sum \iint_{-T}^{T} [b_i(t)b_j(z)-a_i(t)a_j(z)]\cdot H_{ij}^N(t,z)\cdot dtdz\right\}$$

$r_i(t)$, the input of the ith channel, appears only in the first term of Eq. (3-7). Since a(t) and b(t) are assumed known exactly, the second term thus is a constant and may be incorporated in the threshold. Let

$$(3\text{-}8) \qquad s(t) = b(t) - a(t)$$

Then, from Eq. (3-7), an equivalent likelihood ratio test (ELRT) is

$$(3\text{-}9) \qquad \text{ELRT} \triangleq \sum_{i,j=1}^{m}\sum \iint_{-T}^{T} r_i(t)s_j(z) \cdot H_{ij}^{\infty}(t,z) \cdot dt\, dz$$

$$\underset{H_a}{\overset{H_b}{\gtrless}} \quad \text{threshold}$$

where we have taken the limit as $N \to \infty$:

$$(3\text{-}10) \quad H_{ij}^{\infty}(t,z) = \lim_{N\to\infty} H_{ij}^{N}(t,z)$$

$$= \lim_{N\to\infty} \sum_{\ell,n=1}^{N} q_{[(i-1)N+\ell][(j-1)N+n]}\, \phi_{\ell}(t)\, \phi_{n}(z)$$

$$= \frac{\delta_{ij}}{h_w} \int_{-T}^{T} \delta[t-t'+(m-i)\nu] \cdot \delta[z-t'+(m-j)\nu] \cdot dt'$$

$$- \frac{1}{h_w} \sum_{k=1}^{\infty} \frac{\lambda_k - h_w}{m\lambda_k-(m-1)h_w} \iint_{-T}^{T} \delta[t-t'+(m-i)\nu] \cdot$$

$$\cdot \delta[z-u'+(m-j)\nu] \cdot \phi_k(t')\, \phi_k(u') \cdot dt'\, du'$$

Substituting Eq. (3-10) into Eq. (3-9), yields

$$\text{ELRT} = \frac{1}{h_w} \sum_{i=1}^{m} \int_{-T}^{T} r_i(t_i) s_i(t_i) dt$$

$$- \sum_{i,j=1}^{m} \iint_{-T}^{T} r_i(t_i) s_j(z_j) \cdot \Psi(t,z) \cdot dt\, dz$$

where

$$(3\text{-}11) \quad t_i \triangleq t-(m-i)\nu$$

$$(3\text{-}12) \quad z_j \triangleq z - (m-j)\nu$$

and

$$(3\text{-}13) \quad \Psi(t,z) \triangleq \sum_{\ell=1}^{\infty} \frac{\phi_{\ell}(t)\phi_{\ell}(z)}{m + \frac{h_w}{\lambda_{\ell} - h_w}}$$

Let η be the threshold. The optimum detection system is defined by

$$(3\text{-}14) \qquad L(R) \triangleq \sum_{i=1}^{m} \int_{-T}^{T} r_i(t_i) s_i(t_i) \cdot dt$$

$$- \sum_{i,j=1}^{m} \int_{-T}^{T} r_i(t_i) s_j(z_j) \cdot \Psi(t,z) \cdot dt\, dz$$

$$\underset{H_a}{\overset{H_b}{\gtrless}} \eta$$

The likelihood ratio test leads us to the test statistic L(R), which can be generated by correlating the delayed signal $r_i(t_i)$ with some known functions. We compare L(R) to a threshold to make the decision.

In Eq. (3-14), the known signal s(t) and the array received signal $r_i(t)$ are time-shifted, because

$$(3\text{-}15) \qquad s_i(t_i) = s_i[t-(m-i)\nu]$$

$$= b[t-(i-1)\tau-(m-i)\nu] - a[t-(i-1)\tau-(m-i)\nu]$$

and

$$(3\text{-}16) \qquad r_i(t_i) = r_i[t-(m-i)\nu]$$

The delay time $(i-1)\tau$ occurs because each array element has unequal distance to the signal source. But the additional delay $(m-i)\nu$ results from computing the Q matrix using the transformation C. The double summation term in the test statistic L(R) is influenced by the power spectrum of the interference, for $\Psi(t,z)$ is obtained from the integral equation defined by Eq. (2-11). The double summation term may be rewritten as

$$(3\text{-}17) \qquad \sum_{i=1}^{m} \int_{-T}^{T} r_i(t_i) \cdot \left\{ \sum_{j=1}^{m} \left[\sum_{\ell=1}^{\infty} \frac{s^*_{j\ell}}{m + \frac{h_w}{\lambda_\ell - h_w}} \phi_\ell(t) \right] \right\} dt$$

where

$$(3\text{-}18) \qquad s^*_{j\ell} \triangleq \int_{-T}^{T} s_j(z_j) \phi_\ell(z) \cdot dz$$

Hence, $r_i(t_i)$ is, in general, correlated with m distorted known signals $s_j(z_j)$ because $s^*_{j\ell}$'s are weighted unequally. For the case when the interference is a white noise process with autocorrelation function $R(t-u) = h_n \cdot \delta(t-u)$, it is found by solving Eq. (2-11) that $\lambda_\ell - h_w = h_n$ for all ℓ. Thus the weights for the $s^*_{j\ell}$'s are identical and the test statistic takes a much simpler form:

(3-19)

$$L(R) = \sum_{i=1}^{m} \int_{-T}^{T} r_i(t_i)s_i(t_i)dt - \frac{1}{m + \frac{h_w}{h_n}} \sum_{i,j=1}^{m} \int_{-T}^{T} r_i(t_i)s_j(t_j)dt$$

A scheme for processing the input of the ith channel based on Eq. (3-14) is shown in Fig. 3-1.

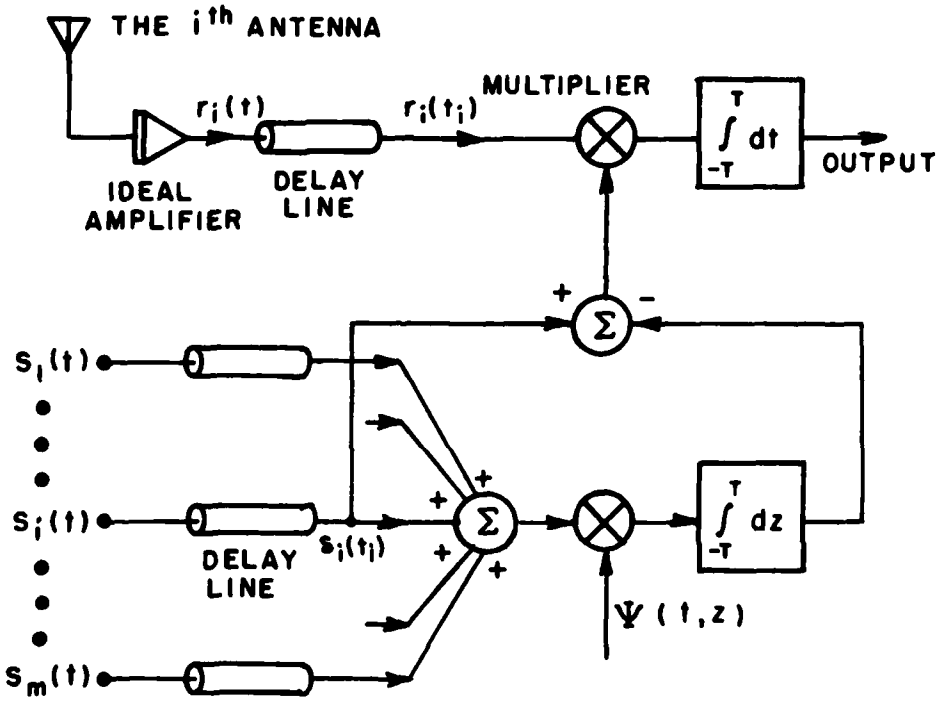

Fig. 3-1--The ith channel processing unit.

B. Receiver Operating Characteristic

Since the test statistic L(R) is obtained by the linear operation indicated by Eq. (3-14) on $r_i(t_i)$, it is a Gaussian random variable under either hypothesis. The density of L(R) is found once its mean and variance are determined.

The mean of L(R) is readily obtained if we replace $r_i(t_i)$ in Eq. (3-14) by its expectation, i.e.,

(3-20)

$$m_{La} \triangleq E\{L(R)\,|H_a\}$$
$$= \sum_{i=1}^{m} \int_{-T}^{T} a_i(t_i)s_i(t_i)dt - \sum_{i,j=1}^{m}\sum \iint_{-T}^{T} a_i(t_i)s_j(z_j)\cdot\psi(t,z)\cdot dt\, dz$$

and

(3-21)

$$m_{Lb} \triangleq E\{L(R)\,|H_b\}$$
$$= \sum_{i=1}^{m} \int_{-T}^{T} b_i(t_i)s_i(t_i)dt - \sum_{i,j=1}^{m}\sum \iint_{-T}^{T} b_i(t_i)s_j(z_j)\cdot\psi(t,z)\cdot dt\, dz$$

The variance of L(R) under either hypothesis may be calculated from the following relation

(3-22) $$\text{var}\{L(R)\,|H_k\} = E\{L^2(R)\,|H_k\} - E^2\{L(R)\,|H_k\}$$

Evaluating the variance is straightforward but tedious. The derivation is given in Appendix B. We find that the variance of L(R) equals

(3-23)

$$\sigma_L^2 \triangleq \text{var}\{L(R)\,|H_k\}$$
$$= h_w\left\{\sum_{i=1}^{m} \int_{-T}^{T} s_i^2(t_i)dt - \sum_{i,j=1}^{m}\sum \iint_{-T}^{T} s_i(t_i)s_j(z_j)\cdot\psi(t,z)\cdot dt\, dz\right\}$$

By expressing $s_i(t_i)$ as,

$$s_i(t_i) = b_i(t_i) - a_i(t_i),$$

it can be shown that the variance σ_L^2 may be written in terms of the distance between the means of the test statistic under either hypotheses as

$$\sigma_L^2 = h_w (m_{Lb} - m_{La}) \tag{3-24}$$

Since σ_L^2 is nonnegative, one concludes that

$$m_{Lb} \geq m_{La} \tag{3-25}$$

We next formulate the equations for the probabilities of false and correct detection. Let the probability of choosing H_b when H_a is present be denoted by P_F and that of choosing H_b when H_b is present by P_D. Then, as illustrated in Fig. 3-2, the probability of false detection is+

$$P_F = \int_{\eta}^{\infty} p(L(R)|H_a) \cdot dL(R) \tag{3-26}$$

$$= \frac{1}{\sqrt{2\pi}\,\sigma_L} \int_{\eta}^{\infty} e^{-\frac{(L-m_{La})^2}{2\sigma_L^2}} dL = \text{erfc}_*\left(\frac{\eta - m_{La}}{\sigma_L}\right)$$

and the probability of correct detection is

+$\text{erfc}_*(x)$ is defined as $\int_x^{\infty} \frac{1}{\sqrt{2\pi}} e^{-\frac{y^2}{2}} dy$

$$(3\text{-}27) \qquad P_D = \int_{\eta}^{\infty} p(L(R)|H_b) \cdot d\,L(R)$$

$$= \frac{1}{\sqrt{2\pi}\,\sigma_L} \int_{\eta}^{\infty} e^{-\frac{(L-m_{Lb})^2}{2\sigma_L^2}} dL = \text{erfc}_*\left(\frac{\eta - m_{Lb}}{\sigma_L}\right)$$

The P_F-P_D plot is referred to as the receiver operating characteristic (ROC).

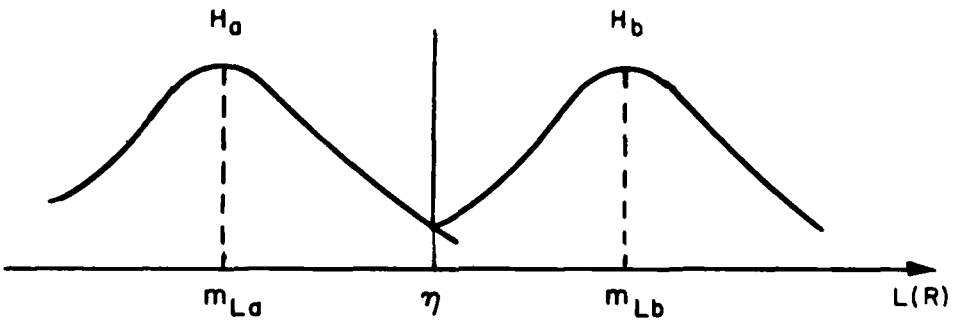

Fig. 3-2--Probability density functions of L(R).

For a communication system, we are usually interested in the total probability of making incorrect decisions. If the a priori probabilities of the source are equal, i.e., if $P_r[H_a] = P_r[H_b] = \frac{1}{2}$, then, P_ε, the total probability of making error is simply

$$(3\text{-}28) \qquad P_\varepsilon = \tfrac{1}{2} P_F + \tfrac{1}{2} (1 - P_D)$$

For a given m_{La}, m_{Lb} and σ_L, the probability of error varies with the threshold η. The threshold η_o which minimizes Eq. (3-28) may be determined by solving

$$(3\text{-}29) \qquad \frac{dP_\varepsilon}{d\eta} = 0$$

for η. The solution is

$$(3\text{-}30) \qquad \eta_o = \tfrac{1}{2} (m_{Lb} + m_{La})$$

The corresponding probability of error, $P_\varepsilon(\eta_0)$, is found to be equal to

$$(3\text{-}31) \qquad P_\varepsilon(\eta_0) = \text{erfc}_*\left(\frac{m_{Lb}-m_{La}}{2\sigma_L}\right)$$

which implies that $P_\varepsilon(\eta_0)$ may be minimized by maximizing $(m_{Lb}-m_{La})/\sigma_L$. Alternatively, by substituting Eq. (3-24) into Eq. (3-31), we obtain another expression for $P_\varepsilon(\eta_0)$,

$$(3\text{-}32) \qquad P_\varepsilon(\eta_0) = \text{erfc}_*\left(\tfrac{1}{2}\sqrt{\frac{m_{Lb}-m_{La}}{h_w}}\right) \quad .$$

CHAPTER IV
THE DIRECTIONAL CHARACTERISTICS AND THE ERROR RATE PERFORMANCE

A. Introduction

To make the general theory developed in the last chapter clearer, we shall treat the case when the binary signals are of the form.

$$(4\text{-}1) \qquad H_a: \quad a(t) = e_a(t) \cdot \cos(\omega t + \phi_s)$$

$$(4\text{-}2) \qquad H_b: \quad b(t) = e_b(t) \cdot \cos(\omega t + \phi_s)$$

The signals given above represent the amplitude-shift keying (ASK) binary signals if the modulating signals $e_a(t)$ and $e_b(t)$ only differ in amplitudes. If the modulating signals are related by $e_a(t) = - e_b(t)$, then the signals given in Eq. (4-1) and Eq. (4-2) are biphase modulated binary signals.

The optimum communication system contains an array and an optimum signal processor. The task for the system is to detect the binary signals arriving from angle θ in the presence of an interfering signal from the given angle ϕ. To accomplish this goal, we intuitively expect the system to function in favor of the signal arriving from the desired angle θ. To investigate this aspect, we study how the system treats a testing signal arriving from an arbitrary angle $\hat{\theta}$. Since the detection system is based on a comparison of the processor output L(R) with a threshold, we examine L(R) to determine the system characteristics. One important characteristic of L(R) is its mean. Hence, we study the mean instead. The performance of a detector is judged mainly by its ability to make correct decisions. For this reason, we shall also discuss the error rate performance and the methods of optimizing it.

Here, we shall assume that the waveform for the testing signal is the same as the signal a(t). The reasons for this choice are (1) to simplify the mathematics involved, and (2) to understand the behavior of the mean m_{La} through studying the directional characteristics of the optimum system. The output from the optimum detector (θ,ϕ) when a signal a(t) arrives from angle $\hat{\theta}$ is given by*

*We use "detector (θ,ϕ)" to mean a detector designed to detect the desired communication signal arriving from angle θ in the presence of the interfering signal with incident angle ϕ.

$$(4\text{-}3) \qquad L(\hat{R}) = \sum_{i=1}^{m} \int_{-T}^{T} \hat{r}_i(t_i) s_i(t_i) dt$$

$$- \sum_{i,j=1}^{m} \sum \iint_{-T}^{T} \hat{r}_i(t_i) s_j(z_j) \cdot \Psi(t,z) \cdot dt\, dz,$$

where $\hat{r}_i(t_i)$ is defined as

$$\hat{r}_i(t_i) \triangleq n_i(t_i) + w_i(t_i) + \hat{a}_i(t_i)$$

$$\triangleq n_i(t_i) + w_i(t_i) + a[t - (i-1)\frac{d}{c} \cos \hat{\theta} - (m-i)\nu]$$

The mean of the system output $L(\hat{R})$ is

$$(4\text{-}4) \qquad m_{La}(\theta,\phi;\hat{\theta}) \triangleq E\{L(\hat{R})\}$$

$$= \sum_{i=1}^{m} \int_{-T}^{T} \hat{a}_i[t-(m-i)\nu] \cdot s_i[t-(m-i)\nu] \cdot dt$$

$$- \sum_{i,j=1}^{m} \sum \iint_{-T}^{T} \hat{a}_i[t-(m-i)\nu] \cdot s_j[z-(m-j)\nu] \cdot$$

$$\cdot \Psi(t,z) \cdot dt\, dz$$

We write m_{La} as a function of the angles to emphasize its dependence on these angles. The m_{La} appearing in the last chapter is just $m_{La}(\theta,\phi;\theta)$.

The closed form representation for $m_{La}(\theta,\phi;\hat{\theta})$ will be derived in the next section. In Sections IV.C and IV.E, the directional characteristics and the error rate performance are investigated. The discussions are restricted to the case when the interfering signal is a white noise process and the desired signals are biphase modulated. Section IV.F generalizes these results to the case when the interference is a general Gaussian, wide-sense stationary process with arbitrary power spectrum.

B. The Mean of $L(\hat{R})$

We assume that the frequencies contained in the modulating signals $e_a(t)$ and $e_b(t)$ are much lower than the carrier frequency so the following approximation may be made*

$$e_{ki}[t-(m-i)\nu] \approx e_k(t), \quad k = a \text{ and } b. \tag{4-5}$$

Hence, $a_i[t-(m-i)\nu]$ may be approximated by

$$a_i[t-(m-i)\nu] \approx e_a(t) \cdot \cos\{\omega[t-(m-1)\nu] + \phi_s-(i-1)\omega(\tau-\nu)\}. \tag{4-6}$$

In the same manner,

$$s_i[t-(m-i)\nu] \approx e(t) \cdot \cos\{\omega[t-(m-1)\nu] + \phi_s-(i-1)\omega(\tau-\nu)\}, \tag{4-7}$$

where $e(t) \triangleq e_b(t) - e_a(t)$.

By making use of the identities

$$\sum_{i=1}^{m} \cos(i-1)x = \frac{\sin\left(\frac{m}{2}x\right) \cdot \cos\left(\frac{m-1}{2}x\right)}{\sin\left(\frac{x}{2}\right)},$$

and

$$\sum_{i=1}^{m} \sin(i-1)x = \frac{\sin\left(\frac{m}{2}x\right) \cdot \sin\left(\frac{m-1}{2}x\right)}{\sin\left(\frac{x}{2}\right)},$$

it can be shown from Eq. (4-6) and Eq. (4-7) that

---

*This approximation introduces a maximum time shift of d/c (m-1) seconds in the modulation envelope. We assume this time shift to be negligible at the maximum modulation frequency.

(4-8) $$\sum_{i=1}^{m} s_i[t-(m-i)\nu]$$

$$= \frac{\sin \frac{m}{2}\omega(\tau-\nu)}{\sin \frac{\omega}{2}(\tau-\nu)} \cdot e(t) \cdot \cos\{\omega[t - \frac{m-1}{2}(\tau+\nu)] + \phi_s\{$$

(4-9) $$\sum_{i=1}^{m} \hat{a}_i[t-(m-i)\nu]$$

$$= \frac{\sin \frac{m}{2}\omega(\hat{\tau}-\nu)}{\sin \frac{\omega}{2}(\hat{\tau}-\nu)} \cdot e_a(t) \cdot \cos\{\omega[t - \frac{m-1}{2}(\hat{\tau}+\nu)] + \phi_s\}$$

and

(4-10) $$\sum_{i=1}^{m} \hat{a}_i[t-(m-i)\nu] \cdot s_i[t-(m-i)\nu]$$

$$= \frac{e(t)e_a(t)}{2} \cdot \frac{\sin \frac{m}{2}\omega(\hat{\tau}-\tau) \cdot \cos \frac{m-1}{2}\omega(\hat{\tau}-\tau)}{\sin \frac{\omega}{2}(\hat{\tau}-\tau)}$$

$$+ \frac{e(t)e_a(t)}{2} \cdot \frac{\sin \frac{m}{2}\omega(\hat{\tau}-\tau-2\nu)}{\sin \frac{\omega}{2}(\hat{\tau}+\tau-2\nu)}.$$

$$\cdot \quad \cos\{2\omega(t - \frac{m-1}{2}\nu)+2\phi_s - \frac{m-1}{2}(\hat{\tau}-\tau)\}$$

Substituting Eqs. (4-8), (4-9) and (4-10) into (4-4), we obtain

(4-11)

$$m_{La}(\theta,\phi;\hat{\theta}) = \frac{\sin \frac{m}{2}\omega(\hat{\tau}+\tau-2\nu)}{\sin \frac{\omega}{2}(\hat{\tau}+\tau-2\nu)} \cdot \int_{-T}^{T} \frac{e_a(t)e(t)}{2},$$

$$\cdot \cos[2\omega(t - \frac{m-1}{2}\nu) + 2\phi_s - \frac{m-1}{2}\omega(\hat{\tau}+\tau)] \cdot dt$$

(4-11)
(Cont.)

$$+\frac{\sin\frac{m}{2}\omega(\hat{\tau}-\tau)\cdot\cos\frac{m-1}{2}\omega(\hat{\tau}-\tau)}{\sin\frac{\omega}{2}(\hat{\tau}-\tau)}\cdot\int_{-T}^{T}\frac{e_a(t)\,e(t)}{2}\,dt$$

$$-\frac{\sin\frac{m}{2}\omega(\hat{\tau}-\nu)}{\sin\frac{\omega}{2}(\hat{\tau}-\nu)}\cdot\frac{\sin\frac{m}{2}\omega(\tau-\nu)}{\sin\frac{\omega}{2}(\tau-\nu)}\cdot\sum_{\ell=1}^{\infty}\frac{1}{m+\frac{h_w}{\lambda_\ell-h_w}}\cdot$$

$$\cdot\iint_{-T}^{T}e_a(t)e(z)\cdot\phi_\ell(t)\phi_\ell(z)\cdot\cos\{\omega[t-\tfrac{m-1}{2}(\hat{\tau}+\nu)]+\phi_s\}\cdot$$

$$\cdot\cos\{\omega[z-\tfrac{m-1}{2}(\tau+\nu)]+\phi_s\}\cdot dt\,dz\ .$$

If ω is large, the first term in Eq. (4-11) is comparatively small and may be neglected for computation.

When the interference is a Gaussian white noise process with spectral height h_n, Eq. (4-11) reduces to a very simple form,

(4-12)

$$m_{La}(\theta,\phi;\hat{\theta})\approx\int_{-T}^{T}\frac{e(t)e_a(t)}{2}\,dt\cdot\cos\frac{m-1}{2}\omega(\hat{\tau}-\tau)\cdot$$

$$\cdot\left\{\frac{\sin\frac{m}{2}\omega(\hat{\tau}-\tau)}{\sin\frac{\omega}{2}(\hat{\tau}-\tau)}-\frac{1}{m+\frac{h_w}{h_n}}\cdot\frac{\sin\frac{m}{2}\omega(\tau-\nu)}{\sin\frac{\omega}{2}(\tau-\nu)}\cdot\frac{\sin\frac{m}{2}\omega(\hat{\tau}-\nu)}{\sin\frac{\omega}{2}(\hat{\tau}-\nu)}\right\}$$

where numerically small terms in Eq. (4-11) have been neglected.

C. The Directional Characteristics

The detection system is assumed to operate with two signal sources, the desired communication signal and the interference. The incident angles for these signals are θ and ϕ, respectively. Hence, the behavior of $m_{La}(\theta,\phi;\hat{\theta})$ at $\hat{\theta}=\theta$ and $\hat{\theta}=\phi$ interest us most. For this reason, we next study $m_{La}(\theta,\phi;\theta)$ and $m_{La}(\theta,\phi;\phi)$. In this section, the interfering signal is assumed to be a Gaussian white noise process of spectral height h_n.

The test function L(R) is obtained by processing the sum of the desired signal, the interference and the internal noise in the manner given in Eq. (3-14). The quantity $m_{La}(\theta,\phi;\theta)$ is the mean of the

processor output L(R) under hypothesis H_a. Since the interference and the internal noise have been assumed to be zero-mean, $m_{La}(\theta,\phi;\theta)$ in fact is equal to the component contributed to L(R) by the signal a(t) from the desired source for which the processor is designed to be optimum. Letting $\hat{\theta}=\theta$ (i.e., $\hat{\tau}=\tau$) in Eq. (4-12), we obtain

$$(4\text{-}13)\quad m_{La}(\theta,\phi;\theta) = \left\{ m - \frac{1}{m + \frac{h_w}{h_n}} \frac{\sin^2 \frac{m}{2}\omega(\tau-\nu)}{\sin^2 \frac{\omega}{2}(\tau-\nu)} \right\} \int_{-T}^{T} \frac{e_a(t)e(t)}{2}\, dt$$

For the same reason, $m_{La}(\theta,\phi;\phi)$ is equal to the component contributed to $L(\hat{R})$ by the signal $a(t)$ arriving from the angle identical to that of the interference. Letting $\hat{\theta}=\phi$ (i.e., $\hat{\tau}=\nu$) in Eq. (4-12), we find that

$$(4\text{-}14)\quad m_{La}(\theta,\phi;\phi) = \cos \frac{m-1}{2}\omega(\tau-\nu) \cdot \frac{\sin \frac{m}{2}\omega(\tau-\nu)}{\sin \frac{\omega}{2}(\tau-\nu)} \cdot \left\{ 1 - \frac{m}{m + \frac{h_w}{h_m}} \right\}$$

$$\cdot \int_{-T}^{T} \frac{e_a(t)e(t)}{2}\, dt \quad .$$

It can be shown that $m_{La}(\theta,\phi;\theta)$ never changes sign for a given

$$\int_{-T}^{T} e_a(t)e(t) \cdot dt$$

as the angles of arrival or the number of elements are varied. More precisely, the sign of $m_{La}(\theta,\phi;\theta)$ is always the same as the sign of

$$\int_{-T}^{T} e_a(t)e(t)\, dt.$$

It can be shown from Eq. (4-14) that $m_{La}(\theta,\phi;\phi)$ vanishes if*

---

*Equation (4-15) is derived from setting $\sin \frac{m}{2}\omega(\tau-\nu)=0$. λ is the free-space wavelength associated with the carrier. The quantity $m_{La}(\theta,\phi;\phi)$ also vanishes if $\cos \frac{m-1}{2}\omega(\tau-\nu) = 0$.

(4-15) $$m \frac{d}{\lambda} |\cos \theta - \cos \phi| = k$$

where $\theta \neq \phi$ and $k = 1,2,3 \cdots$. Furthermore, the absolute values of $m_{La}(\theta,\phi;\theta)$ and $m_{La}(\theta,\phi;\phi)$ are bounded as functions of the incident angles θ and ϕ. We find that

(4-16)
$$\left| \int_{-T}^{T} \frac{e_a(t)e(t)}{2} \, dt \cdot m \cdot \left(1 - \frac{m}{m + \frac{h_w}{h_n}} \right) \right| \leq |m_{La}(\theta,\phi;\theta)|$$

$$\leq \left| \int_{-T}^{T} \frac{e_a(t)e(t)}{2} \, dt \cdot m \right|$$

and

(4-17)
$$0 \leq |m_{La}(\theta,\phi;\phi)| \leq \left| \int_{-T}^{T} \frac{e_a(t)e(t)}{2} dt \cdot m \cdot \left(1 - \frac{m}{m + \frac{h_w}{h_n}} \right) \right|$$

Since the upper bound for $|m_{La}(\theta,\phi;\phi)|$ is just the lower bound for $|m_{La}(\theta,\phi;\theta)|$, the former will never become greater than the latter. They are equal only when $\theta=\phi$.

The bounds given in Eq. (4-16) and Eq. (4-17) indicate that the processor produces unequal outputs for the signal a(t) when this signal arrives from different angles. More precisely, the processor functions in favor of the signal a(t) when it arrives from the desired angle θ and suppresses it if the incident angle is ϕ.

For a fixed m and d, the ability of each processor to suppress the signal a(t) arriving from the angle ϕ depends on the angular separation between the incident angles θ and ϕ. To show this, two typical plots of $m_{La}(\theta,\phi;\phi)$ vs θ for $\phi=45^0$ are shown in Fig. 4-1 and Fig. 4-2. The spacing for which each detection system is designed to be optimum is 0.5λ. Also, we let $e_a(t)=-e_b(t)$ so that the binary signals are biphase modulated. Furthermore, we assume that

(4-18) $$\frac{1}{2} \int_{-T}^{T} e_a^2(t)dt = 1$$

In the neighborhood of 45^0, it is observed that $|m_{La}(\theta,45^0;\theta)|$ increases rapidly and eventually reaches the maximum at 45^0.

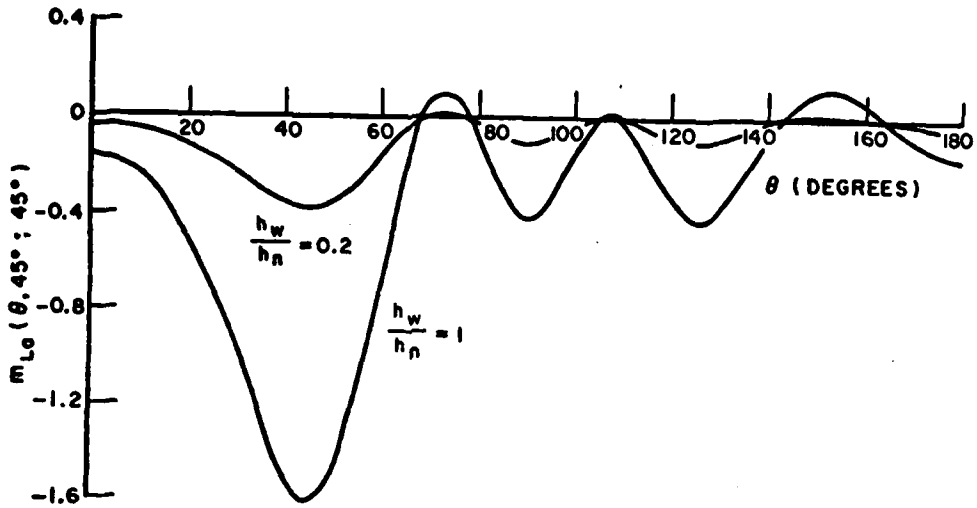

Fig. 4-1--$m_{La}(\theta,45^{o};45^{o})$ vs. θ given m=4 and d= $\frac{\lambda}{2}$.

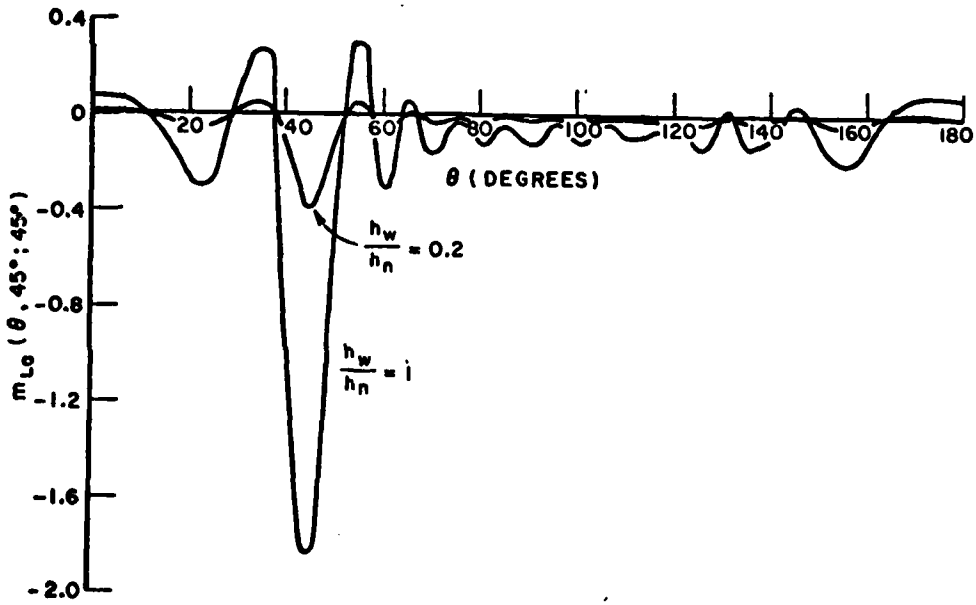

Fig. 4-2--$m_{La}(\theta,45^{o};45^{o})$ vs. θ given m=12 and d= $\frac{\lambda}{2}$.

These two figures indicate that the detection system is capable of suppressing the signal a(t) very effectively if the separation of θ and ϕ is large. As the incident angles θ and θ get very close, the suppression becomes very poor.

We now consider the case when the signal a(t) propagates into the array from the desired angle θ. The ability of the processor to favor this signal is also dependent on the angular separation. In Fig. 4-3 and Fig. 4-4, we plot $m_{La}(\theta,\phi;\theta)$ vs θ, given $\phi=45^o$. The antenna spacing used by each system is again equal to 0.5λ. In Fig. 4-3, where m=4, we observe that $|m_{La}(\theta,45^o;\theta)|$ begins to decrease steadily at $\theta=0^o$ and $\theta=70^o$. In Fig. 4-4, where m=12, the absolute value of each processor output decreases sharply in the neighborhood of $\theta=45^o$ which is the incident angle for the interfering signal.

For a constant m and d, the difference between the delay times τ and ν decreases as the incident angles θ and ϕ get closer and closer. When the separation between θ and ϕ is large enough, the change of the difference between τ and ν causes the sine and cosine functions in Eq. (4-10) and Eq. (4-15) to fluctuate periodically. When θ and ϕ get closer and closer, the distinction between the signals from θ and ϕ diminishes gradually. Consequently, the processor becomes less capable of favoring one type of signal and suppressing another type and vice versa. Finally, the two signals get equal treatment when $\theta=\phi$.

The upper bound of $|m_{La}(\theta,45^o;\theta)|$ for m=12 should be three times higher than m=4. This property is reflected in Fig. 4-3 and Fig. 4-4. One of the differences between $m_{La}(\theta,\phi;\theta)$ and $m_{La}(\theta,\phi;\phi)$ is shown in those figures, i.e., the former does not change sign whereas the latter does change sign as θ is varied.

We pointed out earlier that $m_{La}(\theta,\phi;\phi)$ vanishes if θ,ϕ and n satisfy Eq. (4-15). It can be shown from Eq. (4-13) that Eq. (4-15) is also the condition for $|m_{La}(\theta,\phi;\theta)|$ to reach its upper bound. From the discussion given earlier, it appears that an antenna array with spacing d satisfying this condition, for a given θ,ϕ and m, would optimize the error rate performance of the system. We shall discuss Eq. (4-15) more later. The upper bound of $|m_{La}(\theta,\phi;\phi)|$ increases linearly with m. The function

$$(4\text{-}19) \qquad f(m,h_w h_n^{-1}) = m\left(1 - \frac{m}{1+\frac{h_w}{h_n}}\right)$$

which appears in the upper bound for $|m_{La}(\theta,\phi;\phi)|$, is plotted in Fig. 4-5 for three values of h_w/h_n. It is seen that increasing m

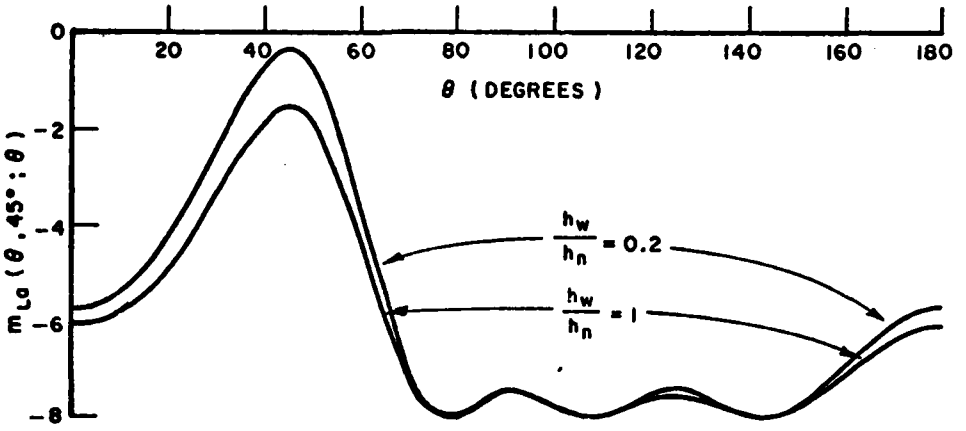

Fig. 4-3--$m_{La}(\theta,45^{o};\theta)$ vs. θ given m=4 and $d = \frac{\lambda}{2}$.

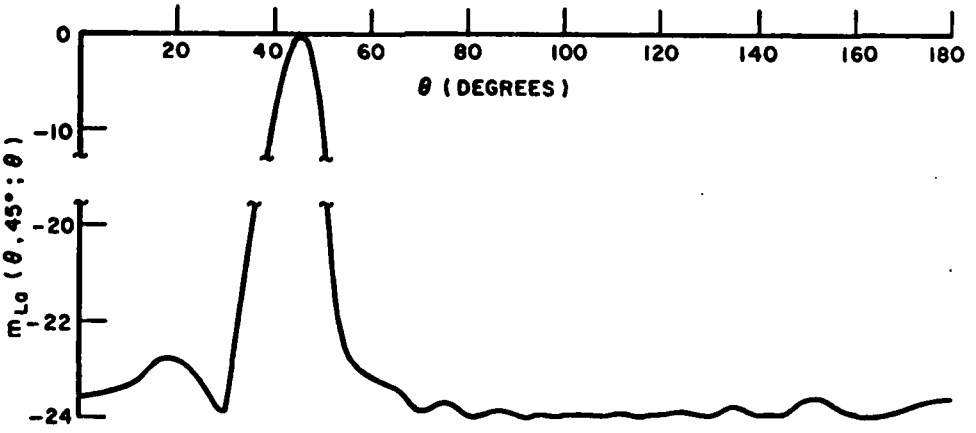

Fig. 4-4--$m_{La}(\theta,45^{o};\theta)$ vs. θ given m=12 and $d = \frac{\lambda}{2}$.

does not increase $f(m,h_w h_n^{-1})$ drastically. We also observe that $f(m,h_w h_n^{-1})$ tends to approach $h_w h_n^{-1}$ as m gets large. In fact, by expanding Eq. (4-19) into a power series, we find that

$$\lim_{m\to\infty} f(m,h_w h_n^{-1}) = \frac{h_w}{h_n} \tag{4-20}$$

Equation (4-20) suggests that the upper bound for $|m_{La}(\theta,\phi;\phi)|$ can not be raised appreciably by increasing m. Hence, we can widen the difference between $m_{La}(\theta,\phi;\theta)$ and $m_{La}(\theta,\phi;\phi)$ by using a large array.

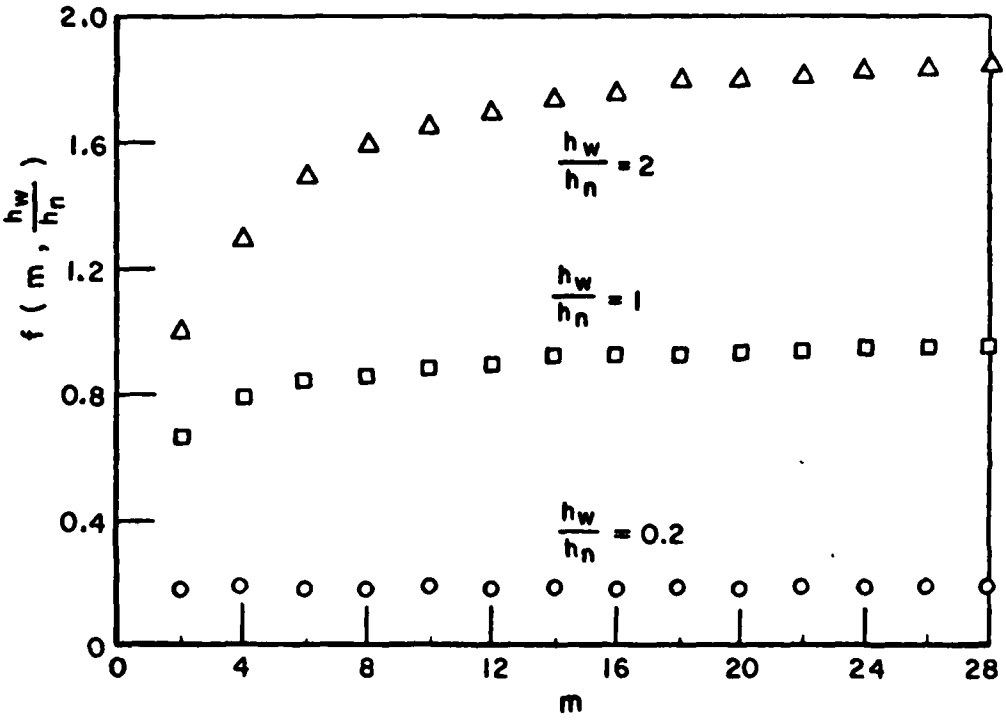

Fig. 4-5--$f(m,h_w h_n^{-1})$ vs. m.

The difference in the magnitudes of $|m_{La}(\theta,\phi;\theta)|$ and $|m_{La}(\theta,\phi;\phi)|$ can be best indicated by the ratio

$$20 \log \left| \frac{m_{La}(\theta,\phi;\phi)}{m_{La}(\theta,\phi;\theta)} \right| \triangleq \text{D.F.}$$

which we may call the discrimination figure (D.F.) because it shows the extent that the processor favors one signal and suppresses another signal. The D.F. for the detector using a 4-element array with spacing $d = 0.5\lambda$ is shown in Fig. 4-6. The incident angle for the interfering signal is 45^o. As can be seen, the D.F. is usually quite high if the separation between θ and ϕ is large, but decreases sharply as θ get closer to ϕ. Ultimately, this figure goes to zero at $\theta=\phi$, because $m_{La}(\theta,\phi;\theta)$ and $m_{La}(\theta,\phi;\phi)$ become equal when $\theta=\phi$. For a constant m, the D.F. changes with the antenna spacing d. Figure 4-7 shows a comparison of the D.F. for $d = 0.5\lambda$ and for $d = 0.75\lambda$ given m=2. A plot of this figure, given $\theta=60^o$ and $\phi=45^o$, of a 4-element array detector vs h_w/h_n is shown in Fig. 4-8. The quantities $|m_{La}(\theta,\phi;\theta)|$ and $|m_{La}(\theta,\phi;\phi)|$ increase with $h_w|h_n$ at different rates. Since the denominator in the expression of D.F. increases faster with $h_w|h_n$ than the numerator, the D.F. declines as $h_w|h_n$ increases. This indicates that the more internal noise, the poorer is the figure.

To broaden the study of the directional characteristics of the detection system, we also examine the behavior of $m_{La}(\theta,\phi;\hat{\theta})$ at an arbitrary angle $\hat{\theta}$. In order to compare easily the treatment of the signal a(t) from $\hat{\theta}$ with that of the same signal from the desired angle θ, we study the normalized ratio defined as follows:

$$F(\theta,\phi;\hat{\theta}) = 20\cdot\log\left|\frac{m_{La}(\theta,\phi;\hat{\theta})}{m_{La}(\theta,\phi;\theta)}\right|$$

For a given θ and ϕ, the $F(\theta,\phi;\hat{\theta})$ vs. $\hat{\theta}$ plot shows relative angular response of the system to the testing signal a(t) from an arbitrary angle $\hat{\theta}$.

Several typical curves of $F(40^o,\phi;\hat{\theta})$ vs. $\hat{\theta}$ of a 4-element array processor are shown in Figs. 4-9 through 4-12. The spacing d for the array is 0.5λ and h_w/h_n is set equal to 0.2. The incident angle ϕ for the interference in Fig. 4-9 is 85^o. The figure shows that $F(40^o,80^o;\hat{\theta})$ reaches its maximum at $\hat{\theta}=\phi$ and becomes a relative minimum at $\hat{\theta}=\phi$. But $F(\theta,\phi;\hat{\theta})$ does not always behave in this manner. In Fig. 4-10, where $\phi=45^o$, the θ which equals the incident angle for the desired signal does not correspond to the maximum, nor does that for the interference correspond to a relative minimum. Before giving an explanation for this, we show the response curves for systems using larger antenna arrays in Fig. 4-11 and Fig. 4-12. The spacing for each system is 0.5λ. In Fig. 4-11, where m=8, the discrimination figure increases to the neighborhood of 20 dB. In Fig. 4-12, where m=12, $F(40^o, 45^o; \hat{\theta})$ reaches the peak value near $\hat{\theta}=\theta$ and becomes a relative minimum at $\hat{\theta}=\phi$ even though the separation between θ and ϕ is only 5^o.

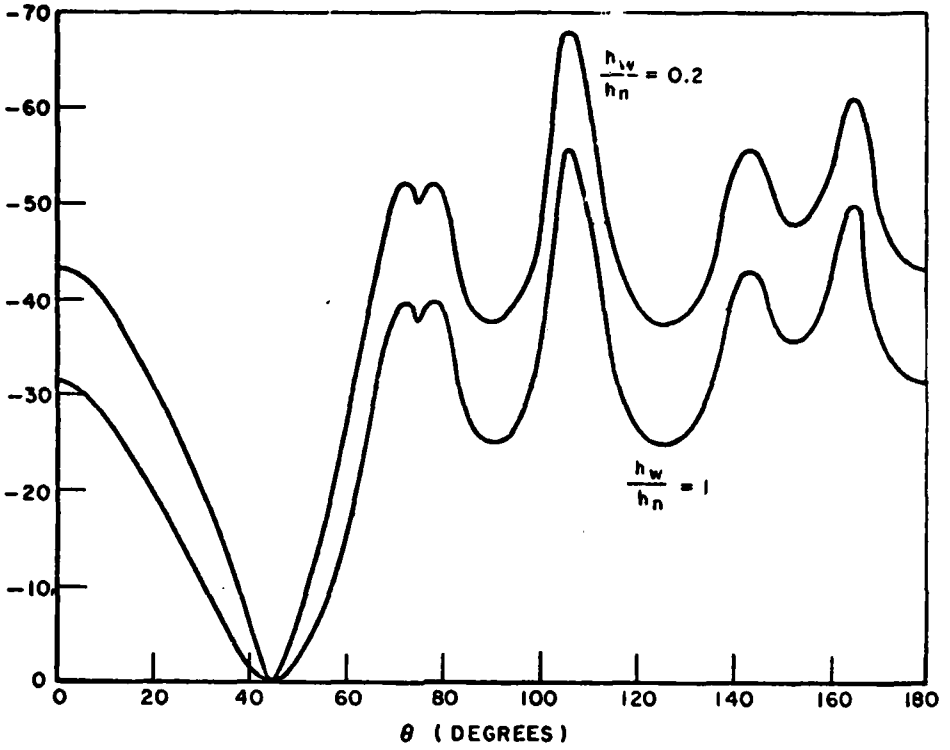

Fig. 4-6--Discrimination figure given m=4, d= $\frac{\lambda}{2}$ and $\phi = 45^{o}$.

For a given θ and ϕ, the conditions for $F(\theta,\phi;\hat{\theta})$ to be minimum can be found from Eq. (4-12). The absolute minimum of $F(\theta,\phi;\hat{\theta})$ is $-\infty$ dB which occurs if

$$\cos \frac{m-1}{2} \omega(\hat{\tau}-\tau) = 0$$

or

$$\frac{\sin \frac{m}{2} \omega(\hat{\tau}-\tau)}{\sin \frac{\omega}{2} (\hat{\tau}-\tau)} - \frac{1}{m + \frac{h_w}{h_n}} \frac{\sin \frac{m}{2} \omega(\tau-\nu)}{\sin \frac{\omega}{2} (\tau-\nu)} \cdot \frac{\sin \frac{m}{2} \omega(\hat{\tau}-\nu)}{\sin \frac{\omega}{2} (\hat{\tau}-\nu)} = 0$$

Obviously, these two conditions are not automatically satisfied when $\theta=\phi$. The relative angular response at $\hat{\theta}=\theta$ is the maximum for the given incident angles if

$$|m_{La}(\theta,\phi;\hat{\theta})| \leq |m_{La}(\theta,\phi;\theta)|$$

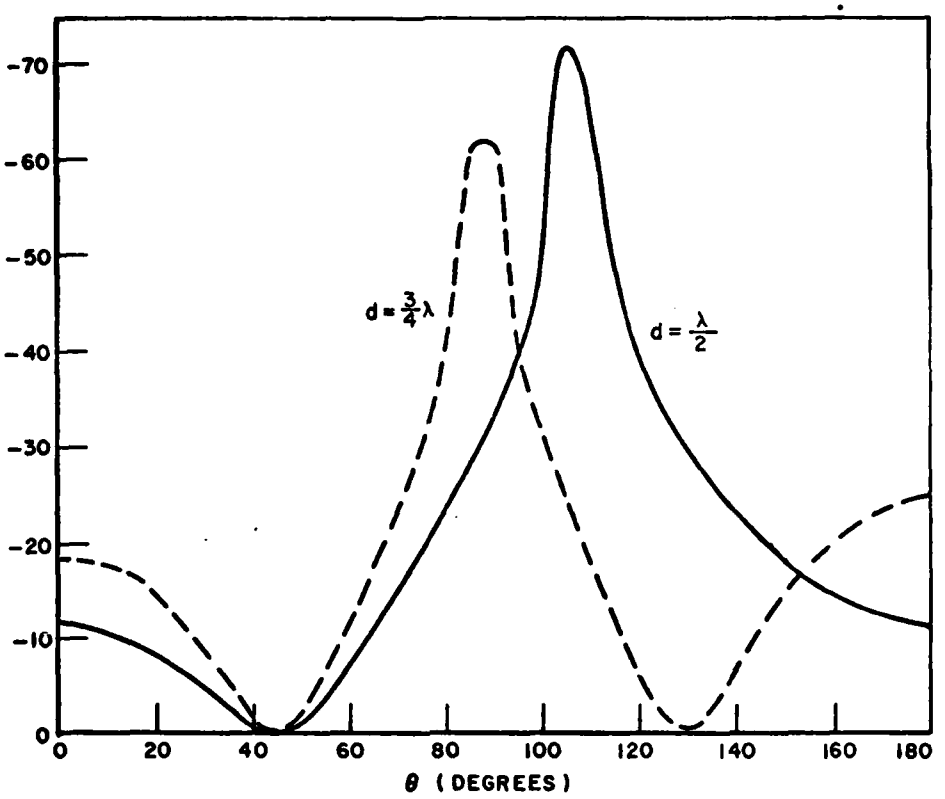

Fig. 4-7--Discrimination figure given m=2, $\phi=45^{o}$ and $h_n h_w^{-1}=0.2$.

for all $\hat{\theta}$'s. From Eq. (4-12) we find that the condition given above is satisfied if

$$\sin \frac{m}{2} \omega(\tau-\nu) = 0 \qquad (4\text{-}21)$$

where $\tau \neq \nu$(i.e., $\theta \neq \phi$). It is interesting to point out that this condition also makes the response curve become the absolute minimum ($-\infty$ dB) at $\theta=\phi$.

Since $m_{La}(\theta,\phi;\theta)$ is equal to the component contributed to L(R) by the signal a(t) from the desired source, large $|m_{La}(\theta,\phi;\theta)|$ will reduce the influence of the interference on making decisions. The fact that each curve in Fig. 4-10 through Fig. 4-12 fails to assume the maximum value at $\theta=\theta$ indicates that the condition given in Eq. (21) is not satisfied for each corresponding detector.

The optimum system is assumed to operate with one desired source and one interfering source. The incident angle for the desired signal is θ. The angular response curves shown in Fig. 4-9 through Fig. 4-12 suggest that it might be possible for a certain detector

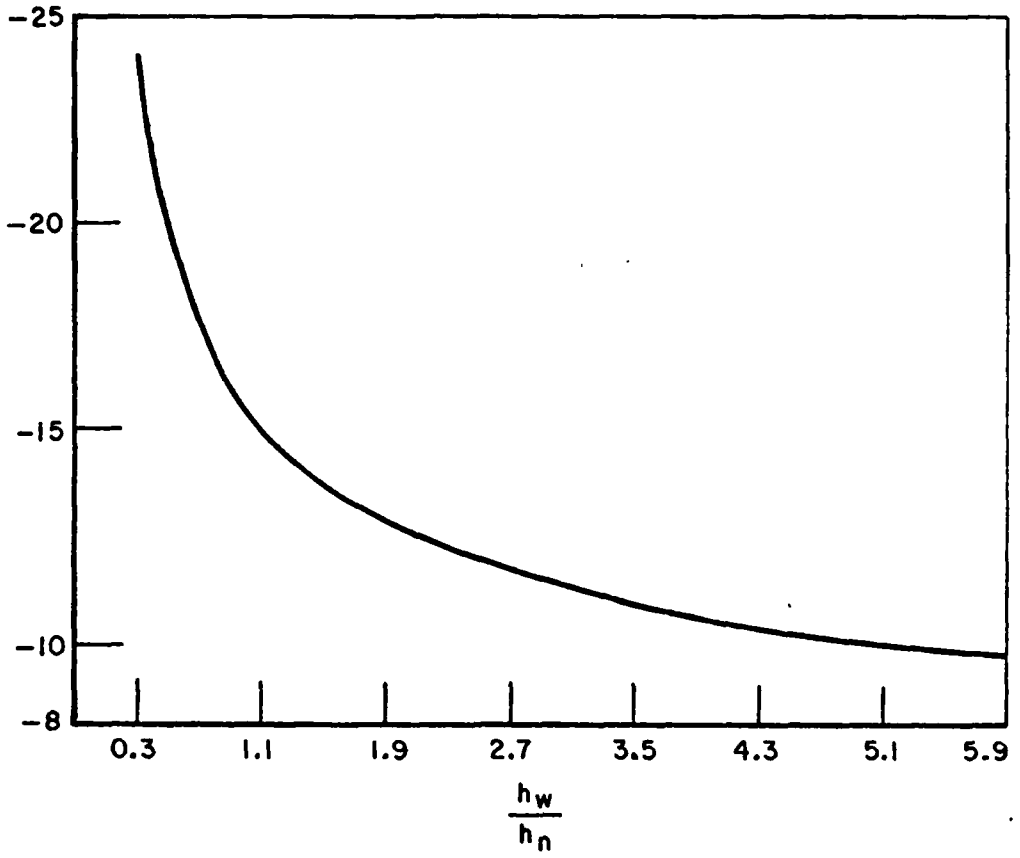

Fig. 4-8--Discrimination figure vs h_w/h_n given m=4, d= $\frac{\lambda}{2}$, $\theta=60^0$ and $\phi=45^0$.

to be optimum for two desired angles. This is indeed true if the second desired source also transmits the binary signals of the same waveforms. This will be shown by an example given in Section IV.F.

D. The Probability of Error

The discussion so far concerns the nature of how the optimum detection system treats the signal a(t) from different incident angles. With this background we next examine the system performance. For a digital communication system, the performance of the system is judged mainly by its ability to make correct decisions. For this reason, the technique of minimizing $P_\varepsilon(\eta_0)$ defined in Eq. (3-32) is investigated. As will become clear, minimization will involve choosing the total number of antennas and the spacing d used by the antenna array. In this section, we assume that the interfering signal is a white noise process with spectral height h_n. The desired binary signals are assumed biphase modulated in the sense that $e_a(t)=-e_b(t)$.

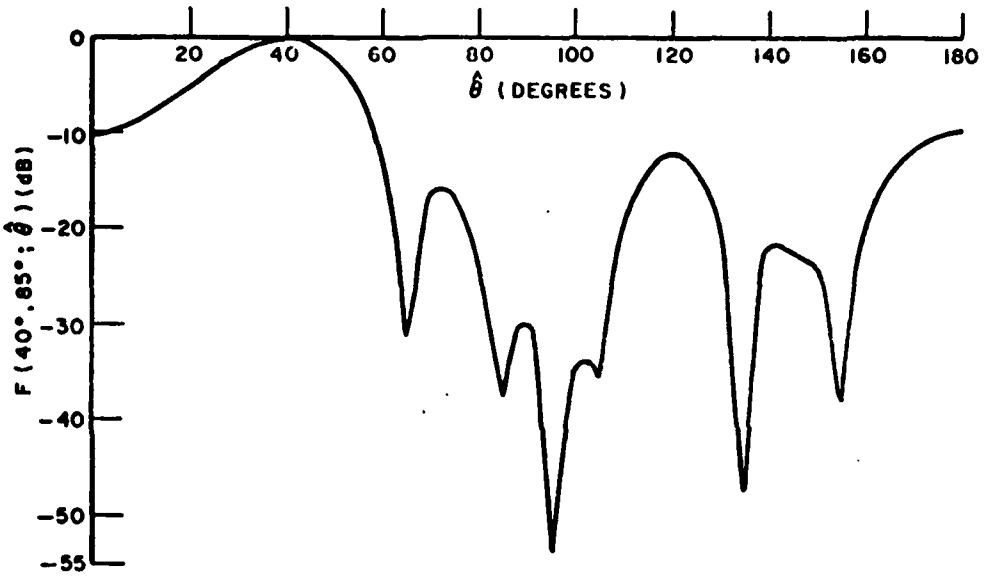

Fig. 4-9--$F(40^0,45^0;\hat{\theta})$ vs. $\hat{\theta}$ given m=4, d= $\frac{\lambda}{2}$ and h_w/h_n = 0.2

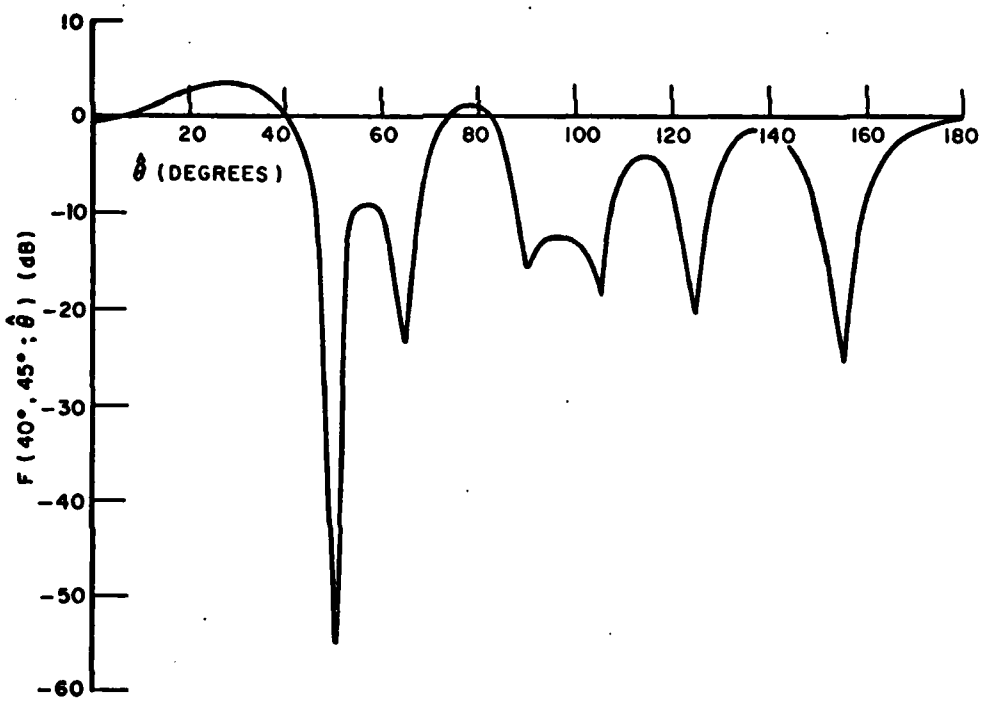

Fig. 4-10--$F(40^0,45^0;\hat{\theta})$ vs. $\hat{\theta}$ given m=4, d= $\frac{\lambda}{2}$ and h_w/h_n = 0.2.

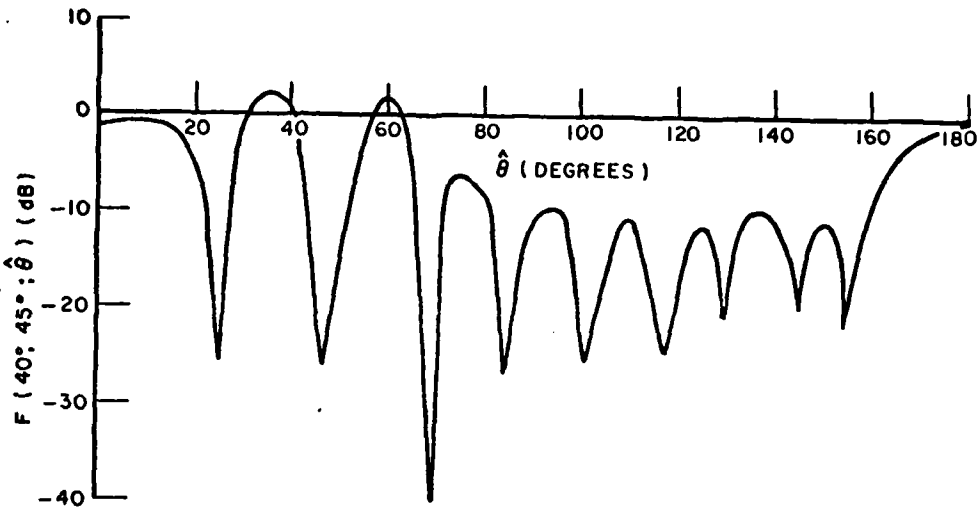

Fig. 4-11--$F(40^0,45^0;\hat{\theta})$ vs. $\hat{\theta}$ given m=8, d= $\frac{\lambda}{2}$ and h_w/h_n=0.2

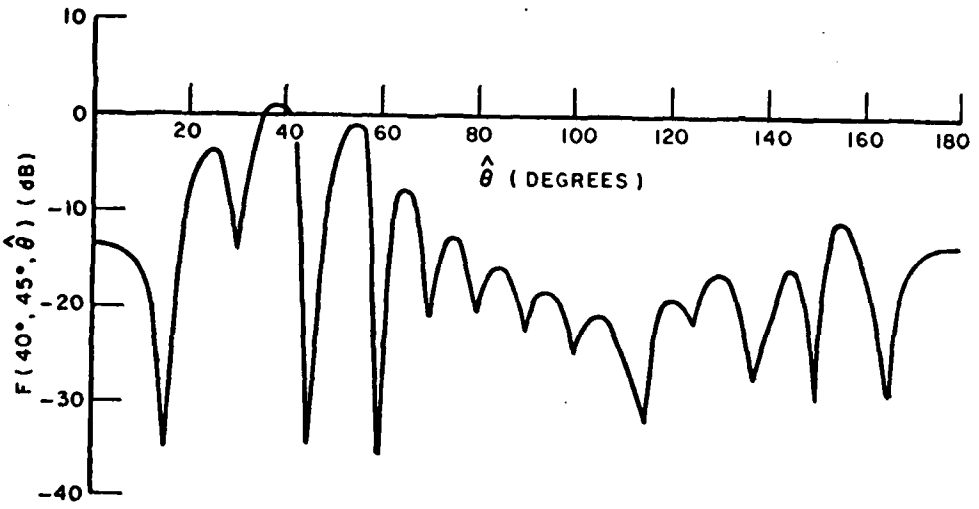

Fig. 4-12--$F(40^0,45^0;\hat{\theta})$ vs. $\hat{\theta}$ given m=12, d= $\frac{\lambda}{2}$ and $h_w h_n^{-1}$=0.2.

Hence, the difference of the means of the processor output L(R) under hypotheses H_b and H_a is equal to

$$m_{Lb}-m_{La} = \left\{ m - \frac{1}{m + \frac{h_w}{h_n}} \cdot \frac{\sin^2 \frac{m}{2}\omega(\tau-\nu)}{\sin^2 \frac{\omega}{2}(\tau-\nu)} \right\} \cdot \int_{-T}^{T} \frac{[e_b(t)-e_a(t)]^2}{2}\, dt$$

where

$$\omega(\tau-\nu) = 2\pi \frac{d}{\lambda} (\cos\theta - \cos\phi)$$

A convenient figure for showing how badly the interference and noise are for this problem is the ratio*

$$(S/N) \triangleq \frac{\int_{-T}^{T} a^2(t)dt}{h_w + h_n} = \frac{\int_{-T}^{T} b^2(t)dt}{h_w + h_n}$$

which in fact is a signal energy to the noise power density ratio. By making use of the assumption given in Eq. (4-19), we may write that

$$(4\text{-}22) \qquad h_w = \frac{1}{(S/N) \cdot \left(1 + \frac{h_n}{h_w}\right)}$$

This equation enables us to specify h_w in terms of the spectral height ratio h_w/h_n and the quantity (S/N).

We now consider the detection system which used a 4-element array and is designed for $\theta=55^0$ and $\phi=45^0$. The array spacing d is 0.5λ. Table 4-1 shows P_F, P_D and P_ε vs the ratio η/σ_L (η is the threshold setting). This system is assumed to operate under the conditions that (S/N) = 1.78 (2.5 dB) and h_n is five times higher than h_w. The spectral height for the internal white noise is assumed equal to 0.0093. From Table 4-1 we see that the probability of making incorrect decisions assumes its lowest value 0.6846×10^{-3} at $\eta = 0$ which agrees with Eq. (3-30) because m_{La} is equal to $-m_{Lb}$ here. To

*The notation (S/N) does not imply the ratio is the signal-to-noise ratio.

reduce the detection error $P_\varepsilon(\eta_0)$, it is clear from Eq. (3-31) that we should increase

$$(4\text{-}23) \qquad \frac{m_{Lb}-m_{La}}{\sigma_L} = 2\left\{\frac{1}{h_w}\left[m - \frac{1}{m + \frac{h_w}{h_n}} \cdot \frac{\sin^2 \frac{m}{2}\,\omega(\tau-\nu)}{\sin^2 \frac{\omega}{2}(\tau-\nu)}\right]\right\}^{\frac{1}{2}}$$

The value for $(m_{Lb}-m_{La})\sigma_L^{-1}$ may be increased by adjusting the spacing d or by varying m as indicated by the equation itself. A plot of $(m_{Lb}-m_{La})\sigma_b^{-1}$ vs m is shown in Fig. 4-13 for three different values of h_w/h_n. The angles θ and ϕ are assumed 55^0 and 45^0, respectively. In plotting this figure, we also let (S/N) = 1.78 and d = 0.5λ. When h_w/h_n = 0.2, $(m_{Lb} - m_{La})\sigma_L^{-1}$ at m=6 is about 10.6, which is higher than the value at m=4. Hence, we expect that the detection error $P_\varepsilon(\eta_0)$ when m=6 would be lower than 0.6846×10^{-3}. In fact, $P_\varepsilon(\eta_0)$ for m=6 is 0.4640×10^{-7}.

TABLE 4-1
P_F, P_D and $P_r(\varepsilon)$ vs. η/σ_L.

η/σ_L	P_F		P_D		P_ε	
-5.00	.96388233E	0	.10000000E	1	.4819E	0
-4.00	.78745639E	0	.10000000E	1	.3937E	0
-3.00	.41981232E	0	.10000000E	1	.2099E	0
-2.00	.11460924E	0	.10000000E	1	.5740E	-1
-1.00	.13818979E	-1	.99998689E	0	.6916E	-2
0.00	.68460932E	-3	.99931550E	0	.6046E	-3
1.00	.13207964E	-4	.98618102E	0	.6916E	-2
2.00	.98379510E	-7	.88539076E	0	.5730E	-1
3.00	.27808902E	-9	.58018768E	0	.2099E	0
4.00	.29586578E	-12	.21254361E	0	.3937E	0
5.00	.11784304E	-15	.36117673E	-1	.4987E	0

The internal noise degrades the error rate performance. To show this, curves of $P_\varepsilon(\eta_0)$ vs h_w/h_n for the detectors (55^0, 45^0) with m=4 and 6 respectively are shown in Fig. 4-14. As can be seen from Eq. (4-22), the spectral height h_w increases with the ratio h_w/h_n if the quantity (S/N) is constant. In plotting Fig. 4-14 we have let (S/N) = 1.78 which is about 2.5 dB. In Fig. 4-15, we show the curves of $P_\varepsilon(\eta_0)$ vs (S/N) for the detector (55^0,45^0) using a 4-element array. The antenna spacing is again equal to 0.5λ. It can be seen from these curves that the internal noise degrades the error rate performance drastically.

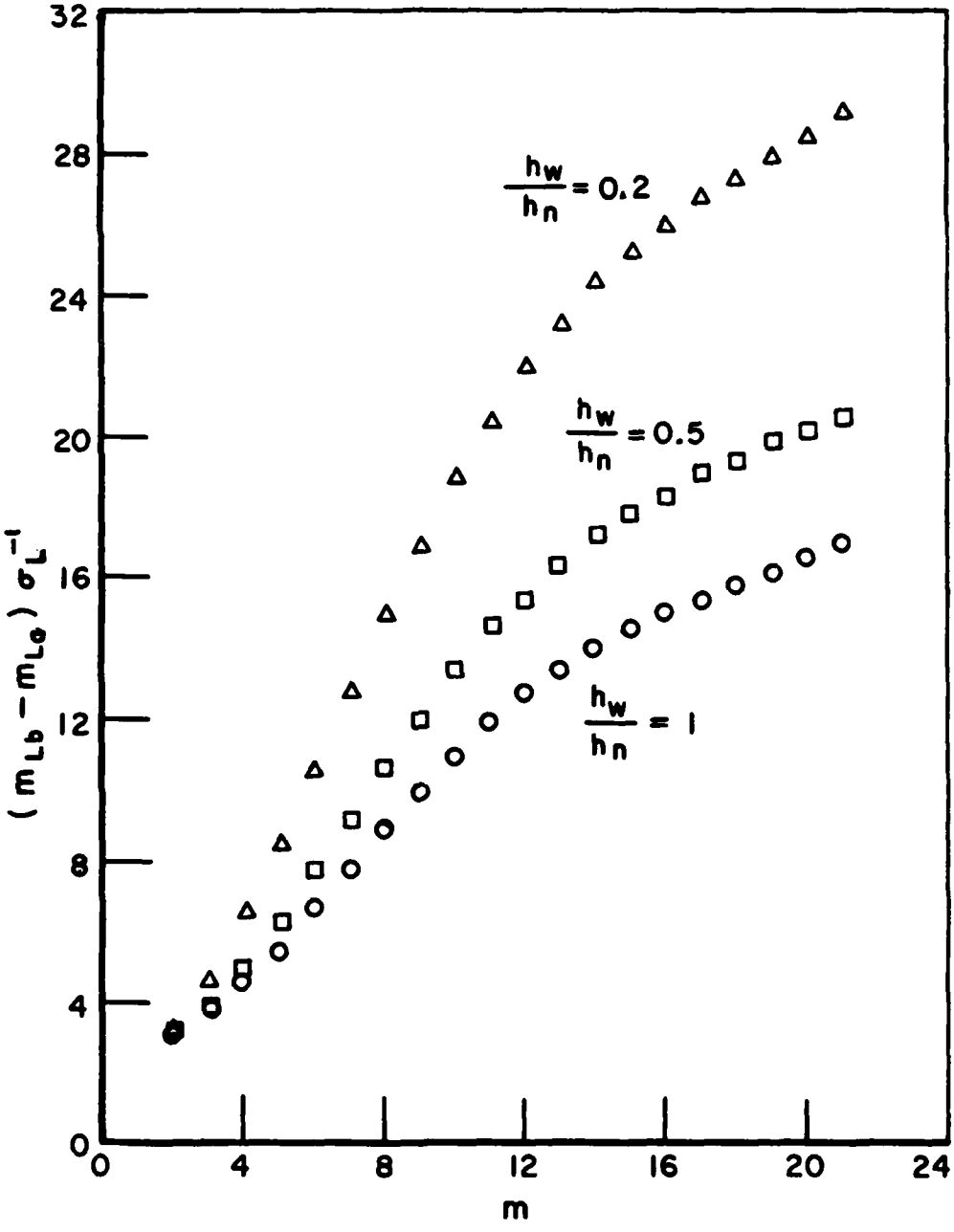

Fig. 4-13--$(m_{La}-m_{Lb})\sigma_L^{-1}$ vs. m given $\theta=55^0$, $\phi=45^0$, (S/N)=1.78 and $d=0.5\lambda$.

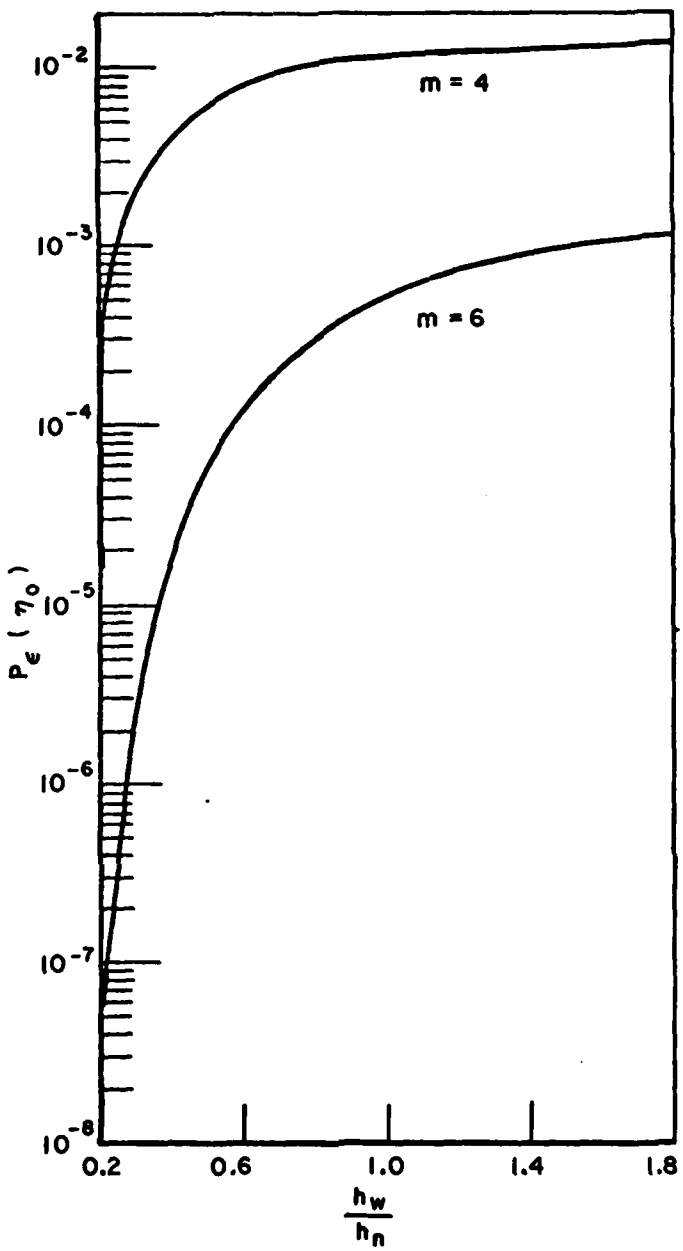

Fig. 4-14--$P_\epsilon(\eta_0)$ vs. h_w/h_n given $\theta=55^0$, $\phi=45^0$, (S/N)=1.78 and d = 0.5λ.

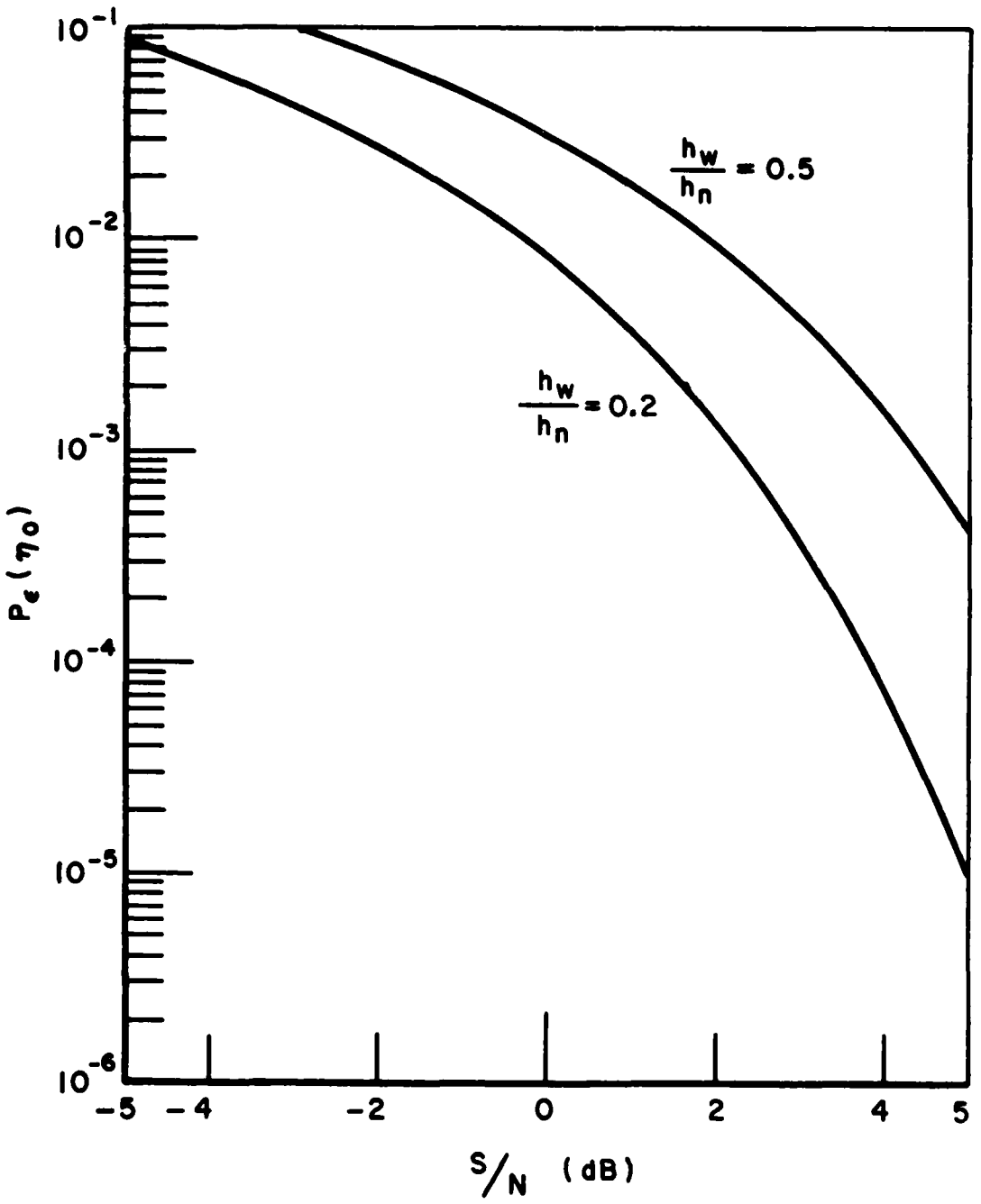

Fig. 4-15--$P_\epsilon(\eta_0)$ vs. (S/N) given $\theta=55^o$, $\phi=45^o$, m=4 and d =0.5λ.

We have shown that it is necessary to increase $(m_{Lb}-m_{La})\sigma_L^{-1}$ in order to reduce $P_\varepsilon(\min)$. For the example given above, we accomplished this by increasing the total number of antennas. But increasing m is not the only way. As a matter of fact, the best approach to this problem is to choose the proper spacing for the elements of the antenna array.

E. The Optimum Spacing

It has been pointed out earlier that for the case when the interference is a Gaussian white noise process $|m_{La}|$ becomes equal to its upper bound if θ,ϕ, m and d are related by Eq. (4-15). Solving Eq. (4-15) for d, one finds the solution is many-valued because k can be any integer. We define the optimum spacing d_{op} as the solution when k=1 is chosen, i.e.,

$$d_{op} \triangleq \frac{\lambda}{m|\cos\theta - \cos\phi|}, \quad \cos\theta - \cos\phi \neq 0. \tag{4-24}$$

Since Eq. (4-15) is not valid if $\theta=\phi$, there does not exist an optimum spacing when $\theta=\phi$.

Equation (3-32) indicates that the error $P_\varepsilon(\eta_0)$ decreases as $(m_{Lb}-m_{La}) \cdot h_w^{-1}$ increases, regardless of the power spectrum of the interfering signal or the waveforms for the desired signals. When the interference is a white noise process, we conclude from Eq. (4-23) that the smallest value for $P_\varepsilon(\eta_0)$ is obtained if d is equal to the optimum spacing. The reason is that the quantity $(m_{Lb}-m_{La})\sigma_L^{-1}$ has the peak value at this particular spacing.

Referring to Eq. (3-14), we see that the amount of time-shifting on s(t) and the amount of time-delaying on r(t) depend on the incident angles and the antenna spacing. When the spacing is changed, we must adjust each delay line to provide the correct delay.

Referring to Eq. (4-23), we find that $(m_{Lb}-m_{La})\sigma_L^{-1}$ may be rewritten as

$$\frac{m_{Lb}-m_{La}}{\sigma_L} = 2\left\{\frac{1}{h_w}\left[m - \frac{1}{m+\frac{h_w}{h_n}} \cdot \frac{\sin^2\left(\frac{d}{d_{op}}\pi\right)}{\sin^2\left(\frac{d}{d_{op}}m\pi\right)}\right]\right\}^{\frac{1}{2}}$$

where the ratio d/d_{op} may be called the normalized spacing. In order to compare the error rate performance for systems optimized for different spacings, several curves of $P_\varepsilon(\eta_0)$ vs. d/d_{op} are shown in Fig. 4-16. In plotting these curves, we let (S/N) = 1.78

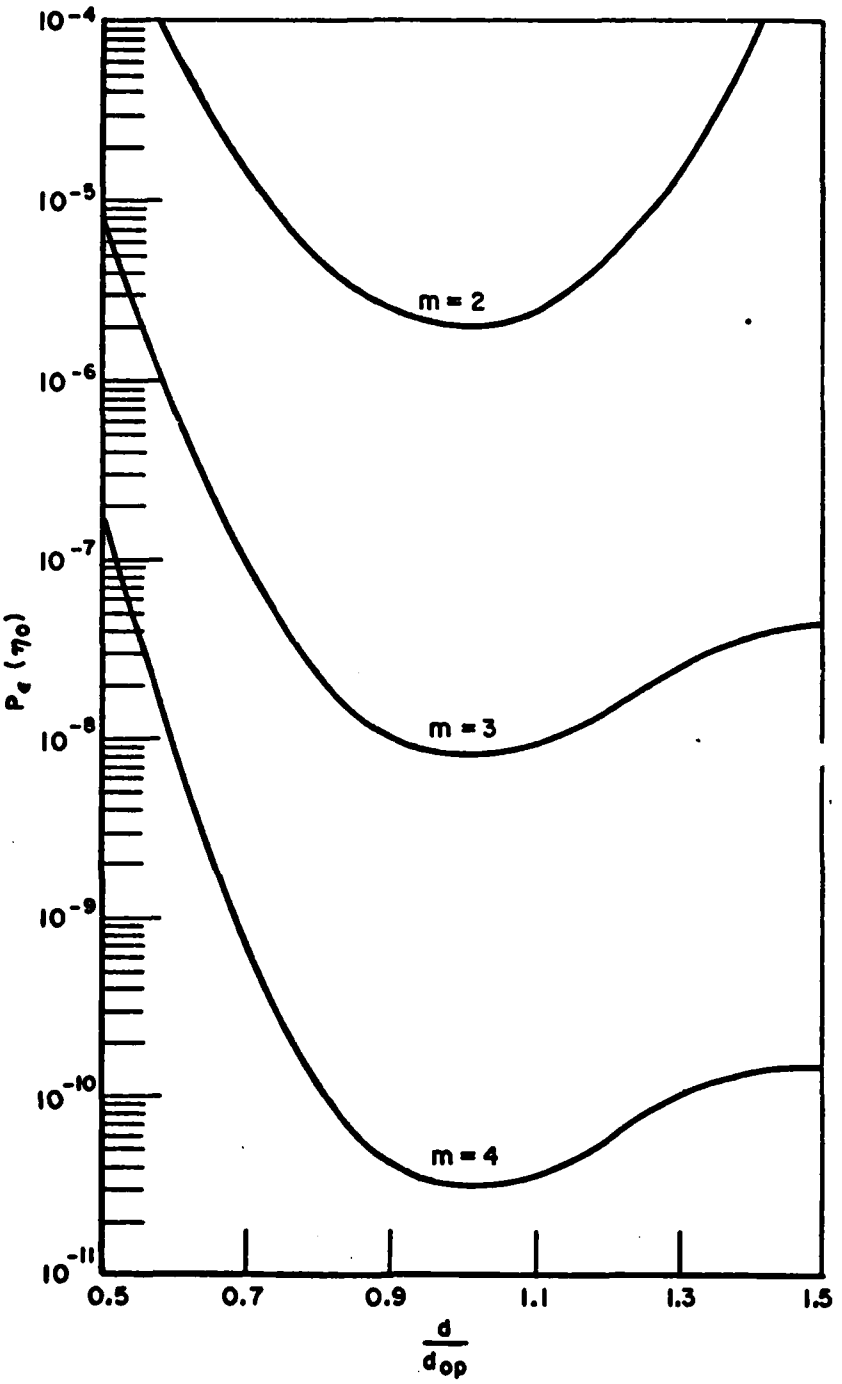

Fig. 4-16--$P_\varepsilon(\eta_0)$ vs. d/d_{op} given (S/N) = 1.78 and h_w/h_n = 0.2.

and $h_w/h_n = 0.2$. In Fig. 4-16, each curve reaches the minimum at $d/d_{op} = 1$ as we have expected. The error $P_\varepsilon(\eta_0)$ at $d/d_{op} = 1$ for $m = 3$ is almost one thousand times lower than the value at 0.5. This clearly points out that the spacing d plays a very important role in the error rate performance. We shall use $P_\varepsilon(\min)$ to denote the error rate for the system which is designed for an optimum spacing.

To show the lowest detection error available to a given array size, the curves of $P_\varepsilon(\min)$ vs. (S/N) for m=2 through 5 given $h_w/h_n = 0.2$, 0.5 and 1.0 are shown in Fig. 4-17 through Fig. 4-19. These curves are valid for arbitrary incident angles θ and ϕ as long as the spacing used by each system is equal to the optimum spacing for the given θ and ϕ. The reason for this is given in the next section.

F. Arbitrary Power Spectrum

The optimum spacing d_{op} defined by Eq. (4-24) is found by examining the behavior of $m_{La}(\theta,\phi;\hat{\theta})$ under the assumption that the interfering signal is a white noise process. In this section, we shall show that this particular spacing also optimizes the error rate performance even though the interfering signal is characterized by a different power spectrum. The signal waveforms considered in this section are assumed to have the general expressions as given in Eq. (4-1) and Eq. (4-2).

For an arbitrary power spectrum, the difference between the means of the test function L(R) under hypotheses H_b and H_a may be derived from Eq. (3-14). The result may be written as

(4-25)

$$m_{Lb} - m_{La} \triangleq E\{L(R)|H_b\} - E\{L(R)|H_a\}$$

$$= \sum_{i=1}^{m} \int_{-T}^{T} s_i^2(t_i)dt - \sum_{i,j=1}^{m} \iint_{-T}^{T} s_i(t_i)s_j(z_j)\cdot\Psi(t,z)\cdot dt\, dz$$

$$= \sum_{i=1}^{m} \int_{-T}^{T} s_i^2(t_i)dt - \sum_{\ell=1}^{\infty} \frac{1}{m + \frac{h_w}{\lambda_\ell - h_w}} \left\{ \int_{-T}^{T} \sum_{i=1}^{m} s_i(t_i)\phi_\ell(t)dt \right\}^2$$

Since the eigenvalues $(\lambda_\ell - h_w)$ are always positive and s(t) and $\phi_\ell(t)$ are real functions, we may write that

(4-26) $$m_{Lb} - m_{La} \leq \sum_{i=1}^{m} \int_{-T}^{T} s_i^2(t_i)dt$$

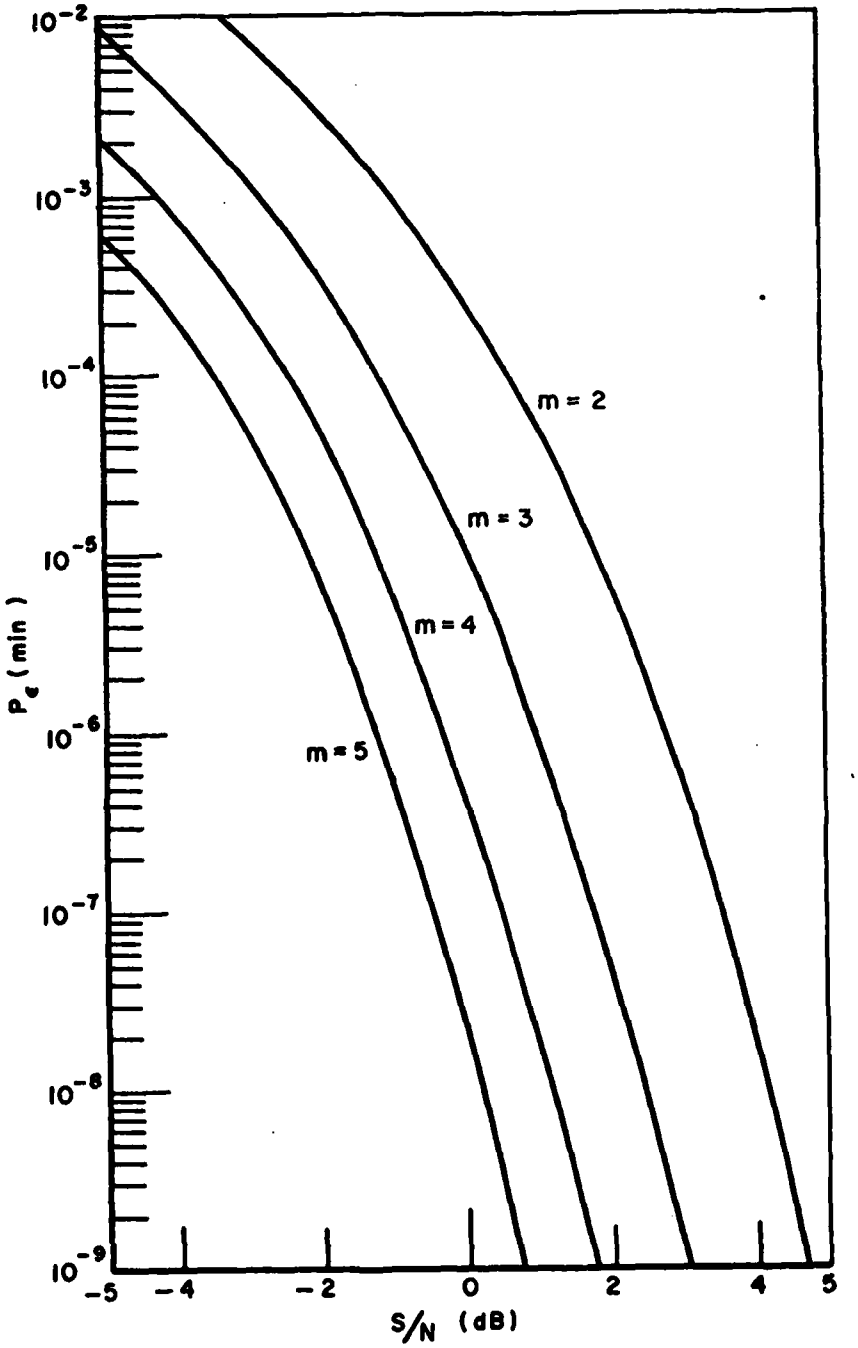

Fig. 4-17--P_ε(min) vs. (S/N) given h_w/h_n = 0.2.

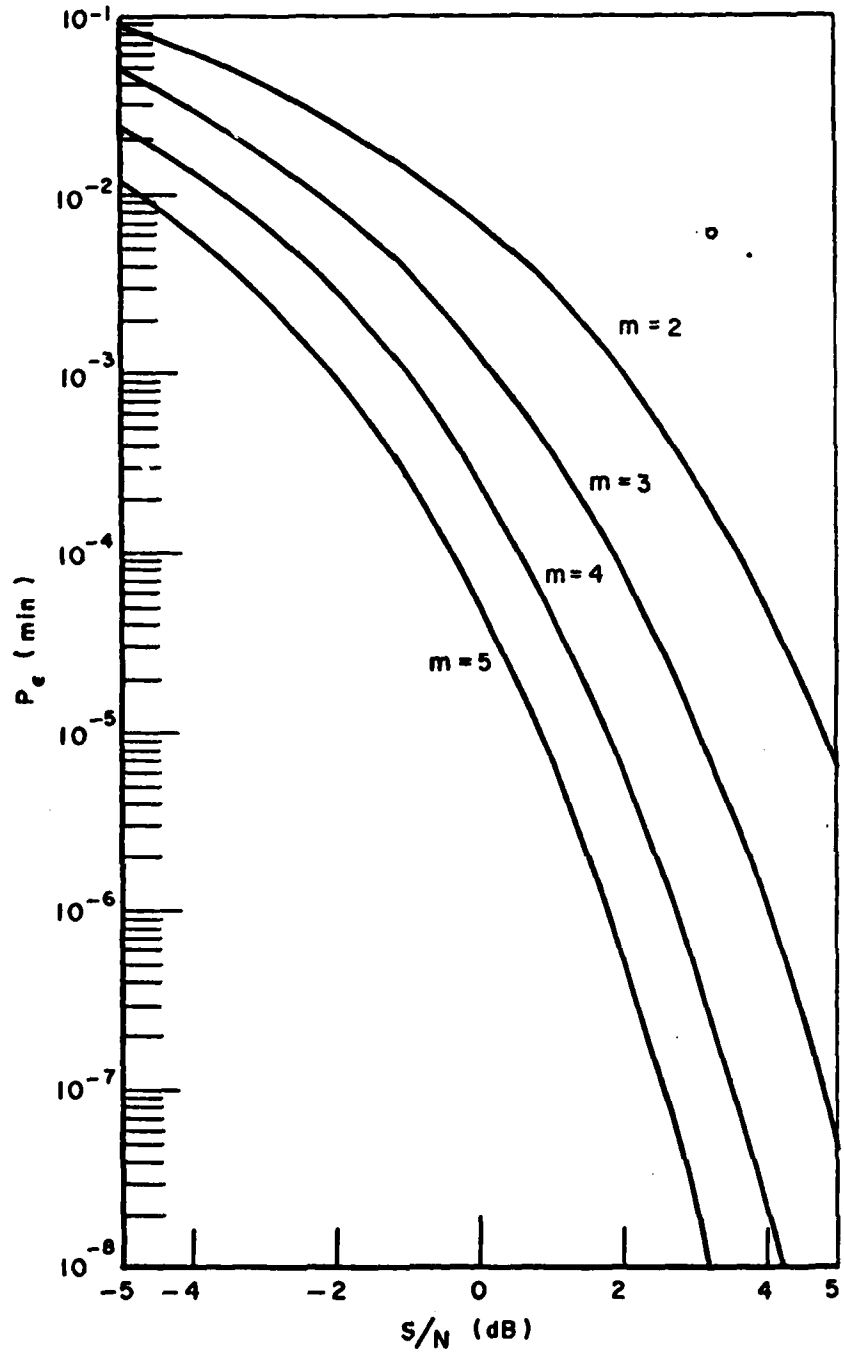

Fig. 4-18--P_ε(min) vs. (S/N) given h_w/h_n = 0.5.

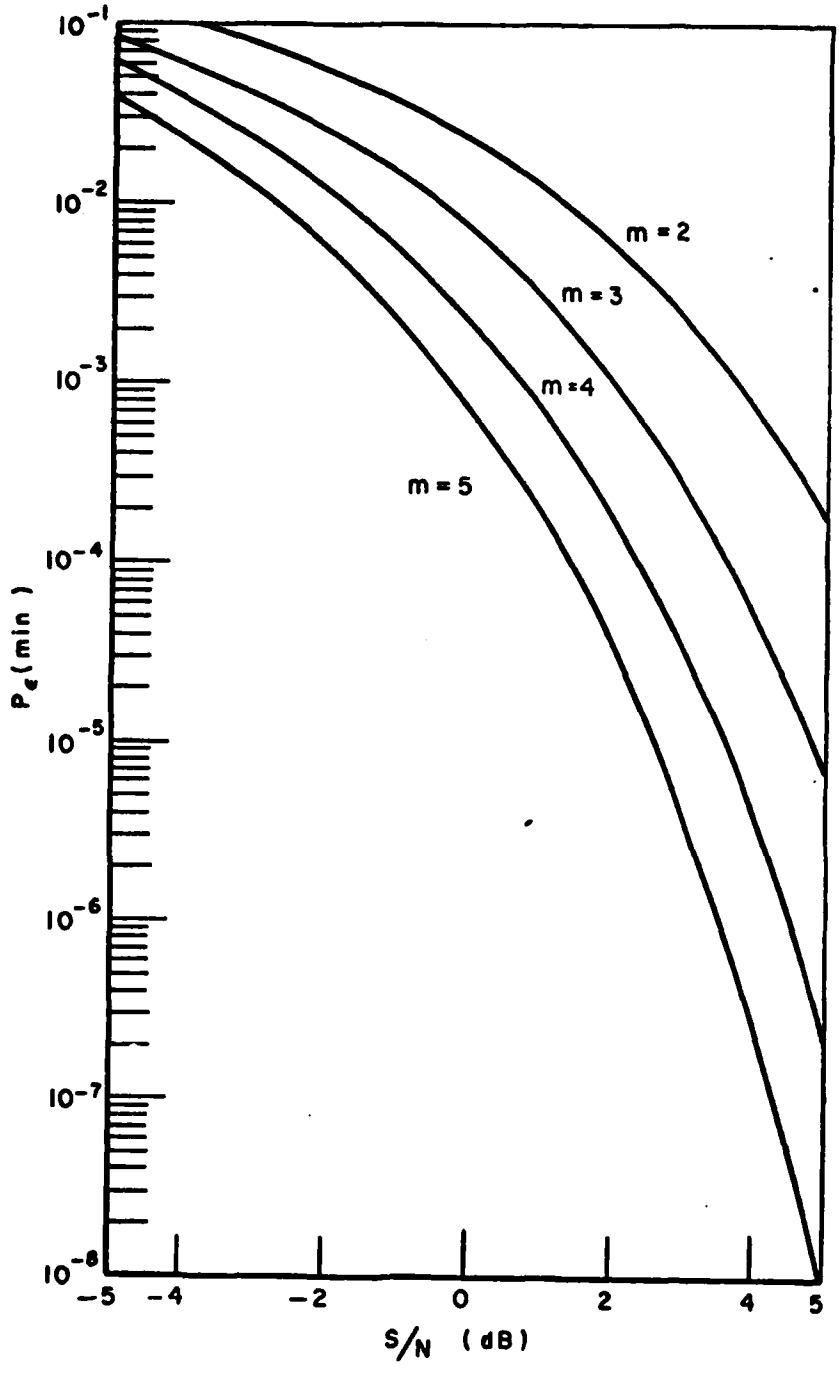

Fig. 4-19--P_ε(min) vs. (S/N) given $h_w/h_n = 1$.

The closed form expression for

$$\sum_{i=1}^{m} s_i^2(t_i)$$

is readily obtained when we replace $\hat{\tau}$ and $e_a(t)$ in Eq. (4-10) by τ and $e(t)$, respectively. Hence,

(4-27)

$$\sum_{i=1}^{m} \int_{-T}^{T} s_i^2(t_i)dt = m \cdot \int_{-T}^{T} \frac{e^2(t)}{2}\, dt + \frac{\sin m\omega(\tau-\nu)}{\sin \omega(\tau-\nu)} \cdot \int_{-T}^{T} \frac{e^2(t)}{2} \cdot \cos\left\{2\omega\left(t - \frac{m-1}{2}\,\nu\right) + 2\phi_s - (m-1)\omega\tau\right\} dt$$

The second term of Eq. (4-27) is much smaller than the first term. Thus the upper bound of $(m_{Lb}-m_{La})$ is approximately equal to

$$\frac{m}{2} \int_{-T}^{T} e^2(t) \cdot dt.$$

When the array is spaced according to Eq. (4-24), we find that

(4-28) $$\sin \frac{m}{2}\,\omega(\tau-\nu) = \sin m\omega(\tau-\nu) = 0$$

As a result, we conclude from Eq. (4-8) that

$$\sum_{i=1}^{m} s_i(t_i) = 0$$

Consequently, the left side of Eq. (4-26) is equal to the right side. Also, the second term of Eq. (4-27) vanishes because $\sin m\omega(\tau-\nu) = 0$. Hence, we obtain

(4-29) $$m_{Lb} - m_{La} = \frac{m}{2} \int_{-T}^{T} e^2(t)\, dt$$

which is very close to the highest value of $(m_{Lb}-m_{La})$ we can get. Substituting Eq. (4-29) into Eq. (3-32), we obtain the detection error

$$(4\text{-}30) \qquad P_\varepsilon(\min) = \operatorname{erfc}_*\left(\frac{1}{2}\sqrt{\frac{m}{h_w}\int_{-T}^{T}\frac{e^2(t)}{2}\,dt}\right)$$

This is the lowest error rate available for a given array size.

Equation (4-30) does not contain the incident angles θ and ϕ. This implies that this error rate does not depend on the angular separation between the interfering source and the desired signal source. The optimum spacing is a function of θ, ϕ and m. To obtain this lowest error rate, we need to change the antenna spacing and adjust the delay lines when the incident angles θ and ϕ vary.

We also notice that Eq. (4-30) does not contain the parameter which characterizes the interfering signal. This points out that this lowest possible error rate is independent of the power spectrum of the interfering signal. The reason is that at this particular antenna spacing the interfering signal is completely cancelled by the optimum processor. A formal proof of this statement will be given in Chapter VI.

In plotting the curves in Fig. 4-17 through Fig. 4-19, we have used the optimum spacing for the antenna elements. Hence, these curves are also valid for other types of power spectrums if the desired signals are biphase modulated in the sense that $e_a(t)=-e_b(t)$.

If we let the signal $a(t) = 0$, then Eq. (4-1) and Eq. (4-2) represent an on-off keying binary signals. The structure for the optimum processor becomes simpler as can be seen by the test statistics

(4-31)

$$L_o(R) \triangleq \sum_{i=1}^{m}\int_{-T}^{T} r_i(t_i)b_i(t_i)dt - \sum_{i,j=1}^{m}\iint_{-T}^{T} r_i(t_i)b_j(z_j)\cdot$$

$$\cdot\,\Psi(t,z)\cdot dt\,dz,$$

which is obtained by replacing s(t) in Eq. (3-14) by b(t). Accordingly, the threshold that minimizes the detection error is

$$\eta_o = \frac{1}{2}m_{Lb}$$

The lowest error rate for a given array size may be derived from Eq. (4-30). We find that

$$(4\text{-}32) \qquad P_\varepsilon(\min) = \operatorname{erfc}_* \left(\frac{1}{2} \sqrt{\frac{m}{h_w} \int_{-T}^{T} \frac{e_b^2(t)}{2} \, dt} \right)$$

Hence, for this on-off binary signals detector, the error rate performance can be made as good as the biphase-binary detector by increasing the amplitude of the signal b(t).

It was pointed out in Section IVC that some detectors may be optimum for two desired sources if they transmit the same type of binary signals. We now consider a detection system which is designed to be optimum for $\theta=\cos^{-1}(0.457)$, $\phi=45^{o}$, m=4 and $d/\lambda = 1$. We find that the conditions given in Eq. (4-28) are satisfied by the data given above. Hence we obtain

$$(4\text{-}33) \qquad m_{Lb} - m_{La} = 2 \int_{-T}^{T} e^2(t) dt$$

When the same binary signals propagate into the array for the same detection systems from angle $\theta=\cos^{-1}(0.957)$, we find that Eq. (4-28) is again satisfied. Hence, the difference of the means is identical to Eq. (4-33). Apparently, the same system provides the same error rate performance to two incident angles.

CHAPTER V
THE DETECTOR FOR BINARY SIGNALS HAVING A RANDOM PHASE AND AMPLITUDE

A. The Optimum Processor

This chapter considers the case where the desired signal is no longer assumed to be known exactly, but instead has certain random parameters.

In a realistic situation, there are always at least some parameters characterizing the communication signal that are not known. For instance, in high frequency communication via the ionosphere and in channels employing tropospheric propagation, the signal received usually fluctuates in amplitude and phase due to fading and multipath effects. These effects are usually modeled by assuming certain parameters of the communication signal to be random variables. Signal detection in this case is often referred to as the composite hypothesis - testing problem.

The technique for determining an optimum processor for detecting the binary signals having random parameters is straightforward, because the only new feature is finding $p(R|H_k)$, where k=a or b, when certain parameters are random. For the case when the random parameters have the same statistics on both hypotheses, the likelihood ratio is simply given by

(5-1)

$$L.R. = \lim_{N\to\infty} \frac{P(R|H_b)}{P(R|H_a)}$$

$$= \lim_{N\to\infty} \frac{\int p(R|\Gamma,H_b) \cdot p(\Gamma) \cdot d\Gamma}{\int p(R|\Gamma,H_a) \cdot p(\Gamma) \cdot d\Gamma}$$

where $p(\Gamma)$ is the probability density function for the parameter vector Γ, and $p(R|\Gamma,H_k)$ is the density function of R under hypothesis H_k for a given Γ [22].

In this chapter we consider the binary signals of the form:

(5-2)

$$H_a: \quad a(t) = f \cdot e_a(t) \cdot \cos(\omega_a t + \phi_s)$$

$$H_b: \quad b(t) = f \cdot e_b(t) \cdot \cos(\omega_b t + \phi_s)$$

where the amplitude f is a Rayleigh random variable and the phase ϕ_s is assumed uniformly distributed between $-\pi$ and π.

Three commonly used methods for transmitting binary signals over an additive Gaussian noise channel are on-off keying (ASK), frequency-shift keying (FSK) and phase-shift keying (PSK). It is apparent that the model we have here can be applied to either the ASK or FSK case.

The signals given in Eq. (5-2) may be rewritten as

$$(5\text{-}3) \qquad \begin{bmatrix} a(t) \\ \\ b(t) \end{bmatrix} = x \cdot \begin{bmatrix} u_a(t) \\ \\ u_b(t) \end{bmatrix} - y \cdot \begin{bmatrix} v_a(t) \\ \\ v_b(t) \end{bmatrix}$$

where we define

$$(5\text{-}4) \qquad x \triangleq f \cdot \cos \phi_s$$

$$(5\text{-}5) \qquad y \triangleq f \cdot \sin \phi_s$$

$$(5\text{-}6) \qquad u_k(t) \triangleq e_k(t) \cdot \cos \omega_k t, \quad k = a \text{ and } b,$$

and

$$(5\text{-}7) \qquad v_k(t) \triangleq e_k(t) \cdot \sin \omega_k t \ .$$

x and y are independent zero-mean Gaussian random variables with equal variances, say σ_Γ^2 [23]. Let

$$\Gamma \triangleq \begin{bmatrix} x \\ y \end{bmatrix}$$

then the density function for the random vector Γ may be written as

$$(5\text{-}8) \qquad p(\Gamma) = (2\pi\sigma_\Gamma^2)^{-1} \cdot \exp\left(-\frac{x^2 + y^2}{2\sigma_\Gamma^2}\right).$$

Since $u_k(t)$ and $v_k(t)$ do not contain unknown parameters, they are completely known functions. Moreover, they are 90^o out of phase.

The desired signal may then be considered as the sum of two signals for which the amplitudes are Gaussian random variables.

Under hypothesis H_b, the density of R associated with an m-element antenna array and an N-term Karhunen-Loéve expansion is equal to

$$p(R|H_b) = \frac{1}{2\pi\sigma_\Gamma^2} \iint_{-\infty}^{\infty} p(R|\Gamma,H_b) \cdot e^{-\frac{x^2+y^2}{2\sigma_\Gamma^2}} \cdot dx\, dy \tag{5-9}$$

In Eq. (5-9), the conditional density is given by

$$p(R|\Gamma,H_b) = \lim_{N\to\infty} \frac{\exp\left\{-\frac{1}{2}(R-B)^T \cdot Q \cdot (R-B)\right\}}{\sqrt{(2\pi)^{mN}\,|K|}} \tag{5-10}$$

$$= \lim_{N\to\infty} \frac{1}{\sqrt{(2\pi)^{mN}|K|}} \cdot$$

$$\cdot \exp\left\{-\frac{1}{2} \sum_{i,j=1}^{m} \iint_{-T}^{T} r_i(t)r_j(z) \cdot H_{ij}^{\infty}(t,z) \cdot dt\, dz \right.$$

$$+ \sum_{i,j=1}^{m} \iint_{-T}^{T} r_i(t)b_j(z) \cdot H_{ij}^{\infty}(t,z) \cdot dt\, dz$$

$$\left. - \frac{1}{2} \sum_{i,j=1}^{m} \iint_{-T}^{T} b_i(t)b_j(z) \cdot H_{ij}^{\infty}(t,z) \cdot dt\, dz \right\}$$

From Eq. (5-3), we obtain

$$b_i(t)b_j(z) = x^2 \cdot u_{bi}(t)\, u_{bj}(z) + y^2 \cdot v_{bi}(t)\, v_{bj}(z) \tag{5-11}$$

$$- xy \cdot [u_{bi}(t)\, u_{bj}(z) + v_{Di}(t)\, v_{bj}(z)]$$

In terms of the in-phase and quadrature components of b(t), we may rewrite

(5-12)

$$p(R|\Gamma,H_b) = \lim_{N\to\infty} \frac{e^{L_r(r)}}{\sqrt{(2\pi)^{mN}\,|K|}} \cdot \exp\left\{-x^2 \frac{\alpha_b}{2\sigma_\Gamma^2}\right.$$

$$\left. - y^2 \frac{\beta_b}{2\sigma_\Gamma^2} + xy \frac{\gamma_b}{\sigma_\Gamma^2} + x\, L_{bu}(r) + y L_{bv}(r)\right\}$$

where we define

(5-13)

$$\alpha_b \triangleq \sigma_\Gamma^2 \sum_{i,j=1}^{m} \iint_{-T}^{T} u_{bi}(t) \cdot u_{bj}(z) \cdot H_{ij}^{\infty}(t,z) \cdot dt\, dz$$

$$= \frac{\sigma_\Gamma^2}{h_w} \left\{ \sum_{i=1}^{m} \int_{-T}^{T} u_{bi}^2(t_i)dt - \sum_{i,j=1}^{m} \iint_{-T}^{T} u_{bi}(t_i) \cdot u_{bj}(z_j) \cdot \right.$$

$$\left. \cdot \Psi(t,z) \cdot dt\, dz \right\}$$

(5-14)

$$\beta_b \triangleq \sigma_\Gamma^2 \sum_{i,j=1}^{m} \iint_{-T}^{T} v_{bi}(t) \cdot v_{bj}(z) \cdot H_{ij}^{\infty}(t,z) \cdot dt\, dz$$

$$= \frac{\sigma_\Gamma^2}{h_w} \left\{ \sum_{i=1}^{m} \int_{-T}^{T} v_{bi}^2(t_i)dt - \sum_{i,j=1}^{m} \iint_{-T}^{T} v_{bi}(t_i)v_{bj}(z_j) \cdot \right.$$

$$\left. \cdot \Psi(t,z) \cdot dt\, dz \right\}$$

(5-15)

$$\gamma_b \triangleq \sigma_\Gamma^2 \sum_{i,j=1}^{m} \iint_{-T}^{T} u_{bi}(t)v_{bj}(z) \cdot H_{ij}^{\infty}(t,z) \cdot dt\, dz$$

$$= \frac{\sigma_\Gamma^2}{h_w} \left\{ \sum_{i=1}^{m} \int_{-T}^{T} u_{bi}(t_i)v_{bi}(t_i)dt - \sum_{i,j=1}^{m} \iint_{-T}^{T} u_{bi}(t_i)v_{bj}(z_j) \cdot \right.$$

$$\left. \cdot \Psi(t,z) \cdot dt\, dz \right\}$$

(5-16)

$$L_{bu}(r) \triangleq \sum_{i,j=1}^{m}\sum \iint_{-T}^{T} r_i(t)u_{bj}(z) \cdot H_{ij}^{\infty}(t,z) \cdot dt\, dz$$

$$= \frac{1}{h_w} \left\{ \sum_{i=1}^{m} \int_{-T}^{T} r_i(t_i)u_{bi}(t_i)dt \right.$$

$$\left. - \sum_{i,j=1}^{m}\sum \iint_{-T}^{T} r_i(t_i)\cdot u_{bj}(z_j) \cdot \Psi(t,z) \cdot dt\, dz \right\}$$

(5-17)

$$L_{bv}(r) \triangleq - \sum\sum \iint_{-T}^{T} r_i(t)v_{bj}(z) \cdot H_{ij}^{\infty}(t,z) \cdot dt\, dz$$

$$= - \frac{1}{h_w} \left\{ \sum_{i=1}^{m} \int_{-T}^{T} r_i(t_i)v_{bi}(t_i)dt \right.$$

$$\left. - \sum_{i,j=1}^{m}\sum \iint_{-T}^{T} r_i(t_i)v_{bj}(z_j) \cdot \Psi(t,z) \cdot dt\, dz \right\}$$

and

(5-18) $$L_r(r) \triangleq - \frac{1}{2} \sum_{i,j=1}^{m}\sum \iint_{-T}^{T} r_i(t)\, r_j(z) \cdot H_{ij}^{\infty}(t,z)\, dt\, dz$$

Substituting Eq. (5-12) into Eq. (5-9), yields

(5-19)

$$p(R|H_b) = \frac{1}{2\pi\sigma_\Gamma^2} \lim_{N\to\infty} \frac{e^{L_r(r)}}{\sqrt{(2\pi)^{mN}\,|K|}} \cdot$$

$$\cdot \iint_{-\infty}^{\infty} \exp \left\{ - \frac{1}{2\sigma_\Gamma^2} \left[x^2(\alpha_b+1) + y^2(\beta_b+1) - 2xy \cdot \gamma_b \right.\right.$$

$$\left.\left. - 2x\sigma_\Gamma^2 L_{bu}(r) - 2y\, \sigma_\Gamma^2 L_{bv}(r) \right] \right\} \cdot dx\, dy$$

The parameters α_b, β_b and γ_b are not random variables. For a given interfering power spectrum and variance σ_Γ^2, their values are controlled by the spacing d, spectral height h_w, number of element m, etc. $L_{bu}(r)$ and $L_{bv}(r)$ are Gaussian random variables, containing the information needed for decision making. From their expressions, we see that $L_{bu}(r)$ and $L_{bv}(r)$ may be realized by schemes similar to the one shown in Fig. 3-1. It will become clear later that the random variable $L_r(r)$ is irrelevant in the hypothesis testing. Equation (5-19) may be simplified by employing

$$\int_{-\infty}^{\infty} \exp\left\{ - \frac{(z\pm c)^2}{2\sigma^2} \right\} \cdot dz = 2\pi\sigma$$

The procedure for simplification is straightforward but tedious. Let

(5-20) $$\Lambda_b(L_u, L_v) \triangleq (\alpha_b+1)\cdot L_{bv}^2(r) + 2\gamma_b \cdot L_{bu}(r)L_{bv}(r) + (\beta_b+1)\cdot L_{bu}^2(r)$$

and

(5-21) $$\mu_b(\alpha,\beta,\gamma) \triangleq (\alpha_b+1)\cdot(\beta_b+1) - \gamma_b^2 .$$

We find that

(5-22)

$$p(R|H_b) = \lim_{N\to\infty} \frac{e^{L_r(r)}}{\sqrt{(2\pi)^{mN}|K|}} \cdot e^{\frac{\sigma_\Gamma^2}{2}\cdot\frac{\Lambda_b(L_u,L_v)}{\mu_b(\alpha,\beta,\gamma)}} \Big/ \sqrt{\mu_b(\alpha,\beta,\gamma)}$$

Replacing the subscript b by a in Eq. (5-13) through Eq. (5-17), we generate a set of new functions which are the counterparts of α_b, β_b, γ_b, $L_{bu}(r)$ and $L_{bv}(r)$ under hypothesis H_a. We denote them by α_a, β_a, γ_a, $L_{au}(r)$ and $L_{av}(r)$, respectively. For example

$$\alpha_a \triangleq \sum_{i,j=1}^{m} \iint_{-T}^{T} u_{ai}(t)\cdot u_{aj}(z)\cdot H_{ij}^{o}(t,z)\cdot dt\, dz .$$

The density of R under H_a may be formulated in the same manner. $p(R|H_a)$ is readily obtained if $\Lambda_b(L_u,L_v)$ and $\mu_b(\alpha,\beta,\gamma)$ in Eq. (5-22) are replaced by their counterparts $\Lambda_a(L_u,L_v)$ and $\mu_a(\alpha,\beta,\gamma)$, etc. Hence, the likelihood ratio is given by

(5-23)

$$\text{L.R.} = \lim_{N\to\infty} \frac{p(R|H_b)}{p(R|H_a)} = \sqrt{\frac{\mu_a(\alpha,\beta,\gamma)}{\mu_b(\alpha,\beta,\gamma)}} \cdot \exp\cdot\left\{\frac{\sigma_\Gamma^2}{2} - \frac{\Lambda_b(L_u,L_v)}{\mu_b(\alpha,\beta,\gamma)} - \frac{\sigma_\Gamma^2}{2} \cdot \frac{\Lambda_a(L_u,L_v)}{\mu_a(\alpha,\beta,\gamma)}\right\}$$

Taking the logarithm and incorporating common terms and known functions in the threshold, we obtain the equivalent test

(5-24)

$$\Lambda_g(r) = \mu_a(\alpha,\beta,\gamma) \cdot \Lambda_b(L_u,L_v) - \mu_b(\alpha,\beta,\gamma) \cdot \Lambda_a(L_u,L_v) \underset{H_a}{\overset{H_b}{\gtrless}} \text{threshold.}$$

The expression for the test function $\Lambda_g(r)$ is quite complicated. The decision process relies on observing four sufficient statistics $L_{ku}(r)$ and $L_{kv}(r)$, k = a and b, which are Gaussian random variables. From Eq. (5-24), we note that the optimum processor, in general, consists of two similar portions, i.e., $\Lambda_a(L_u,L_v)$ and $\Lambda_b(L_u,L_v)$. A scheme for generating $\Lambda_b(L_u,L_v)$ is shown in Fig. 5-1.

B. The Distribution Function

To find the statistics of the test function $\Lambda_g(r)$, we need to determine its distribution. In theory, the distribution of $\Lambda_g(r)$ under each hypothesis may be calculated by the integral

(5-25)

$$F_\Lambda(\Lambda|H_k) = \iiiint_{\mathcal{R}} p(L_{bu},L_{bv},L_{au},L_{av}|H_k) \cdot dL_{bu}\cdot dL_{bv}\cdot dL_{au}\cdot dL_{av}$$

where $\mathcal{R}$ is the hyperplane defined by Eq. (5-24) and $p(L_{bu},L_{bv},L_{au},L_{av})$ is the joint density of the random variables $L_{au}(r)$, $L_{av}(r)$, $L_{bu}(r)$ and $L_{bv}(r)$ under hypothesis H_k.

The statistics of $L_{ku}(r)$ and $L_{kv}(r)$, where k=a and b, under both hypothesis are given in Appendix B. In general, they are correlated Gaussian random variables with zero-means. Thus the 4 x 4 covariance matrix associated with the density function p (L_{bu}, L_{bv},

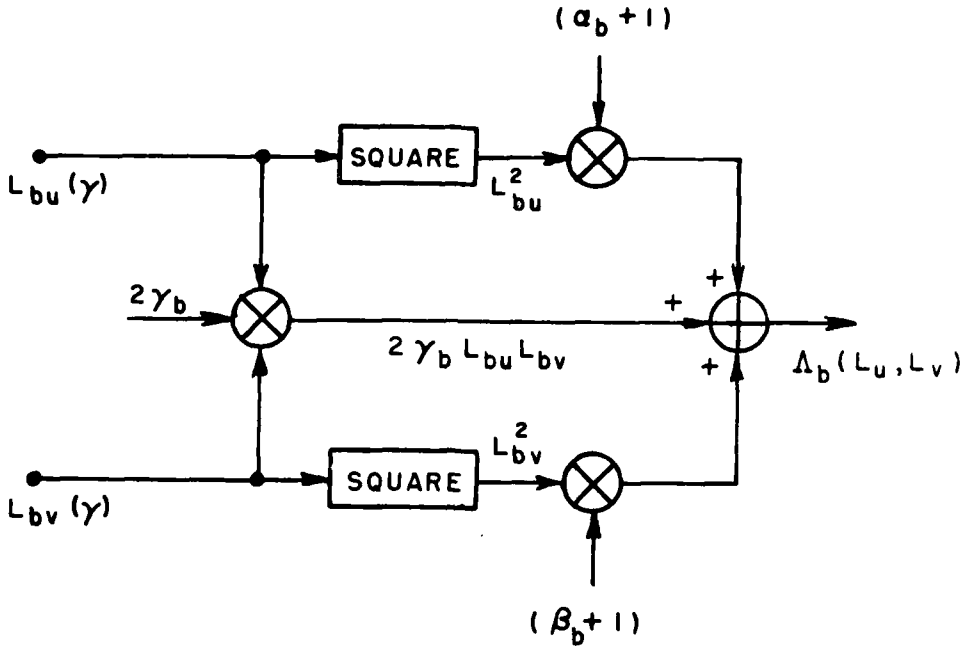

Fig. 5-1--A scheme for generating $\Lambda_b(L_u, L_v)$.

L_{au}, L_{av}) does not have any zero element. We expect that, in general, the inverse of this covariance matrix will not be diagonal. Consequently, the expression for the density function is quite complicated. As can be seen from Eq. (5-24), the geometry of the hyperplane is not simple either. For these reasons, we can see that the quadruple integral in Eq. (5-25) is difficult to evaluate.

For a constant $\Lambda_g(r)$, Eq. (5-24) is the equation of an ellipsoid of four dimensions. To simplify the geometry of $\mathcal{R}$, we shall diagonalize the quadratic equation defining $\mathcal{R}$. The test function $\Lambda_g(r)$ may be written as

$$\Lambda_g(r) = \begin{bmatrix} L_{bv}(r) \\ L_{bu}(r) \\ L_{av}(r) \\ L_{au}(r) \end{bmatrix}^T \begin{bmatrix} \mu_a \cdot (\alpha_b+1) & \mu_a \cdot \gamma_b & 0 & 0 \\ \mu_a \cdot \gamma_b & \mu_a(\beta_b+1) & 0 & 0 \\ 0 & 0 & \mu_b \cdot (\alpha_a+1) & \mu_b \cdot \gamma_a \\ 0 & 0 & \mu_b \cdot \gamma_a & \mu_b \cdot (\beta_a+1) \end{bmatrix} \begin{bmatrix} L_{bv}(r) \\ L_{bu}(r) \\ L_{av}(r) \\ L_{au}(r) \end{bmatrix}$$

Apparently, the coordinates which diagonalize

(5-26)
$$\Lambda_{gk}(r) \triangleq \begin{bmatrix} L_{kv}(r) \\ L_{ku}(r) \end{bmatrix}^T \begin{bmatrix} \mu_q \cdot (\alpha_k + 1) & \mu_q \cdot \gamma_k \\ \mu_q \cdot \gamma_k & \mu_q \cdot (\beta_k + 1) \end{bmatrix} \begin{bmatrix} L_{kv}(r) \\ L_{ku}(r) \end{bmatrix},$$

where

$$k \neq q$$

$$k = a \text{ and } b$$

and

$$q = a \text{ and } b,$$

will also diagonalize the quadratic equation $\Lambda_g(r)$. Let*

(5-27)
$$D_k \triangleq \begin{bmatrix} \sqrt{\xi_{k1}} & 0 \\ 0 & \sqrt{\xi_{k2}} \end{bmatrix}$$

$$\triangleq \frac{\mu_q}{2} \begin{bmatrix} \alpha_k + \beta_k + 2 - \delta_k & 0 \\ 0 & \alpha_k + \beta_k + 2 + \delta_k \end{bmatrix}, \quad k \neq q,$$

where

$$\delta_k \triangleq \sqrt{(\alpha_k - \beta_k)^2 + 4\gamma_k^2}$$

Also, let us define

(5-28)
$$G_k \triangleq \frac{1}{\sqrt{2\delta_k}} \begin{bmatrix} \sqrt{-\alpha_k + \beta_k + \delta_k} & -\sqrt{\alpha_k - \beta_k + \delta_k} \\ \sqrt{\alpha_k - \beta_k + \delta_k} & \sqrt{-\alpha_k + \beta_k + \delta_k} \end{bmatrix} \triangleq \begin{bmatrix} g_{k11} & g_{k12} \\ g_{k21} & g_{k22} \end{bmatrix}$$

---

* ξ_{k1} and ξ_{k2} are the eigenvalues associated with the 2 x 2 symmetric matrix given in the right side of Eq. (5-26).

G_k is an orthonormal matrix. Then we find that in terms of the normal coordinates $\mathcal{L}_{bu}(r), \mathcal{L}_{bv}(r), \mathcal{L}_{au}(r)$ and $\mathcal{L}_{av}(r)$, where

$$(5\text{-}29) \qquad \begin{bmatrix} \mathcal{L}_{kv}(r) \\ \\ \mathcal{L}_{ku}(r) \end{bmatrix} = D_k \cdot G_k \cdot \begin{bmatrix} L_{kv}(r) \\ \\ L_{ku}(r) \end{bmatrix}$$

the test function $\Lambda_g(r)$ has the simple representation,

$$(5\text{-}30) \qquad \Lambda_g(r) = \mathcal{L}^2_{bv}(r) + \mathcal{L}^2_{bu}(r) - \mathcal{L}^2_{av}(r) - \mathcal{L}^2_{au}(r) \underset{H_a}{\overset{H_b}{\gtrless}} \text{threshold.}$$

As a result, the distribution of $\Lambda_g(r)$ may be evaluated alternatively by

$$F_\Lambda(\Lambda|H_k) = \iiiint_R p(\mathcal{L}_{bu}, \mathcal{L}_{bv}, \mathcal{L}_{au}, \mathcal{L}_{av} \; H_k) \cdot d\mathcal{L}_{bu} \; d\mathcal{L}_{bv} \cdot d\mathcal{L}_{au} \; d\mathcal{L}_{av} \; .$$

The statistics of L_{ku} and L_{kv}, k=a and b, under both hypotheses are given in Appendix B. In general, they are correlated Gaussian random variables with zero-means. Being linear functions of L_{bu}, L_{bv}, L_{au} and L_{av}, the new coordinates are therefore also zero-mean Gaussian random variables. The covariance matrix $K_{\mathcal{L}}$ associated with the normal coordinates is a 4 x 4 matrix

$$(5\text{-}31) \qquad K_{\mathcal{L}} = E\left\{ \begin{bmatrix} \mathcal{L}^2_{bu} & \mathcal{L}_{bu}L_{bv} & \mathcal{L}_{bu}\mathcal{L}_{au} & \mathcal{L}_{bu}\mathcal{L}_{av} \\ \mathcal{L}_{bv}L_{bu} & \mathcal{L}^2_{bv} & \mathcal{L}_{bv}\mathcal{L}_{au} & \mathcal{L}_{bv}\mathcal{L}_{av} \\ \mathcal{L}_{au}L_{bu} & \mathcal{L}_{au\,bv} & \mathcal{L}^2_{au} & \mathcal{L}_{au}\mathcal{L}_{av} \\ \mathcal{L}_{av}L_{bu} & \mathcal{L}_{av\,bv} & \mathcal{L}_{av}\mathcal{L}_{au} & \mathcal{L}^2_{av} \end{bmatrix} \right\}$$

From Eq. (5-29) we find that in general only

$$(5\text{-}32) \qquad E\{\mathcal{L}_{ku}\mathcal{L}_{kv}\} = 0, \quad k = a, b.$$

For this reason the four jointly normal random variables $\mathcal{L}$'s cannot be statistically independent. The variables $\mathcal{L}$'s in the expression for the joint density $p(\mathcal{L}_{bu}, \mathcal{L}_{bv}, \mathcal{L}_{au}, \mathcal{L}_{av})$ are only partially decoupled. As a result of this, the quadruple integral Eq. (5-31) remains difficult to integrate. It appears that a simple, analytical formula for the distribution of the test function $\Lambda_g(r)$ given by Eq. (5-24) seems not obtainable.

C. The Probability Equations, ASK

One commonly used method for transmitting the binary symbols 0 and 1 using ASK signals is to send a specific signal for the symbol 1 and to send no signal at all for the symbol 0. For this special case, only two test variables remain in the equivalent likelihood ratio test defined by Eq. (5-24). Besides, the distribution of the test function may be obtained by evaluating a double integral.

Suppose the signal b(t) is sent for the symbol 1. The signals received by the ith element under both hypotheses are

$$\begin{aligned} H_a:&\quad r_i(t) = n_i(t) + w_i(t) \\ H_b:&\quad r_i(t) = n_i(t) + w_i(t) + x \cdot u_{bi}(t) - y \cdot v_{bi}(t) \end{aligned} \tag{5-33}$$

Setting $u_a(t) = v_a(t) = 0$, we obtain from Eq. (5-24) that

(5-34)

$$\Lambda(r) \triangleq (\alpha_b+1) \cdot L_{bv}^2(r) + 2\gamma_b \cdot L_{bv}(r)L_{bu}(r) + (\beta_b+1) \cdot L_{bu}^2(r)$$

$$\underset{H_a}{\overset{H_b}{\gtrless}} \eta^2$$

The distribution of $\Lambda(r)$ may be evaluated by

$$F_\Lambda(\Lambda|H_k) = \iint p(\mathcal{L}_{bv}, \mathcal{L}_{bu}|H_k) \cdot d\mathcal{L}_{bv} \cdot d\mathcal{L}_{bu}$$

We shall see later that even for this special case, the double integral given above can not be evaluated analytically either. However, comparatively speaking, the expression for the distribution is quite simple.

The structure of the optimum processor for detecting on-off binary signals is just half the general system $\Lambda_g(r)$. In the $L_{bu}(r)$ and $L_{bv}(r)$ plane the hypothesis H_a is chosen whenever $\Lambda(r)$ appears within the ellipse or H_b is chosen whenever otherwise. The geometry (e.g., major axis) of the ellipse is decided by the threshold, α_b, β_b and γ_b. From Eq. (5-29) we know that the quadratic equation Eq. (5-34) may be rewritten as

$$\Lambda(r) = \mathcal{L}_{bv}^2(r) + \mathcal{L}_{bu}^2(r) \underset{H_a}{\overset{H_b}{\gtrless}} \eta^2 \tag{5-35}$$

where*

$$\mathcal{L}_{bv} = \sqrt{\xi_{b1}} \cdot (g_{b11} L_{bv} + g_{b12} L_{bu}) \tag{5-36}$$

$$\mathcal{L}_{bu} = \sqrt{\xi_{b2}} \cdot (g_{b21} L_{bv} + g_{b22} L_{bu}) \tag{5-37}$$

Making use of Eqs. (5-36) and (5-37), we find that the variances of $\mathcal{L}_{bv}(r)$ and $\mathcal{L}_{bu}(r)$ under hypothesis H_k, k=a and b, are equal to

(5-38)

$$\sigma_{bvk}^2 \triangleq E^2\{\mathcal{L}_{bv}^2(r)|H_k\} = \frac{\xi_{b1}}{2\sigma_\Gamma^2}(\alpha_b + \beta_b + \delta_b) \cdot \left[\frac{1}{2}(2+\alpha_b+\beta_b+\delta_b)\right]^{\varepsilon_k}$$

(5-39)

$$\sigma_{buk}^2 \triangleq \text{var}\{\mathcal{L}_{bu}(r)|H_k\} = \frac{\xi_{b2}}{2\sigma_\Gamma^2} \cdot (\alpha_b + \beta_b - \delta_b) \cdot \left[\frac{1}{2}(2+\alpha_b+\beta_b-\delta_b)\right]^{\varepsilon_k}$$

---

*Because the factor $\mu_a(\alpha,\beta,\gamma)$ does not appear in Eq. (5-34), the eigenvalues ξ_{b1} and ξ_{b2} in Eq. (5-36) are equal to $\frac{1}{2}(\alpha_b+\beta_b+2-\delta_b)$ and $\frac{1}{2}(\alpha_b+\beta_b+2+\delta_b)$, respectively.

where $\varepsilon_k = 0$ if $k = a$ $\qquad$ $\varepsilon_k = 1$ if $k = b$

$\Lambda(r)$ is nonnegative because $\mathcal{L}_{bv}$ and $\mathcal{L}_{bu}$ are real functions. The distribution function $F_\Lambda(\Lambda|H_k)$ is simply given by

(5-40)

$$F_\Lambda(\Lambda|H_k) = \frac{1}{2\pi\sigma_{bvk}\sigma_{buk}} \iint_R e^{-\frac{\mathcal{L}_{bv}^2}{2\sigma_{bvk}^2} - \frac{\mathcal{L}_{bu}^2}{2\sigma_{buk}^2}} \cdot d\mathcal{L}_{bv}\, d\mathcal{L}_{bu}$$

$$= \frac{1}{2\pi\sigma_{bvk}\sigma_{buk}} \int_0^{\sqrt{\Lambda}} \int_{\theta=0}^{2\pi} e^{-\frac{(z\sin\theta)^2}{2\sigma_{buk}^2} - \frac{(z\cos\theta)^2}{2\sigma_{buk}^2}} \cdot z\, dz \cdot d\theta$$

The probability density function of the test function $\Lambda(r)$ under hypothesis H_k thus is

(5-41)

$$p_\Lambda(\Lambda|H_k) \triangleq \frac{\partial F_\Lambda(\Lambda|H_k)}{\partial \Lambda} = \frac{1}{2\sqrt{\Lambda}} \left.\frac{\partial F_\Lambda(\Lambda|H_k)}{\partial z}\right\}_{z=\sqrt{\Lambda}}$$

$$= \frac{1}{4\pi\sigma_{bvk}\sigma_{buk}} \cdot \int_0^{2\pi} e^{-\frac{\Lambda}{2}\left(\frac{\sin^2\theta}{\sigma_{bvk}^2} + \frac{\cos^2\lambda}{\sigma_{buk}^2}\right)} \cdot d\theta$$

where $\Lambda \geq 0$. This integral can not be integrated analytically. One may use a numerical integration technique to get the value. Denoting the probability of choosing hypothesis H_b when H_b is present by P_d, and the probability of choosing H_b when H_a is present by P_f and referring to Fig. 5-2, we find that

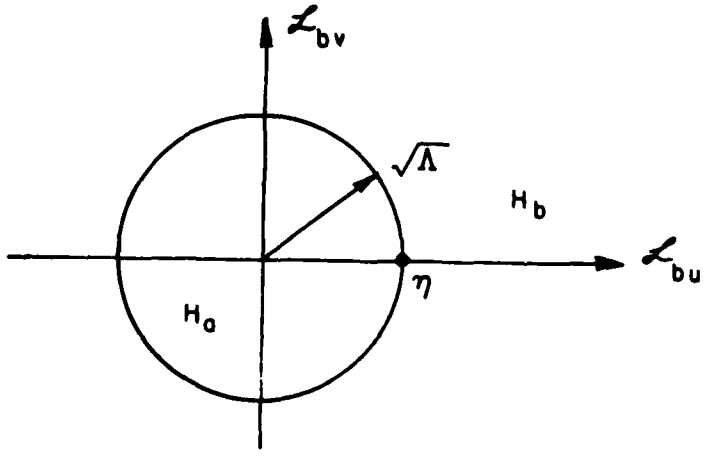

Fig. 5-2--The decision plane.

(5-42)

$$P_d = \int_{\eta}^{\infty} P_{\Lambda}(\Lambda|H_b) \cdot d\Lambda$$

$$= \frac{1}{2\pi\sigma_{bvb}\sigma_{bub}} \cdot \int_0^{2\pi} \frac{e^{-\frac{\eta}{2}\left(\frac{\sin^2\theta}{\sigma^2_{bvb}} + \frac{\cos^2\theta}{\sigma^2_{bub}}\right)}}{\left(\frac{\sin^2\theta}{\sigma^2_{bvb}} + \frac{\cos^2\theta}{\sigma^2_{bub}}\right)} \cdot d\theta$$

and

(5-43) $$P_f = \int_{\eta}^{\infty} P_{\Lambda}(\Lambda|H_a) \cdot d\Lambda$$

whose expression is similar to Eq. (5-42) and can be readily obtained from the same equation when the third subscripts of σ_{bub} and σ_{bvb} are changed from b to a. Before presenting some numerical results, we shall briefly discuss the parameters α_k, β_k and γ_k.

D. On Parameters α_k, β_k and γ_k

Examining the equations for P_d and P_f, we note that they are mainly controlled by the parameters α_b, β_b and γ_b. In the case of the general optimum detection system Eq. (5-24), we expect that the problem of optimizing the system performance would become a problem of designing proper values for α_k, β_k and γ_k, where k=a and b. For this reason, we study the properties of parameters α_b, β_b and γ_b. In practice, the carrier frequency ω_b is much greater than the one used in the modulating signal $e_b(t)$. Very little error would be introduced when we approximate $u_{bi}(t_i)$ and $v_{bi}(t_i)$ by

(5-44) $$u_{bi}(t_i) \approx e_b(t) \cdot \cos\{\omega_b[t-(m-1)\nu]-(i-1)\omega_b(\tau-\nu)\}$$

and

(5-45) $$v_{bi}(t_i) \approx e_b(t) \cdot \sin\{\omega[t-(m-1)\nu]-(i-1)\omega_b(\tau-\nu)\}$$

Thus we obtain the following closed forms:

(5-46)

$$\sum_{i=1}^{m} u_{bi}(t_i) = \frac{\sin \frac{m}{2}\ \omega_b(\tau-\nu)}{\sin \frac{\omega_b}{2}\ (\tau-\nu)} \cdot e_b(t)\cdot\cos\{\omega_b[t - \frac{m-1}{2}\ (\tau+\nu)]\}$$

(5-47)

$$\sum_{i=1}^{m} v_{bi}(t_i) = \frac{\sin \frac{m}{2}\ \omega_b(\tau-\nu)}{\sin \frac{\omega_b}{2}\ (\tau-\nu)} \cdot e_b(t)\cdot\sin\{\omega_b[t - \frac{m-1}{2}\ (\tau+\nu)]\}$$

and

(5-48)

$$\sum_{i=1}^{m} u_{bi}(t_i)v_{bi}(t_i) = \frac{\sin m\omega_b(\tau-\nu)}{\sin \omega_b(\tau-\nu)} \cdot \frac{e_b^2(t)}{2} \cdot \sin\{2\omega_b[t - \frac{m-1}{2}\ (\tau+\nu)]\}$$

Comparing their definitions with the mean of L(R), Eq. (3-4), we conclude that parameters α_b, β_b and $m_{La}(\theta,\phi;\theta)$ possess the same directional property. Using the results just obtained for

$$\sum_{i=1}^{m} u_{bi}(t_i), \quad \sum_{i=1}^{m} v_{bi}(t_i)$$

and

$$\sum_{i=1}^{m} u_{bi}(t_i)\ v_{bi}(t_i),$$

we may derive the closed form representations of α_b, β_b and γ_b. For the sake of saving space we write them in a common expression designated as $g(\theta_1,\theta_2)$.

(5-49)

$$g(\theta_1,\theta_2) \triangleq \frac{\sigma_\Gamma^2}{h_w} \cdot m \cdot \sin(\theta_2-\theta_1) \cdot \int_{-T}^{T} \frac{e_b^2(t)}{2}\, dt$$

$$+ \frac{\sigma_\Gamma^2}{h_w} \cdot \frac{\sin m\omega_b(\tau-\nu)}{\sin \omega_b(\tau-\nu)} \cdot \int_{-T}^{T} \frac{e_b^2(t)}{2} \cdot$$

$$\cdot \sin\{2\omega_b[t - \tfrac{m-1}{2}(\tau+\nu)] + \theta_1+\theta_2\} \cdot dt$$

$$- \frac{\sigma_\Gamma^2}{h_w} \cdot \left[\frac{\sin \frac{m}{2}\omega_b(\tau-\nu)}{\sin \frac{\omega_b}{2}(\tau-\nu)}\right]^2 \cdot \iint_{-T}^{T} e_b(t)e_b(z) \cdot$$

$$\cdot \cos\left\{\omega_b\left[t - \tfrac{m-1}{2}(\tau+\nu) + \theta_1\right]\right\} \cdot$$

$$\cdot \sin\{\omega_b[z - \tfrac{m-1}{2}(\tau+\nu)] + \theta_2\} \cdot \Psi(t,z) \cdot dt\, dz$$

where θ_1 and θ_2 assume different values under different circumstances. In terms of $g(\theta_1,\theta_2)$, we find that

(5-50) $$\alpha_b = g(0\ ,\ \pi/2)$$

$$\beta_b = g(-\ \pi/2,\ 0)$$

and

$$\gamma_b = g(0,0).$$

The function $u_b(t)$ is real, so

$$\sum_{i,j=1}^{m} \iint_{-T}^{T} u_{bi}(t_i) \cdot u_{bj}(z_j) \cdot \psi(t,z) \cdot dt\, dz$$

$$= \sum_{\ell=1}^{\infty} \frac{\left\{ \sum_{i=1}^{m} \int_{-T}^{T} u_{bi}(t_i)\phi_\ell(t) \cdot dt \right\}^2}{m + \frac{h_w}{\lambda_\ell - h_w}} \geq 0$$

From Eqs. (5-13) and (5-14), we thus establish that

$$\alpha_b \leq \frac{\sigma_\Gamma^2}{h_w} \sum_{i=1}^{m} \int_{-T}^{T} u_{bi}^2(t_i)dt \tag{5-51}$$

and

$$\beta_b \leq \frac{\sigma_\Gamma^2}{h_w} \sum_{i=1}^{m} \int_{-T}^{T} v_{bi}^2(t_i)dt \tag{5-52}$$

The upper bounds in Eq. (5-51) and Eq. (5-52) are nonnegative because the integrands $u_{bi}^2(t_i)$ and $v_{bi}^2(t_i)$ are nonnegative. As a matter of fact, these bounds are just equal to the sum of the first two terms of Eq. (5-49). For the case when the interference is a white noise process with flat spectrum height h_n, Eq. (5-49) reduces to

(5-53)

$$g_w(\theta_1,\theta_2) = \frac{\sigma_\Gamma^2}{h_w} \, m \cdot \sin(\theta_2-\theta_1) \cdot \int_{-T}^{T} \frac{e_b^2(t)}{2} dt$$

$$+ \frac{\sigma_\Gamma^2}{h_w} \cdot \frac{\sin m\omega_b(\tau-\nu)}{\sin \omega_b(\tau-\nu)} \cdot \int_{-T}^{T} \frac{e_b^2(t)}{2} \cdot$$

$$\cdot \sin\{2\omega_b[t - \tfrac{m-1}{2}(\tau+\nu)]+\theta_1 + \theta_2\}\, dt$$

$$- \frac{\sigma_\Gamma^2}{h_w} \cdot \frac{1}{m + \frac{h_w}{h_n}} \left\{ \frac{\sin \frac{m}{2}\omega_b(\tau-\nu)}{\sin \frac{\omega_b}{2}(\tau-\nu)} \right\}^2 \cdot$$

(5-53)
(Cont.)

$$\cdot \int_T^T e_b^2(t) \cdot \cos\left\{\omega_b\left[t - \frac{m-1}{2}(\tau+\nu)\right] + \theta_1\right\} \cdot$$

$$\cdot \sin\left\{\omega_b\left[t - \frac{m-1}{2}(\tau+\nu)\right] + \theta_2\right\} \cdot dt$$

Discarding numerically small terms in Eq. (5-53), we obtain the following approximations good for the white noise interference:

(5-54)

$$\alpha_b \approx \beta_b \approx \frac{\sigma_\Gamma^2}{h_w}\left\{m - \frac{1}{m + \frac{h_w}{h_n}}\left(\frac{\sin \frac{m}{2}\omega_b(\tau-\nu)}{\sin \frac{\omega_b}{2}(\tau-\nu)}\right)^2\right\} \cdot \int_{-T}^{T} \frac{e_b^2(t)}{2}\, dt \,.$$

$$\gamma_b \approx 0$$

When the spacing d between two adjacent antennas is

(5-55) $$d = \frac{\lambda_b}{m|\cos\theta - \cos\phi|} \triangleq d_{op},$$

where λ_b is the wavelength corresponding to the angular frequency ω_b, then

(5-56) $$\sin \frac{m}{2}\omega_b(\tau-\nu) = \sin m\omega_b(\tau-\nu) = 0$$

The spacing d_{op} has been referred to as the optimum spacing for the given θ, ϕ and m. As a result of placing an array at this particular spacing, we find that*

(5-57) $$\sum_{i=1}^{m} u_{bi}(\tilde{t}_i) = \sum_{i=1}^{m} v_{bi}(\tilde{t}_i) = 0$$

---

*The definition of t_i is: $t_i \triangleq t-(m-i)\nu = t-(m-i)\, d/c \cos\phi$. When the optimum spacing is used in calculating t_i, we denote the t_i by $\tilde{t}_i$.

$$(5\text{-}58) \qquad \sum_{i=1}^{m} u_{bi}(\tilde{t}_i)v_{bi}(\tilde{t}_i) = 0$$

Later we shall see that these relations are extremely significant. From the general expression Eq. (5-49), we also obtain

$$(5\text{-}59) \qquad \tilde{\alpha}_b = \tilde{\beta}_b = \frac{\sigma_\Gamma^2}{h_w} \cdot m \cdot \int_{-T}^{T} \frac{e_b^2(t)}{2}\, dt$$

$$\tilde{\gamma}_b = 0$$

which are independent of the power spectrum of the interference. Notice that $\tilde{\alpha}_b$ is just equal to the first term of Eq. (5-49). Since it is much greater than the second term of the same equation, $\tilde{\alpha}_b$ is approximately equal to its bound .

We now give a physical interpretation of α_b, β_b and γ_b. The interpretation will also apply to the parameters α_a, β_a and γ_a for the obvious reason. Under hypothesis H_b, the output of the sub-processor $L_{bu}(r)$ may be rewritten as

$$L_{bu}(r) = \frac{1}{h_w}\left\{ \sum_{i=1}^{m} \int_{-T}^{T} \left[n_i(t_i) + w_i(t_i)\right] \cdot u_{bi}(t_i) \cdot dt \right.$$

$$\left. - \sum_{i,j=1}^{m} \iint_{-T}^{T} \left[n_i(t_i) + w_i(t_i)\right] \cdot u_{bj}(z_j) \cdot \psi(t,z) \cdot dt\, dz \right\}$$

$$+ x \cdot \frac{\alpha_b}{\sigma_\Gamma^2} - y \cdot \frac{\gamma_b}{\sigma_\Gamma^2}$$

Thus the component contributed to the output $L_{bu}(r)$ by the desired signal is equal to

$$x \cdot \frac{\alpha_b}{\sigma_\Gamma^2} - y \cdot \frac{\gamma_b}{2}$$

Similarly, the component contributed to the output $L_{bv}(r)$ by the desired signal is equal to

$$y \cdot \frac{\beta_b}{\sigma_\Gamma^2} - x \cdot \frac{\gamma_b}{\sigma_\Gamma^2}$$

Apparently, large α_b and β_b and small γ_b will reduce the influence of the interference in making decisions. Referring to Eq. (5-3), the desired signal b(t) may be decomposed into an in-phase component and a quadrature component, each with a random amplitude. The parameters α_b and β_b represent the bit energies contributed to $L_{bu}(r)$ and $L_{bv}(r)$ by the signals $u_b(t)$ and $v_b(t)$, respectively. The parameter γ_b represents the cross-energy between the $u_b(t)$ and $v_b(t)$.

E. Numerical Results, ASK Signals

In this section, we investigate the characteristics of the optimum detector for detecting the on-off keyed binary signals. We first investigate how the system responds to a testing signal arriving from an arbitrary angle . The testing signal used is assumed to have the same waveform as the desired signal b(t). Again, we consider the case when the interfering signal is a white noise process with spectral height h_η. Later, the error rate performance and methods of optimizing this performance are also discussed.

Letting $\gamma_b \approx 0$ and $\alpha_b \approx \beta_b$ in Eq. (5-34), we thus obtain the processor for detecting the on-off keyed signals corrupted by directional white noise:

$$\Lambda(r) = (\alpha_b + 1)\, L_{bv}^2(r) + (\beta_b + 1)\, L_{bu}^2(r) \underset{H_a}{\overset{H_b}{\gtrless}} \eta^2 \tag{5-60}$$

The detection system makes decisions by comparing its processing output $\Lambda(r)$ to a given threshold. Whenever the processing output is less than η^2 the system signals that H_a is present; otherwise, the system chooses H_b.

The capability of a detection system of doing its job is uniquely decided by how the processing output under one hypothesis is distinct from the output under another, and the value chosen for the threshold. $\Lambda(r)$ is the result of processing the interference-contaminated inputs in the manner specified by the right side of Eq. (5-60). Hence, the characteristics of this detection system are determined by that equation. $\Lambda(r)$ is randomly distributed. One important characteristic of $\Lambda(r)$ is its mean, which we now examine.

Since the testing signal b(t) is assumed to propagate into the array from angle θ, the input to the ith channel of the processor is given by

$$\hat{r}_i(t_i) = n_i(t_i) + w_i(t_i) + x\,\hat{u}_{bi}(t_i) - y\hat{v}_{bi}(t_i) \tag{5-61}$$

where

$$\hat{u}_{bi}(t_i) \triangleq u_b\left[t-(i-1)\frac{d}{c}\cos\hat{\theta} - (m-i)\frac{d}{c}\cos\phi\right] \tag{5-62}$$

and

$$\hat{v}_{bi}(t_i) \triangleq v_b\left[t-(i-1)\frac{d}{c}\cos\hat{\theta} - (m-i)\frac{d}{c}\cos\phi\right] \tag{5-63}$$

The detection system is optimized for the desired signal arriving from angle θ. Hence, the sub-processors $L_{bu}(r)$ and $L_{bv}(r)$ will generate the outputs as follows:

(5-64)

$$\hat{L}_{bu}(r) = \frac{1}{h_w}\left\{\sum_{i=1}^{m}\int_{-T}^{T}\hat{r}_i(t_i)u_{bi}(t_i)dt - \sum_{i,j=1}^{m}\iint_{-T}^{T}\hat{r}_i(t_i)u_{bj}(z_j)\cdot\Psi(t,z)\cdot dt\,dz\right\}$$

and

(5-65)

$$\hat{L}_{bv}(r) = \frac{1}{h_w}\left\{\sum_{i=1}^{m}\int_{-T}^{T}\hat{r}_i(t_i)v_{bi}(t_i)dt - \sum_{i,j=1}^{m}\iint_{-T}^{T}\hat{r}_i(t_i)v_{bj}(z_j)\cdot\Psi(t,z)\cdot dt\,dz\right\}$$

Referring to Eq. (5-61), we see that the first terms of $\hat{L}_{bu}(r)$ and $L_{bv}(r)$ no longer represent the coherent correlators, because the time-shiftings in $\hat{u}_{bi}(t_i)$ and $\hat{v}_{bi}(t_i)$ are not equal to those in $u_{bi}(t_i)$ and $v_{bi}(t_i)$, respectively. The output of the optimum processor is equal to

$$\Lambda(\theta,\phi;\hat{\theta}) = (\alpha_b+1)\hat{L}_{bv}^2(r) + (\beta_b+1)\cdot\hat{L}_{bu}^2(r) \tag{5-66}$$

Equation (5-60) is just the special case of $\Lambda(\theta,\phi;\hat{\theta})$ when $\hat{\theta}=\theta$. The variances of $L_{bu}(r)$ and $L_{bv}(r)$ may be determined from Eq. (B-18) and Eq. (B-19), respectively. It is found that

(5-67) $$\text{var}\{\hat{L}_{bu}(r)|H_b\} = \frac{1}{\sigma_\Gamma^2}(\alpha_b + \hat{\alpha}_b^2 + \hat{\gamma}_b^2)$$

and

(5-68) $$\text{var}\{\hat{L}_{bv}(r)|H_b\} = \frac{1}{\sigma_\Gamma^2}(\beta_b + \hat{\beta}_b^2 + \hat{\gamma}_b^2)$$

where

(5-69) $$\hat{\alpha}_b \triangleq \frac{\sigma_\Gamma^2}{h_w} < \hat{u}_b, u_b >$$

(5-70) $$\hat{\beta}_b \triangleq \frac{\sigma_\Gamma^2}{h_w} <\hat{v}_b, v_b>$$

and

(5-71) $$\hat{\gamma}_b \triangleq \frac{\sigma_\Gamma^2}{h_w} <\hat{u}_b, v_b>$$

Comparing the right side of Eq. (5-6) with that of Eq. (4-2), we find that they are the same if ϕ_s=0. We also find that $v_b(t)$ is equal to Eq. (4-2) if $\phi_s = -\pi/2$. Hence the closed form representation for α_b may be readily obtained from Eq. (4-11) when ϕ_s is set equal to zero and

$$\int_{-T}^{T} e_a(t)\, e(t) \cdot dt$$

is changed to

$$\frac{\sigma_\Gamma^2}{h_w}\int_{-T}^{T} e_b^2(t) \cdot dt \ .$$

As a result, when the interference is a white noise process we find that

(5-72)

$$\hat{\alpha}_b \approx \frac{\sigma_\Gamma^2}{h_w} \int_{-T}^{T} \frac{e_b^2(t)}{2}\,dt \cdot \cos\frac{m-1}{2}\,\omega_b(\hat{\tau}-\tau) \cdot$$

$$\cdot \left\{ \frac{\sin\frac{m}{2}\,\omega_b(\hat{\tau}-\tau)}{\sin\frac{\omega_b}{2}\,(\hat{\tau}-\tau)} - \frac{1}{m+\frac{h_w}{h_n}} \cdot \frac{\sin\frac{m}{2}\,\omega_b(\tau-\nu)}{\sin\frac{\omega_b}{2}\,(\tau-\nu)} \cdot \frac{\sin\frac{m}{2}\,\omega_b(\hat{\tau}-\nu)}{\sin\frac{\omega_b}{2}\,(\hat{\tau}-\nu)} \right\}$$

The closed form representations for $\hat{\beta}_b$ and $\hat{\gamma}_b$ when the interference is a white noise process may be obtained in the same manner. We find that

(5-73) $$\hat{\beta}_b \approx \hat{\alpha}_b$$

and

(5-74) $$\hat{\gamma}_b \approx 0$$

Thus when the interference has a flat spectrum, the mean of $\Lambda(\theta,\phi;\hat{\theta})$ is simply given by,

(5-75) $$E\{\Lambda(\theta,\phi;\hat{\theta})|H_b\} = \frac{2}{\sigma_\Gamma^2}\,(\alpha_b+1) \cdot (\alpha_b + \hat{\alpha}_b^2)$$

For the same reason as given in Chapter IV, we study the directional characteristics of the system by examining the relative angular response.

(5-76) $$F(\theta,\phi;\hat{\theta}) = 20 \cdot \log \frac{E\{\Lambda(\theta,\phi;\hat{\theta})|H_b\}}{E\{\Lambda(\theta,\phi;\theta)|H_b\}}$$

The signal b(t) is a random process. The mean of its energy in the observation interval $[-T,T]$ is equal to

$$E\left\{\int_{-T}^{T} b^2(t)dt\right\} = \sigma_r^2 \int_{-T}^{T} e_b^2(t) \cdot dt$$

We define the signal energy to the total noise power density ratio as

$$(5\text{-}77) \qquad (S/N) = \frac{\sigma_\Gamma^2 \int_{-T}^{T} e_b^2(t)dt}{h_w + h_n}$$

$$= \frac{\sigma_\Gamma^2 \int_{-T}^{T} e_b^2(t)\cdot dt}{h_w} \cdot \frac{1}{1 + \frac{h_w}{h_n}}$$

The quantity

$$\frac{\sigma_\Gamma^2}{h_w} \int_{-T}^{T} e_b^2(t)dt$$

is the signal energy to the internal (white) noise power density ratio. We proceed to investigate the directional characteristics through studying the angular response curve.

Figure 5-3 shows the angular response of the detection system (5^o,45^o) which has a 2-element array with spacing 0.865λ. In plotting this curve, we assume (S/N) = 10, $h_w|h_n = 0.1$ and

$$\sigma_\Gamma^2 \int_{-T}^{T} e_b^2(t)dt = 1.$$

To show the effect of varying the array spacing, the response of the detector (5^o,45^o), which uses the same number of elements with an increased spacing (1.73λ), is given in Fig. 5-4. In Fig. 5-4, $F(5^o,45^o;\hat{\theta})$ is the absolute maximum at $\theta=5^o$ and ϕ becomes a relative minimum at $\theta=45^o$. Physically, this curve implies that when the signal b(t) propagates into the array from the angle θ, the average processor output is the highest. On the other hand the processor generates almost the lowest output (in average) if the same signal arrives from the angle ϕ. As a matter of fact, 1.73λ is the optimum spacing for m=2, $\theta=5^o$ and $\phi=45^o$.

In Fig. 5-5 through Fig. 5-8 we show the angular response curves for the detectors (55^o,45^o) which are designed for different number of antennas and different spacings. It is seen in these curves that the response at the angle corresponding to the incident angle for the interference is always lower than the response at $\theta=\theta$. This suggests that the optimum system possesses the same characteristics as the one discussed in Chapter IV. In fact, $F(\theta,\phi;\theta)$ may be written simply as

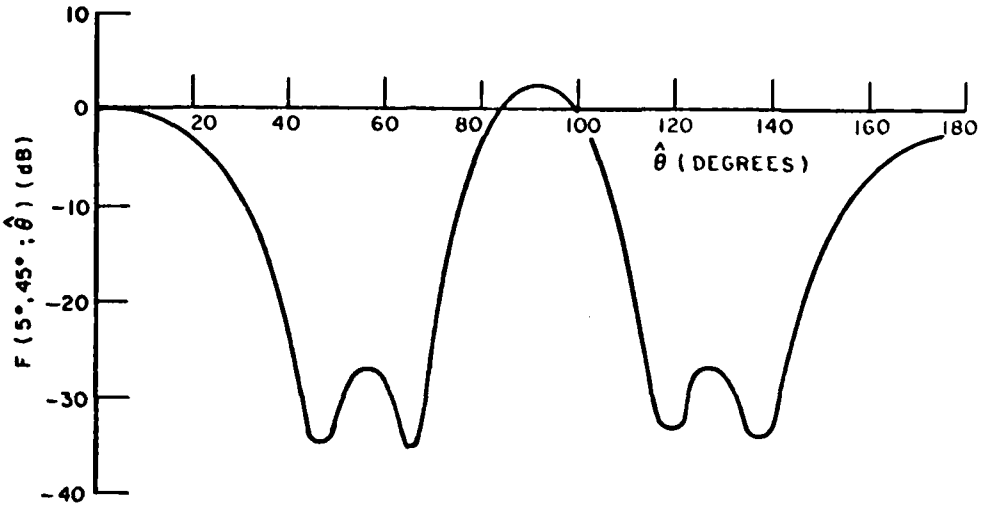

Fig. 5-3--$F(5^{o},45^{o};\hat{\theta})$ vs. $\hat{\theta}$ given m=2, d=0.865λ, (S/N)=10 and h_w/h_n = 0.1.

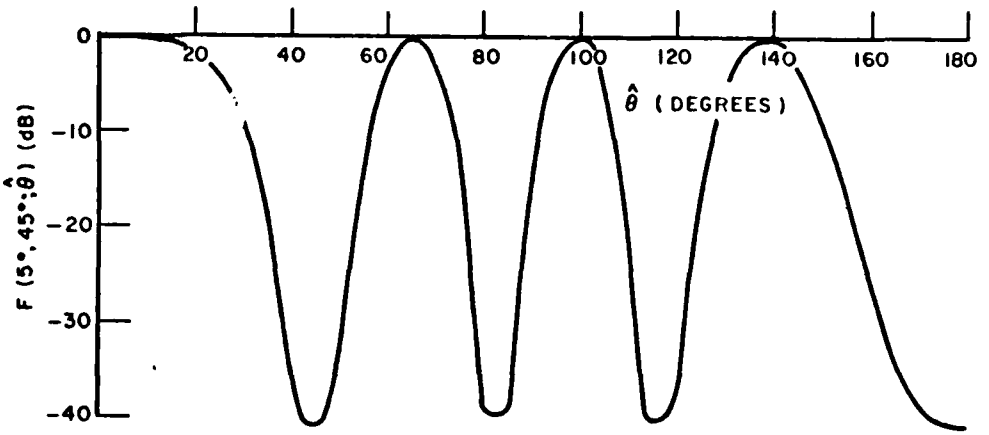

Fig. 5-4--$F(5^{o},45^{o};\hat{\theta})$ vs. $\hat{\theta}$ given m=2, d=1.73λ, (S/N)=10 and h_w/h_n = 0.1.

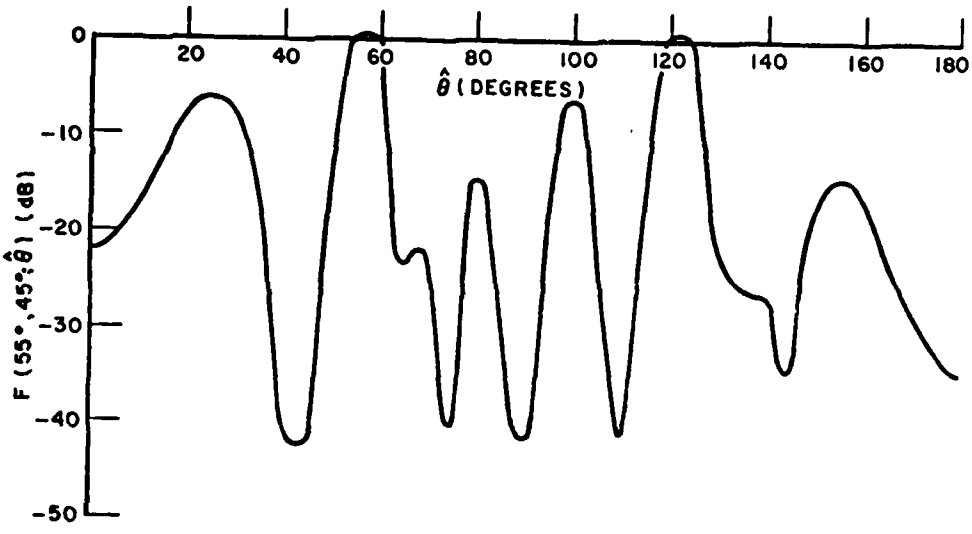

Fig. 5-5--$F(55^{o},45^{o};\hat{\theta})$ vs. $\hat{\theta}$ given m=4, d=0.936λ, (S/N)=10 and h_w/h_n = 0.1.

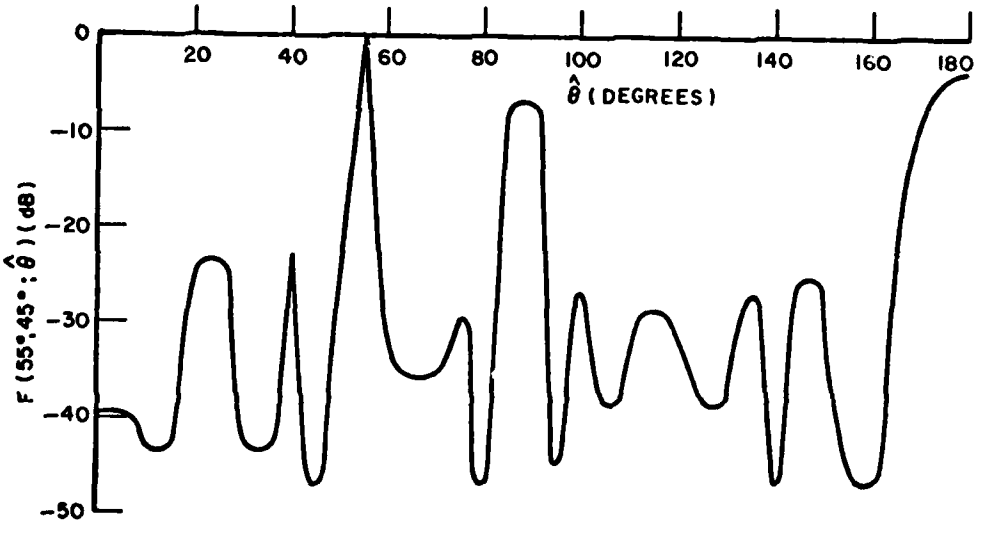

Fig. 5-6--$F(55^{o},45^{o},\hat{\theta})$ vs. $\hat{\theta}$ given m=4, d=1.872λ, (S/N)=10 and h_w/h_n = 0.1.

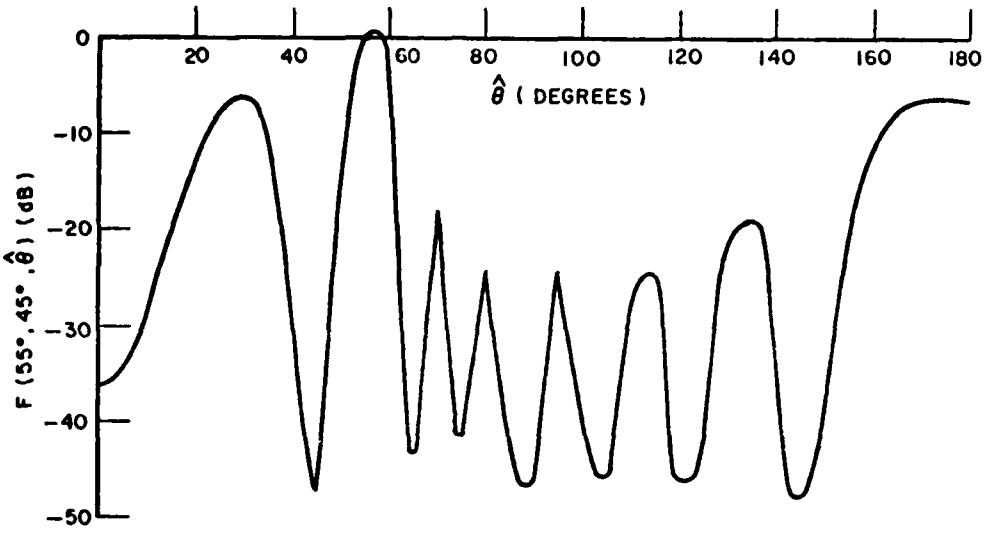

Fig. 5-7--$F(55^{o},45^{o};\hat{\theta})$ vs. $\hat{\theta}$ given m=7, d=0.537λ, (S/N)=10 and h_w/h_n = 0.1.

$$(5\text{-}78) \qquad F(\theta,\phi;\hat{\theta}) = 20 \cdot \log\left(\frac{\alpha_b + \hat{\alpha}_b^2}{\alpha_b + \alpha_b^2}\right)$$

The parameter α_b is often much greater than one, hence $F(\theta,\phi;\hat{\theta})$ may be approximated by

$$(5\text{-}79) \qquad F(\theta,\phi;\hat{\theta}) \approx 40 \cdot \log\left(\frac{\hat{\alpha}_b}{\alpha_b}\right)$$

Because $\hat{\alpha}_b$ and $m_{La}(\theta,\phi;\hat{\theta})$ have the same directional property, it is no surprise that both systems have the similar characteristics. In plotting Fig. 5-5 and Fig. 5-7 an optimum spacing is used by each detector. As a result, the average processor output is always the highest when the signal b(t) propagates into the array from the desired source.

To examine the behavior of $F(\theta,\phi;\hat{\theta})$ when $\theta=\phi$, we show four curves in Fig. 5-9 through Fig. 5-12. In plotting these curves, we again let (S/N) = 10, $h_w|h_n$ = 0.1 and

$$\sigma^2 \int_{-T}^{T} e_b^2(t)dt = 1.$$

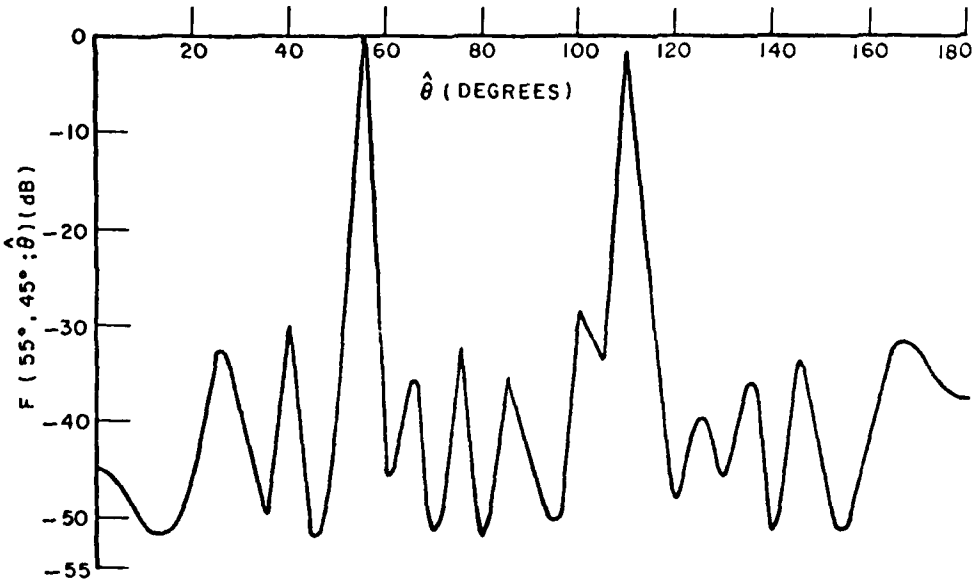

Fig. 5-8--$F(55^{o},45^{o};\hat{\theta})$ vs. $\hat{\theta}$ given m=7, d=1.070λ, (S/N)=10 and h_w/h_n = 0.1.

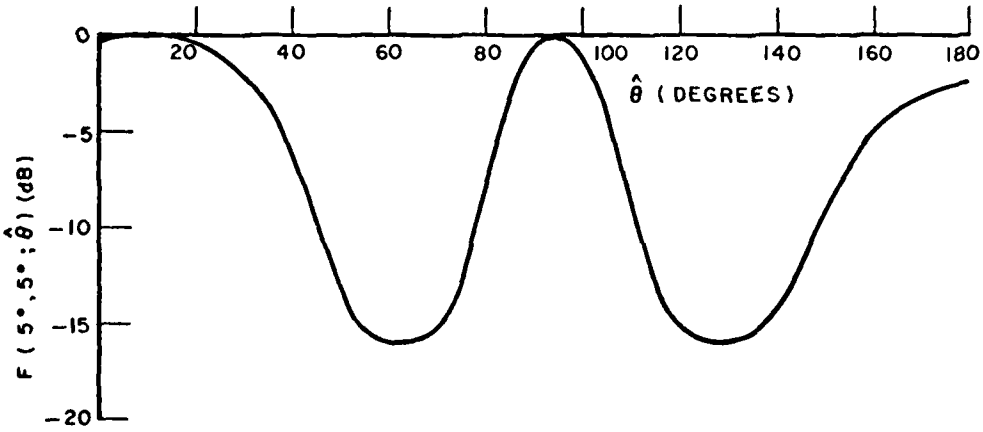

Fig. 5-9--$F(55^{o},5^{o};\hat{\theta})$ vs. $\hat{\theta}$ given m=2, d=0.936λ, (S/N)=10 and h_w/h_n = 0.1.

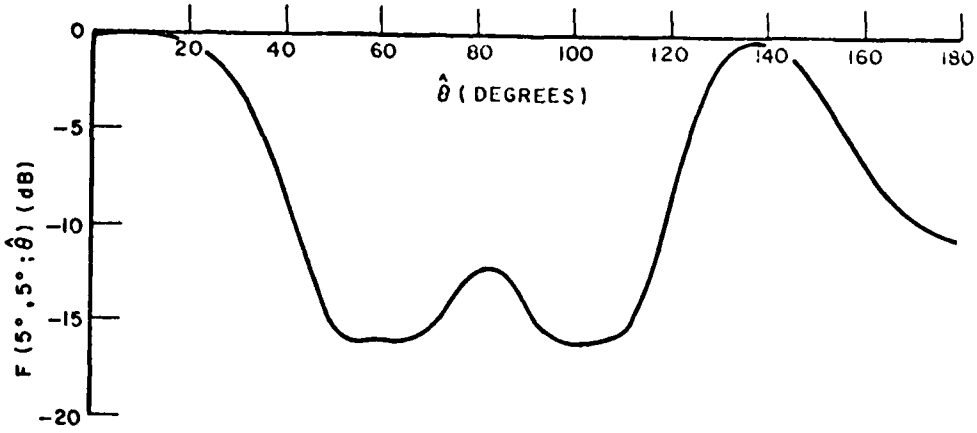

Fig. 5-10--$F(55^{o},5^{o};\hat{\theta})$ vs. $\hat{\theta}$ given m=3, d=0.577λ, (S/N)=10 and h_w/h_n = 0.1.

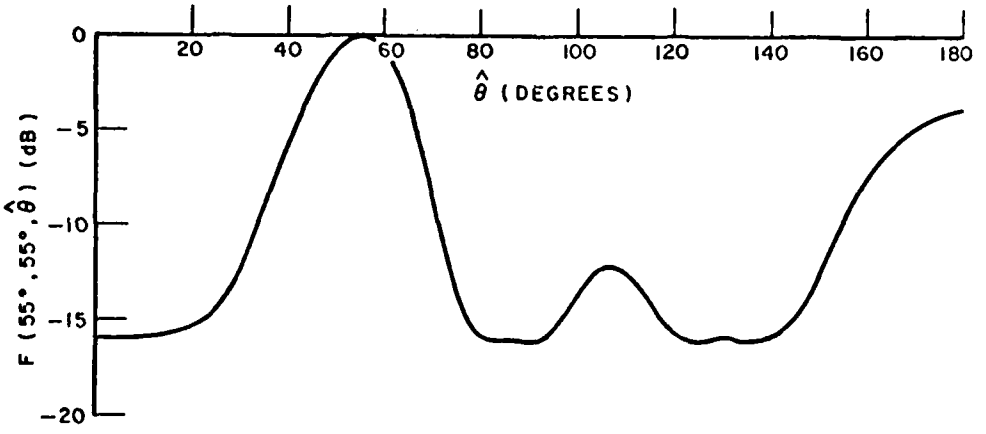

Fig. 5-11--$F(55^{o},5^{o};\hat{\theta})$ vs. $\hat{\theta}$ given m=4, d=0.936λ, (S/N)=10 and h_w/h_n = 0.1.

AD-A122 188 OPTIMUM ARRAY PROCESSING FOR DETECTING BINARY SIGNALS CORRUPTED BY DIRECT.. (U) OHIO STATE UNIV COLUMBUS ELECTROSCIENCE LAB C CHIU DEC 72 ESL-3433-2 2/2

UNCLASSIFIED N00019-72-C-0184 F/G 9/2 NL

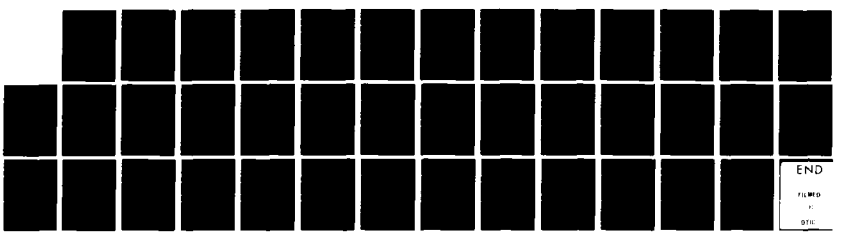

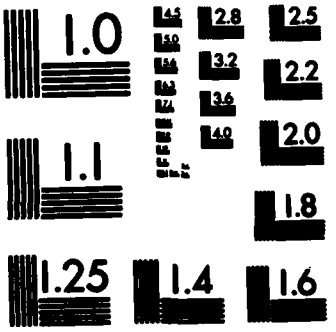

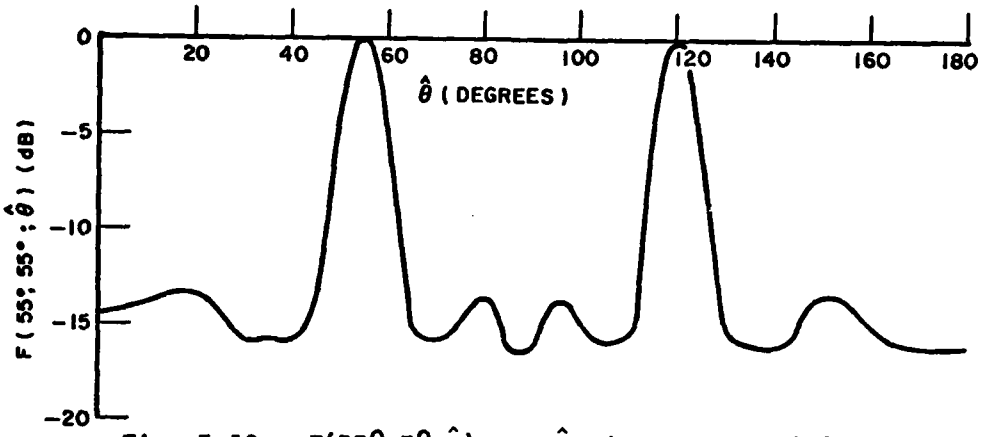

Fig. 5-12. $F(55^{o},5^{o};\hat{\theta})$ vs. $\hat{\theta}$ given m=4, d=0.936λ, (S/N)=10 and $h_w/h_n = 0.1$.

It is seen that $F(\theta,\phi;\hat{\theta})$ always assumes the peak value at $\hat{\theta}=\theta=\phi$ for this extreme case. When m=2, S/N=10 and

$$\sigma_r^2 \int_{-T}^{T} e_b^2(t)dt = 1,$$

the parameter α_b is equal to 110 for the system designed for the optimum spacing. For the case shown in Fig. 5-9, α_b is only equal to 5.238. The detection error is small if α_b is large. (The equation for detection error will be given in Eq. (5-88). Apparently, the error rate performance is extremely poor when $\theta=\phi$.

The basic properties of the response curve discussed in this section do not change if the values chosen for h_w, (S/N), etc. were different. But the error rate performance of the optimum detector does change with these factors. With this background, we next investigate the error rate performance.

There is no need to diagonalize the quadratic equation (5-34) when the interference is a white noise process, because $\gamma_b \approx 0$. But nevertheless, the results shown in Section V.C are still applicable*. Letting $\gamma_b = 0$ and $\alpha_b = \beta b$, from Eqs. (5-38) and (5-39) we obtain

---

*The eigenvalues are $\xi_1 = \beta_b$ and $\xi_2 = \alpha_b + 1$ when $\gamma_b = 0$. The new and the primary coordinates are related by

$$\begin{bmatrix} \mathcal{L}_{bv} \\ \mathcal{L}_{bu} \end{bmatrix} = \begin{bmatrix} 0 & -1 \\ 1 & 0 \end{bmatrix} \begin{bmatrix} L_{bu}(r) \\ L_{bv}(r) \end{bmatrix}$$

$$\sigma_{bvb}^2 = \sigma_{bub}^2 = \frac{\alpha_b}{\sigma_\Gamma^2}(\alpha_b + 1)^2$$

(5-80)
$$\triangleq \sigma_b^2$$

and

$$\sigma_{bva}^2 = \sigma_{bua}^2 = \frac{\alpha_b}{\sigma_\Gamma^2}(\alpha_b+1)$$

(5-81)
$$\triangleq \sigma_a^2$$

Also, as a result of $\gamma_b \approx 0$ and $\alpha_b \approx \beta_b$, the probabilities of making correct and false decisions on whether hypothesis H_b is true reduce to

(5-82) $$P_d \approx e^{-\frac{\eta}{2\sigma_b^2}},$$

and

(5-83) $$P_f \approx e^{-\frac{\eta}{2\sigma_a^2}}$$

In practice, the probabilities for each hypothesis to be present are equal so that the total probability of making wrong decisions on H_b is

(5-84) $$P_e \approx 0.5\, e^{-\frac{\eta}{2\sigma_a^2}} + 0.5\,(1 - e^{-\frac{\eta}{2\sigma_b^2}})$$

The error would be 0.5 if the threshold is set at zero or at infinity. Solving $\partial P_e/\partial \eta = 0$ for η, we find that the lowest total detection error by adjusting the threshold is obtained when

(5-85) $$\eta = 2\frac{\sigma_a^2\,\sigma_b^2}{\sigma_b^2-\sigma_a^2}\ln\left(\frac{\sigma_b^2}{\sigma_a^2}\right)$$

$$= 2\frac{(\alpha_b+1)^2}{\sigma_\Gamma^2}\ln(\alpha_b+1) \triangleq \eta_o$$

At $\eta = \eta_b$, we denote P_d and P_f by $P_d(\eta_b)$ and $P_f(\eta_b)$, respectively. When $\eta = \eta_o$, the two probabilities are related by

$$(5\text{-}86) \qquad P_f(\eta_o) = \frac{\sigma_a^2}{\sigma_b^2} \cdot P_d(\eta_o) = \frac{P_d(\eta_o)}{\alpha_b + 1}$$

where

$$(5\text{-}87) \qquad P_d(\eta_o) = \left(\frac{\sigma_b^2}{\sigma_a^2}\right)^{\frac{\sigma_a^2}{\sigma_a^2 - \sigma_b^2}} = (\alpha_b + 1)^{-\frac{1}{\alpha_b}}$$

The corresponding probability of making wrong decisions on H_b then is

$$(5\text{-}88) \qquad p_e(\eta_o) = 0.5 - 0.5 \cdot \frac{\alpha_b}{\alpha_b + 1} \cdot (\alpha_b + 1)^{-\frac{1}{\alpha_b}}$$

In Eq. (5-55), the parameter α_b is expressed in terms of τ and ν. The delay times τ and ν depend on the incident angles θ and ϕ; so does the optimum spacing. For a given spacing d and the array size m, the ratio d/d_{op} varies with the angles θ and ϕ. Thus the parameter α_b may be written as a function of the normalized spacing d/d_{op},

$$(5\text{-}89) \qquad \alpha_b \approx \frac{\sigma_\Gamma^2}{h_w} \cdot \left\{ m - \frac{1}{m + \frac{h_w}{h_n}} \cdot \frac{\sin^2\left(\frac{d}{d_{op}}\pi\right)}{\sin^2\left(\frac{d}{d_{op}} m\pi\right)} \right\} \cdot \frac{\sigma_\Gamma^2 \int_{-T}^{T} e_b^2(t)dt}{2h_w}$$

We next compare the detection errors $P_e(\eta_o)$ for the systems use the same array size but are designed to be optimum for the different spacings. We shall plot the error $p_e(\eta_o)$ against the normalized spacing. In plotting the curve, we assign values to (S/N) and h_n/h_w. By doing this, the signal energy to the internal noise power density ratio is specified alternatively by

$$(5\text{-}90) \qquad \frac{\sigma_\Gamma^2 \int_{-T}^{T} e_b^2(t) \cdot dt}{h_w} = (S/N) \cdot \left(1 + \frac{h_n}{h_w}\right)$$

In Fig. 5-13 we show $P_e(\eta_o)$ vs d/d_{op}, where $0.2 \leq d/d_{op} \leq 2$, for m=2. The values used for S/N and h_n/h_w are 10 and 31.61, respectively. In Fig. 5-13, $P_e(\eta_o)$ becomes minimum when the

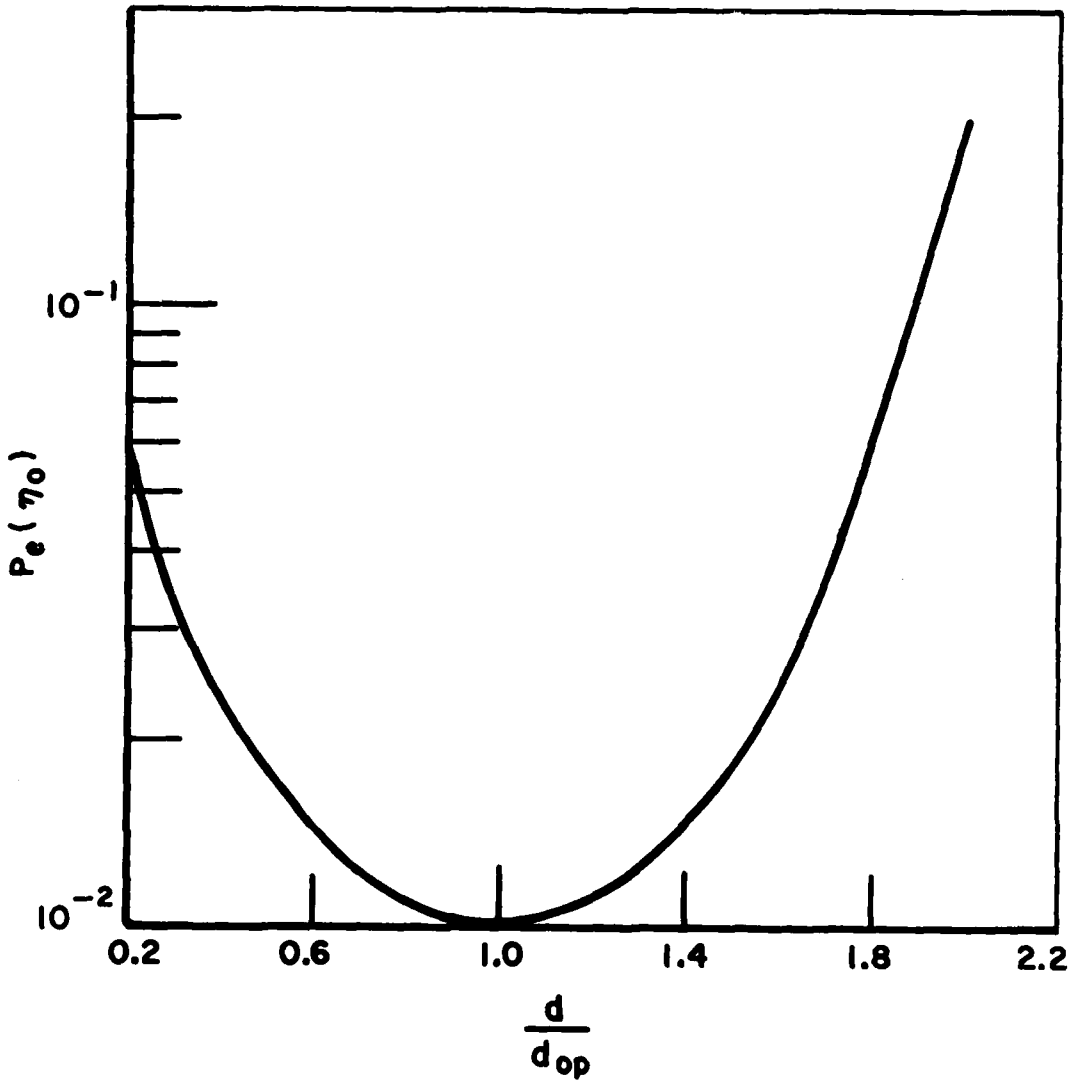

Fig. 5-13--$P_e(\eta_0)$ vs. d/d_{op} given m=2, h_n/h_w=31.61 and (S/N)=10.

normalized spacing is equal to 1, i.e., when the optimum spacing is used by the detection system. The same type of curves given m=4 and 8 are shown in Fig. 5-14 and Fig. 5-15, respectively. Again, the detection errors $P_e(\eta_0)$ assume the lowest value at $d = d_{op}$.

The reason for the detector designed for an optimum spacing to have the fewest decision mistakes can be explained mathematically by the behavior of $P_e(\eta_0)$. In Eq. (5-88) we see that $P_e(\eta_0)$ decreases as α_b increases. Varying the spacing d, we find that

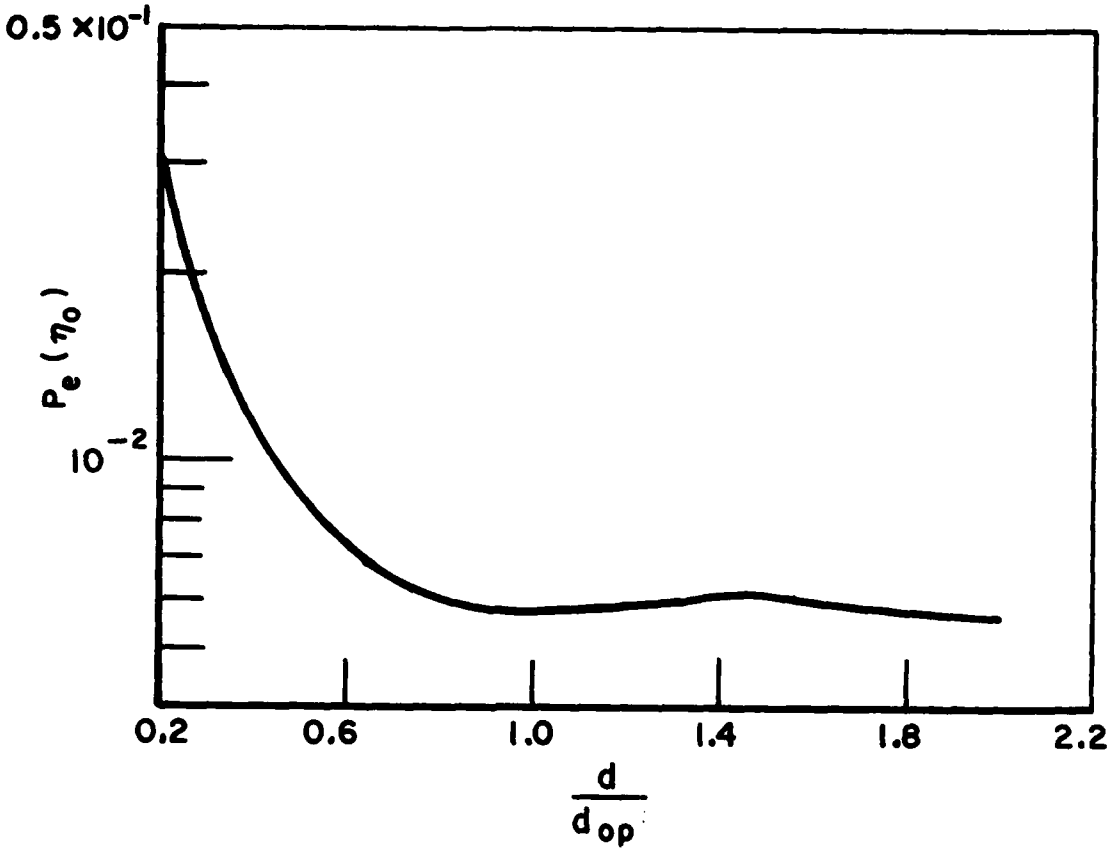

Fig. 5-14--$P_e(\eta_o)$ vs. d/d_{op} given m=4, h_w/h_n=31.61 and (S/N)=10.

α_b reaches the maximum at $d=d_{op}$. Hence the error $P_e(\eta_o)$ reaches the minimum at this particular spacing.

It was pointed out in Section V.D that α_b is proportional to the component contributed to the output of the subprocessor $L_{bu}(r)$ by the desired signal. The ability for the internal noise and external interference to affect the decisions becomes less effective when α_b gets large. Hence, the detection error is minimized when an optimum spacing is employed to design the detector. For the rest of this section, we use $P_e(\text{min})$ to denote the total error rate for the system which sets the threshold at η_o^2 and is designed for an optimum spacing.

To emphasize, $P_e(\text{min})$ is the lowest detection error we can possibly obtain for a given array size and the signal energy to the internal noise power density ratio. Moreover, the error $P_e(\text{min})$ is not affected by the incident angles θ and ϕ. The reason is that the parameters α_b, β_b and γ_b are not dependent on θ and ϕ when the system is designed for an optimum spacing.

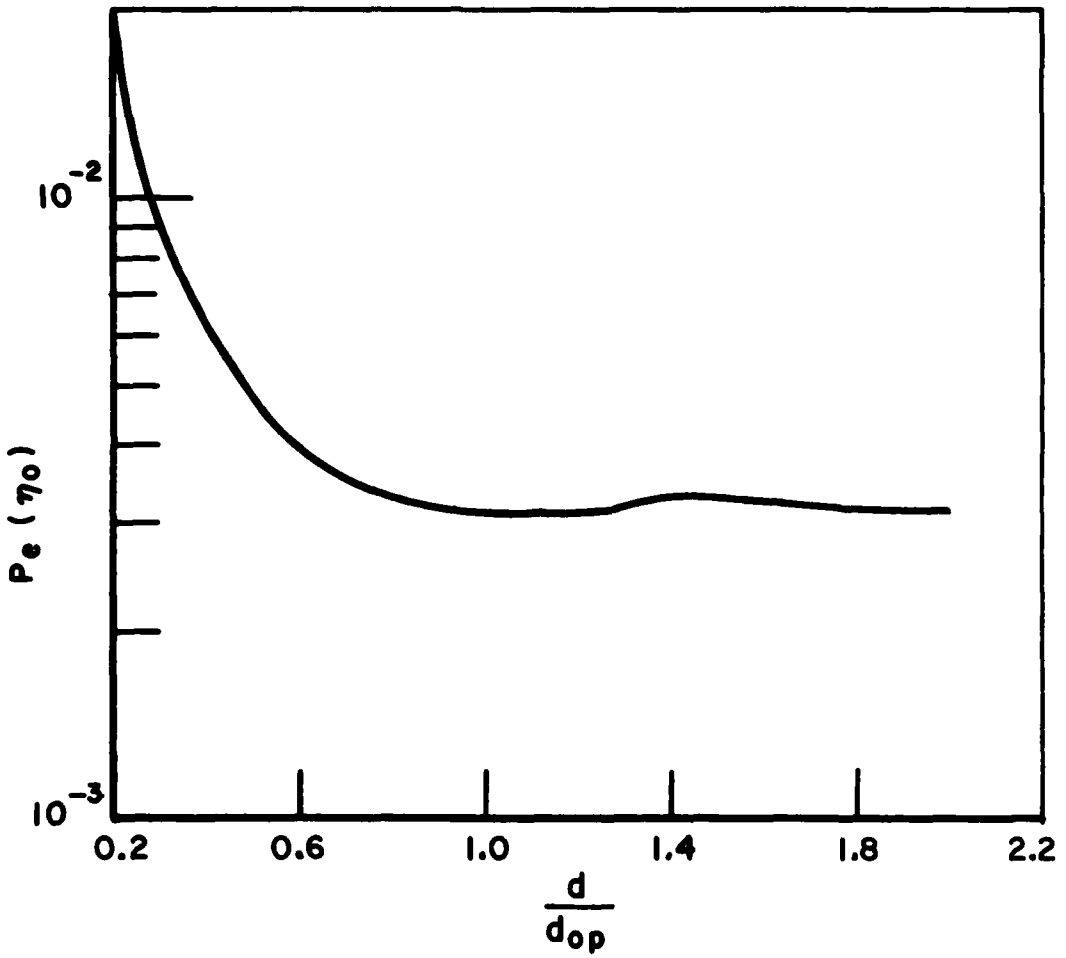

Fig. 5-15--$P_e(\eta_o)$ vs. d/d_{op} given m=8, h_n/h_w=31.61 and (S/N)=10.

Up to this point in this section, the interfering signal is assumed to have a flat power spectrum. The conditions used to get Eq. (5-56) through Eq. (5-88) are $\gamma_b=0$ and $\alpha_b=\beta_b$ which are correct because the interference is a white noise process. In Section V.D we formally show that regardless of the power spectrum these conditions are automatically satisfied for the system designed for the optimum spacing for a given θ,ϕ and m. Hence, replacing α_b by $\hat{\alpha}_b$ in Eq. (5-56) through Eq. (5-88), we obtain the corresponding equations valid for the system designed for the optimum spacing and optimized for an arbitrary power spectrum. The error P_e(min) associated with this detection system is equal to

$$(5\text{-}91) \qquad P_e(\min) = 0.5 - 0.5 \cdot \frac{\tilde{\alpha}_b}{\tilde{\alpha}_b + 1} \left(\tilde{\alpha}_b + 1\right)^{-\frac{1}{\tilde{\alpha}_b}}$$

where

$$(5\text{-}92) \qquad \tilde{\alpha}_b = \frac{m}{2} \cdot \frac{\sigma_\Gamma^2 \int_{-T}^{T} e_b^2(t) \cdot dt}{h_w}$$

Since $\tilde{\alpha}_b$ is invariant to the power spectrum of the interfering signal, it is apparent that this lowest possible error $P_e(\min)$ does not change from one power spectrum to another. Equation (5-92) indicates that the detection error $P_e(\min)$ is uniquely determined by the array size m and the signal energy to the internal noise power density ratio.

We next show the curves of $P_e(\min)$ of several detectors. In plotting these curves, we assume that h_n is constant so that the values assigned to the spectral height ratio h_n/h_w and ratio (S/N) specify the desired signal energy to the internal white noise power density ratio. For a given h_n/h_w, the relation between (S/N) and the signal energy to the internal noise power density ratio is given by Eq. (5-90). Since we shall plot $P_e(\min)$ against (S/N), the relation between (S/N) and the signal energy to the internal noise power density ratio is shown in Fig. 5-16 for convenience.

The error $P_e(\min)$ vs. S/N given m=2 is shown in Fig. 5-17. The values chosen for the spectral height ratio h_n/h_w are 3.161, 10, 31.61 and 100. For a given S/N, the error rate $P_e(\min)$ drops as the ratio h_n/h_w drops. Physically, this means that the lowest possible detection error decreases if the internal noise level decreases. In Chapter IV, we have concluded that the internal noise degrades the performance of the optimum detector L(R). Here we find that the internal noise affects the detector $\Lambda(r)$ in the same manner. For a constant internal noise level, we may either increase the array size or raise the desired signal level for improving the error rate performance. The same type of curves given m=4, 8 and 15 are shown in Fig. 5-18 through Fig. 5-20. It is observed that $P_e(\min)$ drops steadily as the array size increases from 2 to 15.

The lowest detection error available to the detector $\Lambda(r)$ is far greater than the error provided by the system L(R) for detecting the completely known binary signals. The reason for having such a large difference is obviously attributed to the random phase and random amplitude which inevitably cause many decision mistakes for the detector $\Lambda(r)$.

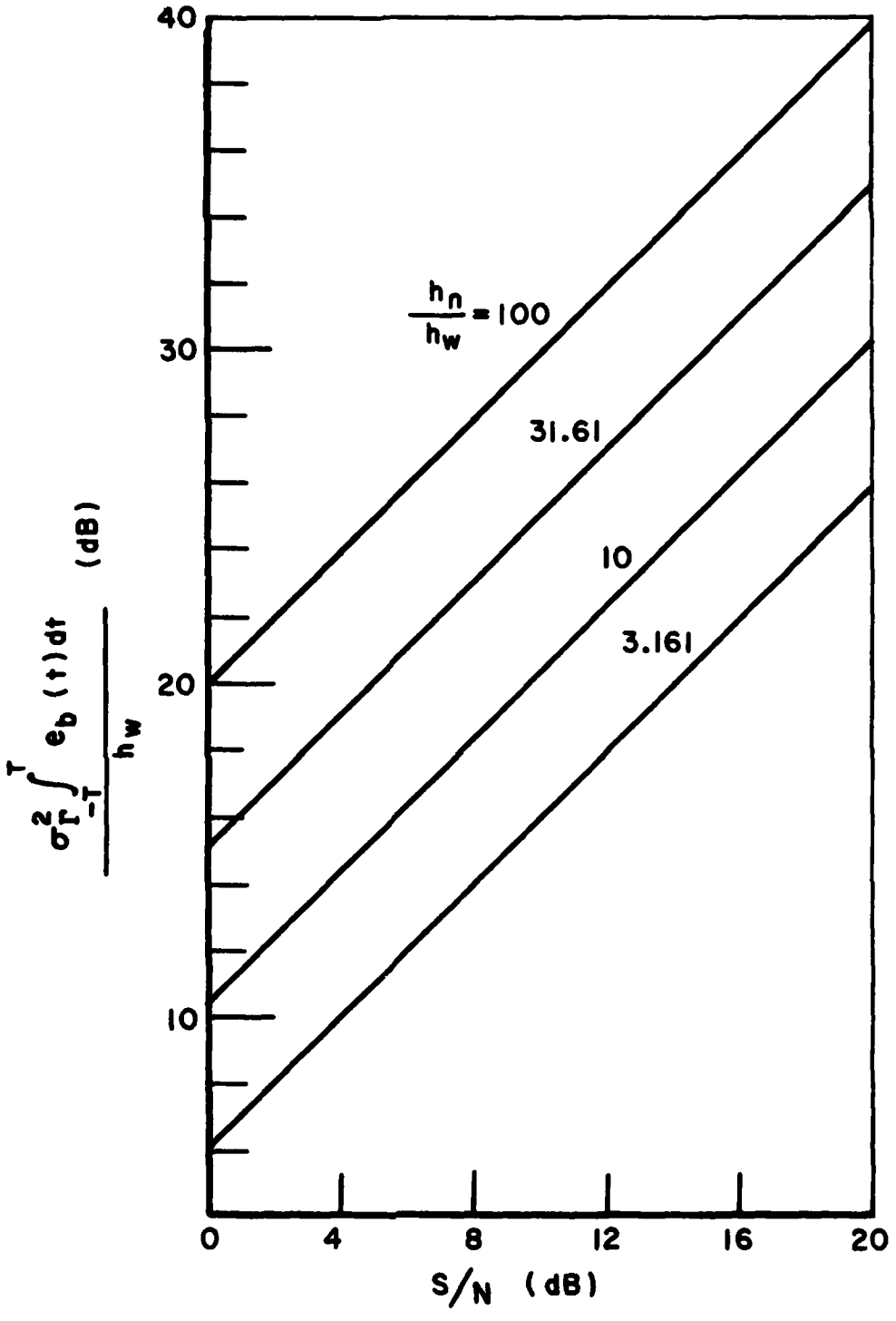

Fig. 5-16--(S/N) vs. $\sigma_T^2 \cdot h_w^{-1} \cdot \int_{-T}^{T} e_b^2(t) \cdot dt$.

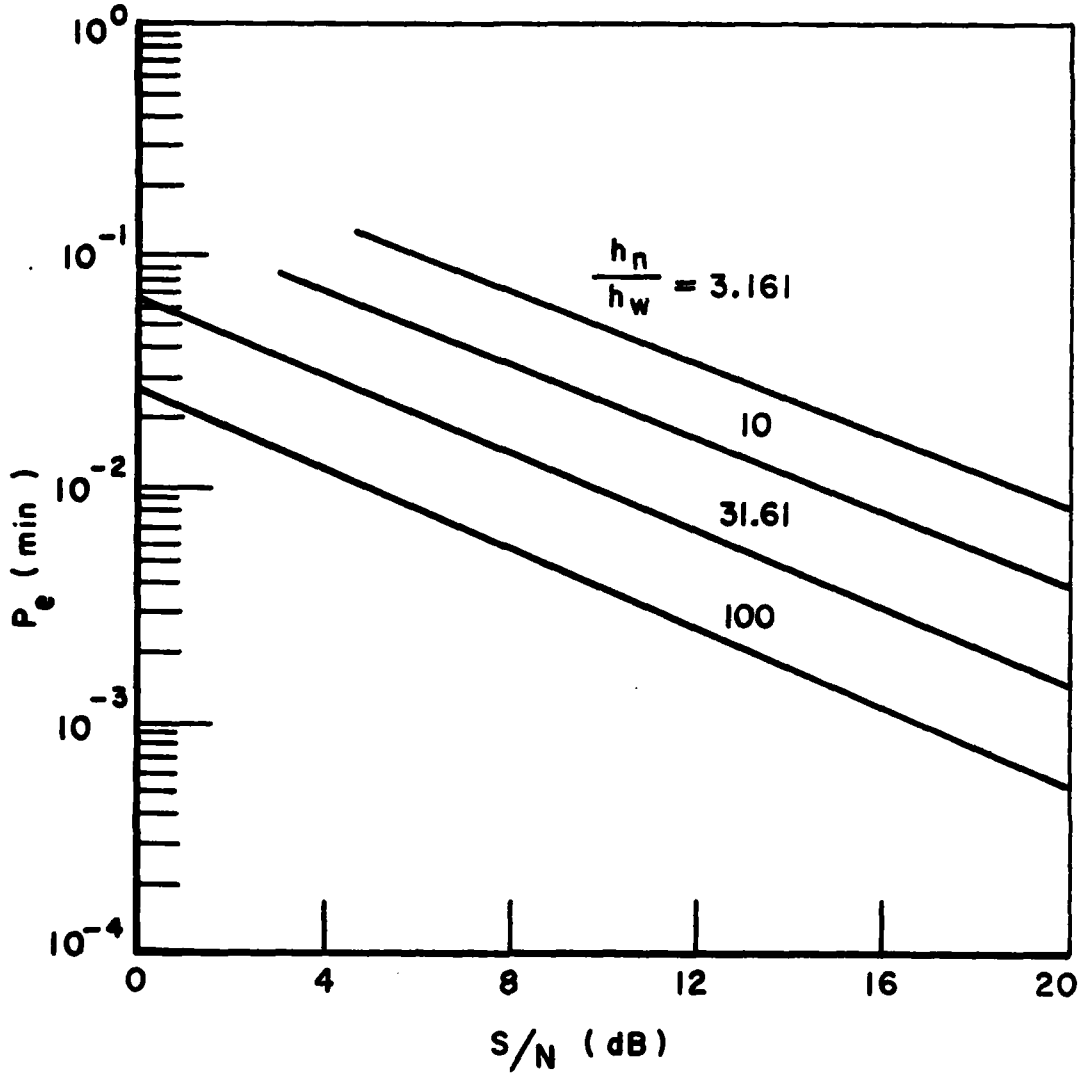

Fig. 5-17--P_e(min) vs. (S/N) given m=2.

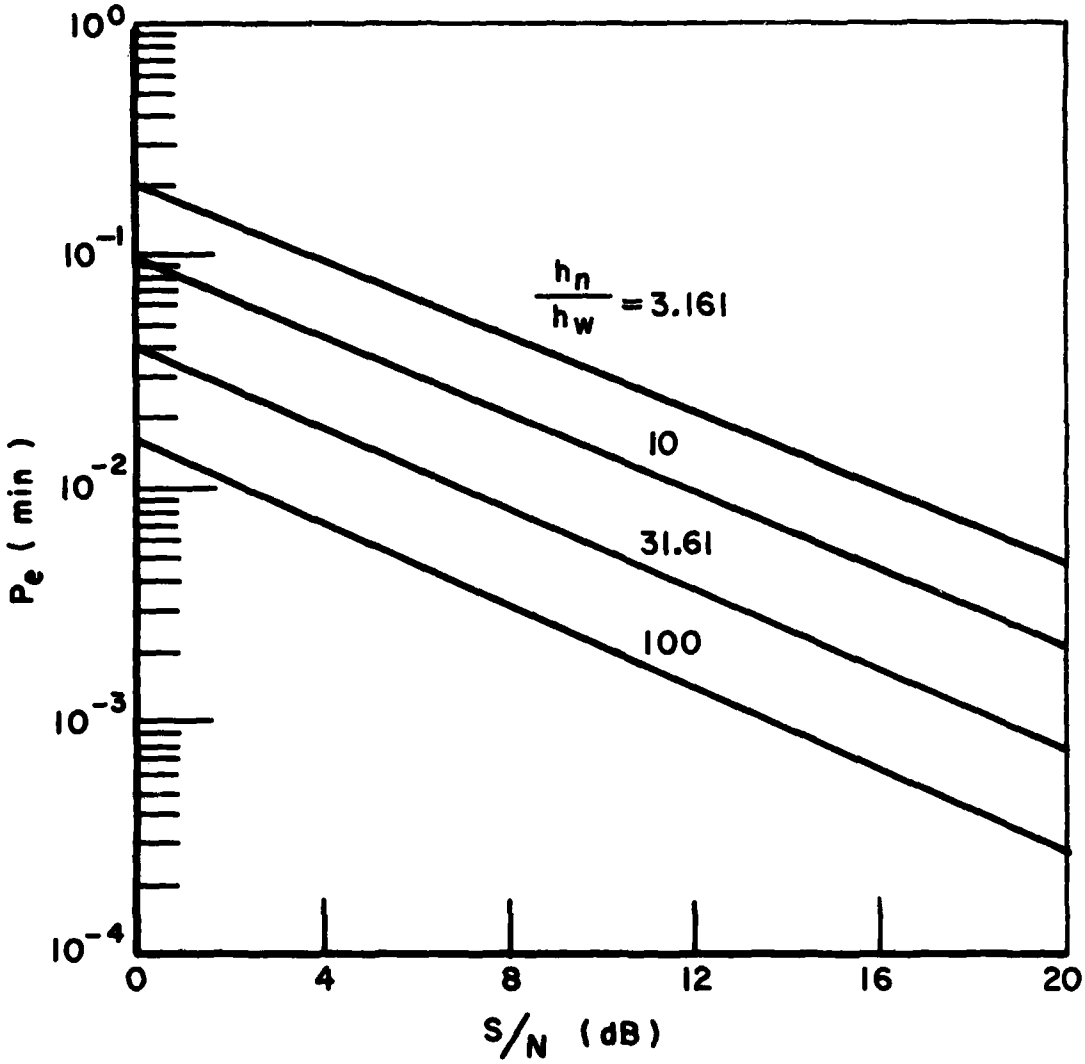

Fig. 5-18--P_e(min) vs. (S/N) given m=4.

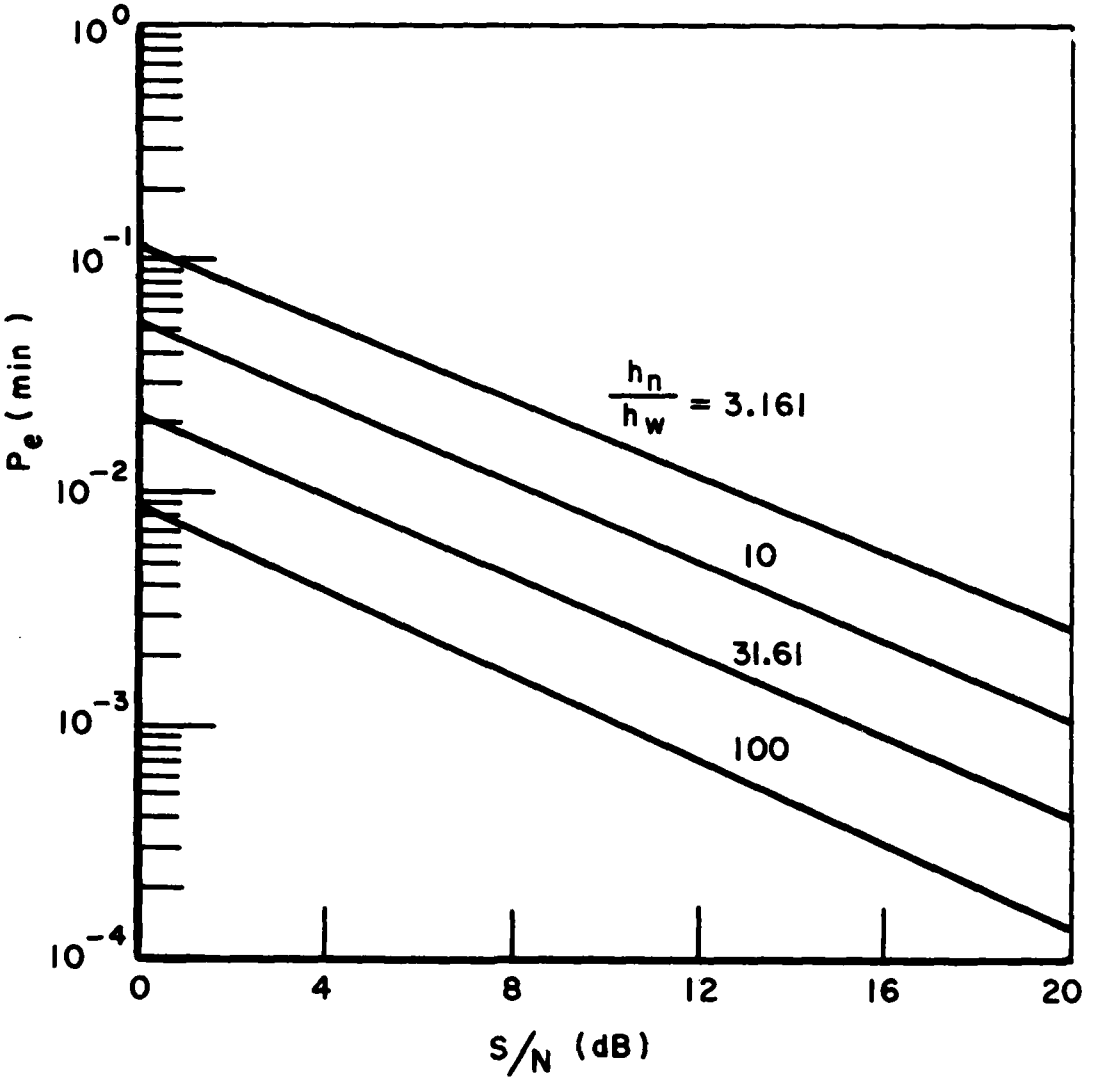

Fig. 5-19--P_e(min) vs. (S/N) given m=8.

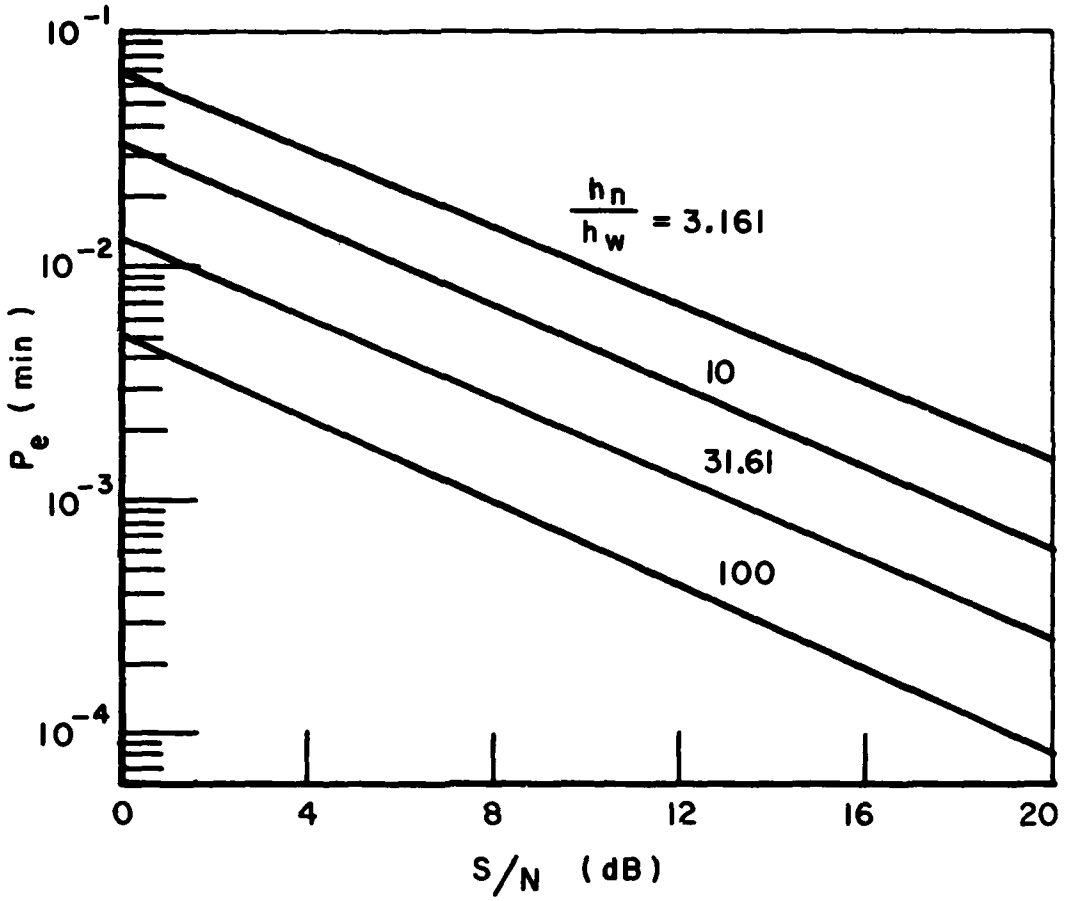

Fig. 5-20--P_e(min) vs (S/N) given m=15.

CHAPTER VI
ON SYSTEMS DESIGNED FOR THE OPTIMUM SPACING

A. The Interference-Free Spacing

When the desired binary signals are known exactly, we have concluded from the detection error given in Eq. (3-32) that the number of wrong decisions is minimized when the detection system is designed for the optimum spacing. The same conclusion is also obtained for the random phase and amplitude ASK binary detector discussed in the last chapter. In this section, we examine $L(R)$, $L_{bu}(r)$ and $L_{bv}(r)$ for a unified explanation for this phenomenon. It will become clear later, the optimum spacing may be called the interference-free spacing.

The definitions for the random variables $L(R)$, $L_{bu}(r)$ and $L_{bv}(r)$ are very similar. They may be represented by the general expression L_g given below

(6-1)

$$L_g \triangleq \int_{-T}^{T} \sum_{i=1}^{m} r_i(t_i) g_i(t_i) \cdot dt$$

$$- \sum_{\ell=1}^{\infty} \frac{1}{m + \dfrac{h_w}{\lambda_\ell - h_w}} \cdot \int_{-T}^{T} \phi_\ell(t) \cdot \sum_{i=1}^{m} r_i(t_i) dt \cdot$$

$$\cdot \int_{-T}^{T} \phi_\ell(z) \sum_{j=1}^{m} g_j(z_j) \cdot dz$$

because $L(R) = L_g$ if $g(t) = s(t)$, $L_{bu}(r) = L_g$ if $g(t) = u_b(t)$ and $L_{bv}(r) = L_g$ when $g(t) = -v_b(t)$. When optimum-spaced arrays are used in both detection systems, we have shown in Section IV.F and Section V.D that

$$\sum_{i=1}^{m} g_i(\tilde{t}_i) = 0 \tag{6-2}$$

and

$$\sum_{i=1}^{m} u_{bi}(\tilde{t}_i)\, v_{bi}(\tilde{t}_i) = 0 \tag{6-3}$$

In Eq. (6-1), as a result of using an optimum-spaced array, the second term, which reflects the characteristics of the interference, vanishes. Hence,

$$(6\text{-}4) \qquad \tilde{L}(R) = \int_{-T}^{T} \sum_{i=1}^{m} r_i(\tilde{t}_i)\, s_i(\tilde{t}_i) \cdot dt$$

$$(6\text{-}5) \qquad \tilde{L}_{bu}(r) = h_w^{-1} \int_{-T}^{T} \sum_{i=1}^{m} r_i(\tilde{t}_i)\, u_{bi}(\tilde{t}_i) \cdot dt$$

and

$$(6\text{-}6) \qquad \tilde{L}_{bv}(r) = -h_w^{-1} \int_{-T}^{T} \sum_{i=1}^{m} r_i(\tilde{t}_i)\, v_{bi}(\tilde{t}) \cdot dt$$

Equation (6-4) through Eq. (6-6) imply that the sub-system which varies with the power spectrum of the interfering signal is no longer needed when the detection system is designed for the optimum spacing. The input to the ith channel under hypothesis H_b is

$$(6\text{-}7) \qquad r_i(\tilde{t}_i) = n\,[t-(m-1)\nu] + w_i(\tilde{t}_i) + b_i(\tilde{t}_i)$$

where the signal b(t) is assumed to be deterministic if $r_i(\tilde{t}_i)$ is substituted into Eq. (6-4), and b(t) is assumed to have a random phase and amplitude when $r_i(t_i)$ is substituted into Eq. (6-5) and Eq. (6-6).

Substituting $r_i(\tilde{t}_i)$ into Eq. (6-4) and simplifying the equation by using Eq. (6-2), we obtain

(6-8)

$$\tilde{L}(R) = \int_{-T}^{T} \sum_{i=1}^{m} b_i(\tilde{t}_i)\, s_i(\tilde{t}_i) \cdot dt + \int_{-T}^{T} \sum_{i=1}^{m} b_i(\tilde{t}_i)\, w_i(\tilde{t}_i) \cdot dt$$

Similarly,

(6-9)

$$\tilde{L}_{bu}(r) = x \cdot \int_{-T}^{T} \sum_{i=1}^{m} u_{bi}^2(\tilde{t}_i)dt + \int_{-T}^{T} \sum_{i=1}^{m} u_{bi}(\tilde{t}_i)\, w_i(\tilde{t}_i) \cdot dt$$

and

(6-10)

$$L_{bv}(r) = y \cdot \int_{-T}^{T} \sum_{i=1}^{m} v_{bi}^2(\tilde{t}_i) \cdot dt - \int_{-T}^{T} \sum_{i=1}^{m} v_{bi}(\hat{t}_i) w_i(\tilde{t}_i) \cdot dt$$

The simplified versions of $\tilde{L}(R)$, $\tilde{L}_{bu}(r)$ and $\tilde{L}_{bv}(r)$ do not contain the external interfering signal $n(t)$. This implies that the influence from the interference in the decision process is eliminated completely by the processor when the detector is designed for an optimum spacing. When the processor output $\tilde{L}(R)$ is compared to the threshold to make decisions, only the internal white noise $w_i(t)$ can cause decision mistakes for the case when the desired signals are completely known. For signals with random amplitude and phase, the uncertainty in the values of x and y also cause decision errors. This explains why the detection error for the optimum system $\Lambda(r)$ is far greater than the system $L(R)$. But, nevertheless, all of $\tilde{L}(R)$, $\tilde{L}_{bu}(r)$ and $\tilde{L}_{bv}(r)$ are interference free. Physically, we may say that the optimum spacing is an interference-free spacing. For a given m, h_w, etc., it is this very property which enables the detector designed for an optimum spacing to have the lowest detection error. Because the eigenfunctions do not appear in $\tilde{L}(R)$, $\tilde{L}_{bu}(r)$ and $\tilde{L}_{bv}(r)$ any more, the structures for detectors $\tilde{L}(R)$ and $\hat{\Lambda}(r)$ do not vary from one power spectrum to another.

B. FSK Binary Detector

Equation (5-2) represents FSK binary signals when $\omega_a \neq \omega_b$. In practice, the carrier frequency under one hypothesis differs from that under the other only slightly. Also, it is a general practice to use identical modulating signals for both hypotheses. Let

(6-11) $\quad e_k(t) = e(t), \quad k = a \text{ and } b,$

and

(6-12) $\quad \omega_k = \omega_o + \varepsilon_k \omega_d \ ,$

where $\omega_d << \omega_o$, $\varepsilon_k = -1$ under hypothesis H_a and $\varepsilon_k = 1$ under hypothesis H_b. For simplicity, we define

(6-13) $\quad u_o(t) \triangleq e(t) \cdot \cos \omega_o t$

and

$$(6\text{-}14) \qquad v_o(t) \triangleq e(t) \cdot \sin \omega_o t$$

Then, from Eq. (5-6), we have

$$(6\text{-}15) \qquad u_k(t) = u_o(t) \cdot \cos \omega_d t - \varepsilon_k \cdot v_o(t) \cdot \sin \omega_d t$$

and

$$(6\text{-}16) \qquad v_k(t) = \varepsilon_k \cdot u_o(t) \cdot \sin \omega_d t + v_o(t) \cdot \cos \omega_d t$$

In this section, we investigate the form of the optimum system for detecting the FSK binary signals in Eq. (5-2) when the spacing chosen for the array is equal to the optimum spacing defined in terms of the wavelength λ_o associated with the angular frequency λ_o. More precisely,

$$(6\text{-}17) \qquad d_{op} \triangleq \frac{\lambda_o}{m\,|\cos\theta - \cos\phi|}$$

At this particular spacing, if $|\cos\theta - \cos\phi|$ is not too small, negligible error will be introduced if we approximate

$$(6\text{-}18) \qquad \omega_d[t - (m-1)\nu - (i-1)(\tau-\nu)] \approx \omega_d t$$

Consequently, $u_{ki}(\tilde{t}_i)$ and $v_{ki}(\tilde{t}_i)$ may be approximated by

$$(6\text{-}19) \qquad u_{ki}(\tilde{t}_i) \approx u_{oi}(\tilde{t}_i) \cdot \cos \omega_d t - \varepsilon_k \cdot v_{oi}(\tilde{t}_i) \cdot \sin \omega_d t$$

and

$$(6\text{-}20) \qquad v_{ki}(\tilde{t}_i) \approx \varepsilon_k \cdot u_{oi}(\tilde{t}_i) \cdot \sin \omega_d t + v_{oi}(\tilde{t}_i) \cdot \cos \omega_d t$$

respectively. Since $\sum_{i=1}^{m} u_{oi}(\tilde{t}_i) = \sum_{i=1}^{m} v_{oi}(\tilde{t}_i) = 0$, we conclude from Eqs. (6-19) and (6-20) that

$$(6\text{-}21) \qquad \sum_{i=1}^{m} u_{ki}(\tilde{t}_i) = 0$$

$$(6\text{-}22) \qquad \sum_{i=1}^{m} v_{ki}(\tilde{t}_i) = 0$$

and

$$(6\text{-}23) \qquad \sum_{i=1}^{m} u_{ki}(\tilde{t}_i)\, v_{ki}(\tilde{t}_i) = 0 \,.$$

The eigenfunction-dependent terms once again drop out of the equation of the test variables $L_{ku}(r)$ and $L_{kv}(r)$; so we find

$$(6\text{-}24) \qquad \tilde{L}_{ku}(r) = h_w^{-1} \int_{-T}^{T} \sum_{i=1}^{m} r_i(\tilde{t}_i)\, u_{ki}(\tilde{t}_i) \cdot dt$$

and

$$(6\text{-}25) \qquad \tilde{L}_{kv}(r) = -h_w^{-1} \int_{-T}^{T} \sum_{i=1}^{m} r_i(\tilde{t}_i)\, v_{ki}(\tilde{t}_i) \cdot dt$$

where $u_{ki}(\tilde{t}_i)$ and $v_{ki}(\tilde{t}_i)$ are given by Eq. (6-19) and Eq. (6-20), respectively. $L_{ku}(r)$ and $\tilde{L}_{kv}(r)$ can be shown free from interfering signal. For this reason, it is believed that the FSK binary detector designed for an optimum spacing also provides the lowest detection error. Because an identical modulating signal is employed under each hypothesis, we know that

$$(6\text{-}26) \qquad \tilde{\alpha}_k = \tilde{\beta}_k = \frac{\sigma_\Gamma^2}{h_w} \cdot m \cdot \int_{-T}^{T} \frac{e^2(t)}{2}\, dt \,, \quad k = a \text{ and } b.$$

Hence,

$$(6\text{-}27) \qquad \tilde{\mu}_a(\alpha,\beta,\gamma) = \tilde{\mu}_b(\alpha,\beta,\gamma)$$

Resetting the threshold, from Eq. (5-24), we obtain a reduced likelihood ratio test for FSK binary signals received by an optimum-spacing array,

(6-28) $$\tilde{\Lambda}_{fsk}(r) \triangleq \tilde{L}^2_{bv}(r) + \tilde{L}^2_{bu}(r) - \tilde{L}^2_{av}(r) - \tilde{L}^2_{au}(r)$$

$$\underset{H_a}{\overset{H_b}{\gtrless}} \text{ threshold}$$

Writing $\tilde{L}_{ku}(r)$ and $\tilde{L}_{kv}(r)$ directly in terms of $u_{oi}(\tilde{t}_i)$ and $v_{oi}(\tilde{t}_i)$, and substituting the new equations for $\tilde{L}_{ku}(r)$ and $\tilde{L}_{kv}(r)$ into Eq. (6-28), we obtain a simpler optimum detector:

(6-29)

$$\tilde{\Lambda}_{fsk}(r) = \int_{-T}^{T} \Lambda_u(\tilde{t}_i) \cdot \sin \omega_d t \cdot dt \cdot \int_{-T}^{T} \Lambda_v(\tilde{t}_i) \cdot \cos \omega_d t \cdot dt$$

$$- \int_{-T}^{T} \Lambda_u(\tilde{t}_i) \cdot \cos \omega_d t \cdot dt \cdot \int_{-T}^{T} \Lambda_v(\tilde{t}_i) \cdot \sin \omega_d t \cdot dt$$

$$\underset{H_a}{\overset{H_b}{\gtrless}} \text{ threshold}$$

where

$$\Lambda_u(\tilde{t}_i) = \sum_{i=1}^{m} r_i(\tilde{t}_i)\, u_{oi}(\tilde{t}_i)$$

and

(6-30) $$\Lambda_v(\tilde{t}_i) = \sum_{i=1}^{m} r_i(\tilde{t}_i)\, v_{oi}(\tilde{t}_i)$$

B. On General Random Phase and Random Amplitude Detector

In this section, we shall briefly discuss the optimum detector for detecting the binary signals whose amplitudes and phases are distributed differently from what were assumed in the last chapter.

In theory, the joint probability density function of the random variables x and y defined in Eq. (5-4) and Eq. (5-5) may be determined once the statistics for the amplitude and the phase are specified. Let the joint density be p(x,y). The density of R is obtained by averaging the conditional density Eq. (5-12) over x and y. For simplicity, we define

$$\iint p(x,y) \cdot e^{\frac{-x^2\alpha_k' - y^2\beta_k' + 2xy\gamma_k'}{2} + x L_{ku}(r) + y L_{kv}(r)} \cdot dx\, dy$$

$$\triangleq p[L_{ku}(r),\ L_{kv}(r),\ \alpha_k',\ \beta_k',\ \gamma_k';\ C_{xy}]$$

where α_k', β_k' and γ_k' are equal to α_k, β_k and γ_k respectively if $\sigma_r^2 = 1$, and C_{xy} represents all parameters which characterize the random variables x and y. Then the density of R under hypothesis H_k, k=a and b, is equal to

$$p(R|H_k) = \lim_{N\to\infty} \frac{e^{L_r(r)}}{\sqrt{(2\pi)^{mN}\ |K|}} \cdot p[L_{ku}(r),\ L_{kv}(r),\ \alpha_k',\ \beta_k',\ \gamma_k',\ C_{xy}]$$

and the likelihood ratio test takes the following general expression

(6-31)

$$LRT = \frac{p[L_{bu}(r), L_{bv}(r),\ \alpha_b',\ \cdots,\ C_{xy}]}{p[L_{au}(r), L_{av}(r),\ \alpha_a'\ \cdots,\ C_{xy}]}$$

$$\triangleq f[L_{bu}(r), L_{bv}(r), \cdots, L_{au}(r), L_{av}(r), \cdots \alpha_b', \alpha_a',\ \cdots,\ C_{xy}]$$

$$\underset{H_a}{\overset{H_b}{\gtrless}} \text{ threshold}$$

If we implement the function $f[\cdot]$, we obtain the optimum detection system. Since $f[\cdot]$ is expressed as a function of α_b', $L_{bu}(r)$, $L_{av}(r)$, etc., evidently, the sub-processors which compute $L_{ku}(r)$ and $L_{kv}(r)$, k=a and b, for the system $\Lambda_g(r)$ are again required by this general optimum detection system Eq. (6-31). In other words, the basic building blocks for the random phase and random amplitude binary detector do not change with the assumptions on the amplitude and phase. But how the outputs of these sub-processors should be processed is determined by the function p(x,y) because $f[\cdot]$ does vary with p(x,y). We have demonstrated that the variables $L_{ku}(r)$ and $L_{kv}(r)$ are free from the interference if the detector $\Lambda(r)$ is designed for an optimum spacing. Even though the formula for the detection error of the system $f[\cdot]$ is not known, there is a reason to believe that for a given array size m, spectral height h_w, etc. the lowest detection error will be provided by the system designed for an optimum spacing.

If we set $\phi_s=0$ in Eq. (5-2), then the binary signals would contain one random parameter which is the amplitude. From Eqs. (5-4) and (5-5) we find that y=0 when $\phi_s=0$. Hence the conditional density for R under H_k becomes

$$(6\text{-}32) \qquad p(R|x,H_k) = \lim_{N\to\infty} \frac{e^{L_r(r)}}{\sqrt{(2\pi)^{mN}|K|}} e^{-\frac{x^2 d'}{2} + xL_{ku}(r)}$$

Accordingly, the likelihood ratio test associated with the random amplitude binary signals is equal to

$$(6\text{-}33) \qquad LRT = \frac{\int p(x) \cdot e^{-\frac{x^2\alpha_b'}{2} + x\, L_{bu}(r)} \cdot dx}{\int p(x) \cdot e^{\frac{-x^2\alpha_a'}{2} + 2\, L_{au}(r)} \cdot dx}$$

Hence, the sub-processors which compute $L_{au}(r)$ and $L_{bu}(r)$ in the system $\Lambda_g(r)$ are the building blocks for the random-amplitude binary detector.

For most cases of interest, the analytic solutions for the likelihood ratio test are not obtainable. As a result, various types of approximations may be needed.

CHAPTER VII
CONCLUSIONS

The goal of this research was to find the optimum detection system for detecting corrupted binary signals received by a linear antenna array in an effort to minimize the detection error. The binary signals may either be completely known or have a random amplitude, which is Rayleigh distributed, and a random phase, uniformly distributed between $-\pi$ and π. The approach used to determine the optimum system was to perform the likelihood ratio test based on the statistical detection theory.

The results presented here are obtained from analytic solutions. It has been possible to obtain these solutions mainly because we have derived an analytic expression for the inverse of the covariance matrix K. Hence this research removes a mathematical difficulty encountered frequently in analyzing problems related to optimum space-time signal processing.

In the completely known signal case, the desired signals considered in Chapter III are the most general ones in the sense that the waveforms may have arbitrary expressions. Hence, the equations formulated for implementing the optimum processor and for determining the system performance are valid for the ASK, FSK and PSK binary signals.

For the case when the amplitude and phase of the desired signal are random, the equation needed for implementing the optimum processor was also derived. Since the phase was assumed uniformly distributed between $-\pi$ and π, the result can not be applied to the PSK binary signals. In general, we shall have to use a numerical method to determine the error rate performance of the system when the signal has a random phase and amplitude. But when the binary signal is an on-off keyed type, a simple analytic formula for the detection error is available.

The optimum processors for both cases are basically correlation receivers. In general, the structures for both types of processors are dependent on the power spectrum of the interfering signal.

The directional characteristics of both detection systems have been investigated through examining how the systems respond to a testing signal arriving from an arbitrary angle. We have found that both processors respond unfavorably to the testing signal in the sense that the processor outputs are suppressed if the signal propagates into the antenna array from the angle ϕ. When the testing signal arrives from the desired angle θ, the processor

outputs are high. The ability for each processor to favor the signal from the angle θ and to suppress the signal from the angle ϕ depends on the angular separation between θ and ϕ. It has been shown that this ability can be improved by either increasing the array size m or by adjusting the spacing d if the angles θ and ϕ are fixed.

The detection error is determined by the array size, the internal noise level, the desired signal power level and the spacing d for which the detection system is designed to be optimum. We have concluded that the detection error is minimized if the array elements are spaced at an optimum spacing, which is solely determined by θ, ϕ and m. The reason for this is that the processor outputs are interference-free when this particular spacing is chosen. Another advantage for using an optimum-spaced array is that the power-spectrum-dependent processing units can be removed from the processor without affecting the error rate performance. Hence, for a given array size, signal power level, and the spectral height h_w, the optimum detection system is also invariant to the power spectrum of the interfering signal.

In a realistic situation, there are always at least some parameters characterizing a communication signal that are not known. In Chapter III we have idealized the situation by assuming the binary signals to be completely known. The detector thus obtained represents an ideal case. The error rate associated with this case will be lower than that for signals with random parameters. Furthermore, this ideal detector is optimum in the sense that for a given condition (e.g., array size, spacing d, etc.) its detection error represents a lower bound for the performance that might be obtained with other types of array processing (such as with adaptive array techniques [24-26]). That is, the error rate given by Eq. (4-30) represents a lower bound for the detection error for all conceivable binary detectors.

When the phase and amplitude are distributed otherwise, we have formally shown that the new likelihood ratio is expressible in terms of random variables $L_{ku}(r)$ and $L_{kv}(r)$ and the parameters α_k, β_k and γ_k. For this reason, discussions given in the latter portion of this research are believed quite general.

APPENDIX A
A PROOF OF EQ. (2-36)

In this appendix, a simple proof of Eq. (2-36) is given. K^* and Q^* are the covariance matrix and its inverse, respectively.

$$K^* = \begin{bmatrix} K^*_{11} & K^*_{12} & \cdots & K^*_{1m} \\ K^*_{21} & K^*_{22} & \cdots & K^*_{2m} \\ \cdot & \cdot & & \cdot \\ \cdot & \cdot & & \cdot \\ \cdot & \cdot & & \cdot \\ K^*_{m1} & K^*_{m2} & \cdots & K^*_{mm} \end{bmatrix} \tag{A-1}$$

$$Q^* = \begin{bmatrix} Q^*_{11} & Q^*_{12} & \cdots & Q^*_{1m} \\ Q^*_{21} & Q^*_{22} & \cdots & Q^*_{2m} \\ \cdot & \cdot & & \cdot \\ \cdot & \cdot & & \cdot \\ \cdot & \cdot & & \cdot \\ Q^*_{m1} & Q^*_{m2} & \cdots & Q^*_{mm} \end{bmatrix} \tag{A-2}$$

The general expression for the submatrix G^*_{ij} of the product of K^* and Q^* is equal to

$$G^*_{ij} = \sum_{p=1}^{m} K^*_{ip} Q^*_{pj}, \quad 1 \le i, j \le m \tag{A-3}$$

We need to prove that G^*_{ij} is the null matrix if $i \neq j$ and G^*_{ii} is the identity matrix. It has been pointed out that both K^*_{ij} and Q^*_{ij} are diagonal, i.e.,

(A-4)

$$K^*_{ij} = \begin{bmatrix} k^*_{[(i-1)N+1][(j-1)N+1]} & 0 & \cdots & 0 \\ 0 & k^*_{[(i-1)N+2][(j-1)N+2]} & \cdots & 0 \\ \vdots & \vdots & & \vdots \\ 0 & 0 & \cdots & k^*_{[(i-1)N+N][(j-1)N+N]} \end{bmatrix}$$

and

(A-5)

$$Q^*_{ij} = \begin{bmatrix} q^*_{[(i-1)N+1][(j-1)N+1]} & 0 & \cdots & 0 \\ 0 & q^*_{[(i-1)N+2][(j-1)N+2]} & \cdots & 0 \\ \vdots & \vdots & & \vdots \\ 0 & 0 & \cdots & q^*_{[(i-1)N+N][(j-1)N+N]} \end{bmatrix}$$

The product of K^*_{ij} and Q^*_{ij} is also diagonal. In terms of the elements of K^*_{ij} and Q^*_{ij}, $g^*_{ij\ell\ell}$, the element of G^*_{ij} at $\ell\ell$ position is equal to

$$(A\text{-}6)\quad g^*_{ij\ell\ell} = \sum_{p=1}^{m} k^*_{[(i-1)N+\ell][(p-1)N+\ell]}\, q^*_{[(p-1)N+\ell][(j-1)N+\ell]}$$

From Eqs. (2-28) and (2-33), we have

$$(A\text{-}7)\quad k^*_{[(i-1)N+\ell][(p-1)N+\ell]} = \lambda_\ell - (1-\delta_{ip})h_w$$

Substituting Eqs. (A-7) and (2-36) into Eq. (A-6), yields

$$(A\text{-}8)\quad g^*_{ij\ell\ell} = \sum_{p=1}^{m}\left(\lambda_\ell - (1-\delta_{ip})h_w\right)\cdot\left(\frac{\delta_{ij}}{h_w} - \frac{\lambda_\ell - h_w}{h_w[m\lambda_\ell-(m-1)h_w]}\right)$$

For $i\neq j$, we have

$$g^*_{ij\ell\ell} = \frac{-(m-2)(\lambda_\ell-h_w)^2}{h_w[m\lambda_\ell-(m-1)h_w]} - \frac{\lambda_\ell(\lambda_\ell-h_w)}{h_w[m\lambda_\ell-(m-1)h_w]}$$

$$+ \frac{(\lambda_\ell-h_w)[\lambda_\ell+(m-2)(\lambda_\ell-h_w)]}{h_w[m\lambda_\ell-(m-1)h_w]} = 0$$

Hence, G^*_{ij}, $i\neq j$, is equal to the null matrix. If $i=j$, we have

$$g^*_{ii\ell\ell} = \frac{-(m-1)(\lambda_\ell-h_w)^2}{h_w[m\lambda_\ell-(m-1)h_w]} + \frac{\lambda_\ell[\lambda_\ell+(m-2)(\lambda_\ell-h_w)]}{h_w[m\lambda_\ell-(m-1)h_w]}$$

$$= 1\ .$$

Hence, G^*_{ij} equals the identity matrix. We complete the proof that Eq. (2-36) is correct.

APPENDIX B
THE STATISTICS OF L(R), $L_{ku}(r)$ and $L_{kv}(r)$

In this appendix, we derive the variances and formulate some useful relations concerning L(R), $L_{ku}(r)$ and $L_{kv}(r)$ defined in Chapter III and Chapter V. The expressions for them are very similar. In order to avoid repetitions, we define two new functions L_f and L_g:

(B-1)

$$\begin{bmatrix} L_f \\ L_g \end{bmatrix} \triangleq \sum_{i=1}^{m} \int_{-T}^{T} \gamma_i(t_i) \cdot \begin{bmatrix} f_i(t_i) \\ g_i(t_i) \end{bmatrix} \cdot dt - \sum_{i,j=1}^{m} \iint_{-T}^{T} \gamma_i(t_i) \begin{bmatrix} f_j(z_j) \\ g_j(z_j) \end{bmatrix} \cdot \Psi(t,z) \cdot dt\, dz$$

where f(t) and g(t) are not random processes,

$$\Psi(t,z) = \sum_{\ell=1}^{\infty} \frac{\phi_\ell(t)\phi_\ell(z)}{m + \frac{h_w}{\lambda_\ell - h_w}}, \text{ and}$$

(B-2)

$$\gamma_i(t) = \begin{cases} n_i(t) + w_i(t) + \varepsilon\, a_i(t), & \text{under } H_a \\ n_i(t) + w_i(t) + \varepsilon\, b_i(t), & \text{under } H_b \end{cases}$$

The signals a(t) and b(t) may contain random parameter Γ. Because the equations to be derived will not be directly expressed in terms of a(t) and b(t), we place ε, ε=0 or 1, in Eq. (B-2) to see the effects when a(t) or b(t) equals zero.

For a given Γ, the means of L_f and L_g under H_b are

(B-3)

$$\begin{bmatrix} E\{L_f|\Gamma\} \\ E\{L_g|\Gamma\} \end{bmatrix} = \sum_{i=1}^{m} \int_{-T}^{T} b_i(t_i) \cdot \begin{bmatrix} f_i(t_i) \\ g_i(t_i) \end{bmatrix} dt -$$

$$- \sum_{i,j=1}^{m} \sum \iint_{-T}^{T} b_i(t_i) \cdot \begin{bmatrix} f_j(z_j) \\ g_j(z_j) \end{bmatrix} \cdot \Psi(t,z) \cdot dt\, dz$$

The product of two conditional means is equal to

(B-4)

$$E\{L_f|\Gamma,H_b\} \cdot E\{L_g|\Gamma,H_b\}$$

$$= \varepsilon^2 \sum_{i,j=1}^{m} \sum \iint_{-T}^{T} b_i(t_i)b_j(z_j) \cdot f_i(t_i) \cdot g_j(z_j)\, dt\, dz$$

$$- \varepsilon^2 \sum_{\ell,i,j=1}^{m} \sum\sum \iiint_{-T}^{T} b_\ell(x_\ell)b_i(t_i) \cdot f_\ell(x_\ell)g_j(z_j) \cdot \Psi(t,z) \cdot dx\, dt\, dz$$

$$- \varepsilon^2 \sum_{\ell,i,j=1}^{m} \sum\sum \iiint_{-T}^{T} b_\ell(x_\ell)b_i(t_i) \cdot g_\ell(x_\ell)f_j(z_j) \cdot \Psi(t,z) \cdot dx\, dt\, dz$$

$$+ \varepsilon^2 \cdot \sum_{\ell,n,i,j=1}^{m} \sum\sum\sum \iiiint_{-T}^{T} b_\ell(x_\ell)b_i(t_i) \cdot f_n(g_n) \cdot g_j(z_j) \cdot$$

$$\cdot \Psi(x,y) \cdot \Psi(t,z) \cdot dx\, dy\, dt\, dz$$

The product of L_f and L_g is given by

(B-5)

$$L_f L_g = \sum_{i,j=1}^{m} \iint_{-T}^{T} \gamma_i(t_i)\,\gamma_j(z_j) \cdot f_i(t_i)\,g_j(z_j) \cdot dt\,dz$$

$$- \sum_{i,\ell,n=1}^{m} \iiint_{-T}^{T} \gamma_\ell(x_\ell)\gamma_i(t_i) \cdot f_\ell(x_\ell) g_j(z_j) \cdot \psi(t,z) \cdot dx \cdot dt\,dz$$

$$- \sum_{\ell,i,j=1}^{m} \iiint_{-T}^{T} \gamma_\ell(x_\ell)\gamma_i(t_i) \cdot f_j(z_j) g_\ell(x_\ell) \cdot \psi(t,z) \cdot dx \cdot dt\,dz$$

$$+ \sum_{\ell,n,i,j=1}^{m} \iiiint_{-T}^{T} \gamma_i(t_i)\gamma_\ell(x_\ell) \cdot f_j(z_j) g_n(y_n) \cdot \psi(t,z) \cdot$$

$$\cdot \psi(x,y) \cdot dx\,dy\,dt\,dz$$

For a given Γ, the mean of $\gamma_i(t_i)\gamma_\ell(x_\ell)$ under hypothesis H_b is given by

(B-6)

$$E\{\gamma_i(t_i)\,\gamma_\ell(x_\ell) \mid \Gamma, H_b\}$$

$$= R(t-x) + h_w \cdot \delta_{i\ell} \cdot \delta(t-x) + \varepsilon^2 \cdot b_i(t_i)\,b_\ell(x_\ell)$$

Hence, the conditional mean of $L_f L_g$ under hypothesis H_b is given by

(B-7)

$$E\{L_f\,L_g \mid \Gamma, H_b\}$$

$$= \sum_{i,j=1}^{m} \iint_{-T}^{T} R(t-z) \cdot f_i(t_i)\,g_j(z_j) \cdot dt\,dz$$

$$- m \sum_{j,\ell=1}^{m} \iiint_{-T}^{T} R(t-x) \cdot [f_\ell(x_\ell) g_j(z_j) + g_\ell(x_\ell) f_j(z_j)] \cdot$$

$$\cdot \psi(t,z) \cdot dx\,dt\,dz$$

(B-7) (Cont)

$$+ m^2 \sum_{j,n=1}^{m} \iiiint_{-T}^{T} R(t-x) \cdot f_j(z_j)\, g_n(y_n) \cdot \psi(t,z) \cdot \psi(x,y) \cdot dt\, dz \cdot dx\, dy$$

$$+ h_w \sum_{i=1}^{m} \int_{-T}^{T} f_i(t_i)\, g_i(t_i) \cdot dt$$

$$- h_w \sum_{i,j=1}^{m} \iint_{-T}^{T} [f_i(t_i) g_j(z_j) + g_i(t_i) f_j(z_j)] \cdot \psi(t,z) \cdot dt\, dz$$

$$+ m\, h_w \cdot \sum_{j,n=1}^{m} \iiint_{-T}^{T} f_j(z_j) \cdot g_n(y_n) \cdot \psi(t,z) \cdot \psi(t,y) \cdot dt\, dz\, dy$$

$$+ \varepsilon^2 \sum_{i,j=1}^{m} \iint_{-T}^{T} b_i(t_i) b_j(z_j) \cdot f_i(t_i)\, g_j(z_j) \cdot dt\, dz$$

$$-\varepsilon^2 \sum_{\ell,i,j=1}^{m} \iiint_{-T}^{T} b_i(t_i) b_\ell(x_\ell) [f_\ell(x_\ell) g_j(z_j) + g_\ell(x_\ell) f_j(z_j)] \cdot \psi(t,z) \cdot dx\, dt\, dz$$

$$-\varepsilon^2 \sum_{\ell,n,i,j=1}^{m} \iiiint_{-T}^{T} b_i(t_i) b_\ell(x_\ell) \cdot f_n(y_n) g_j(z_j) \cdot \psi(x,y) \cdot \psi(t,z) \cdot dx\, dy\, dt\, dz$$

The expression given above may be simplified by applying the following relations:

(B-8)

$$\int_{-T}^{T} \phi_\ell(t)\, \phi_n(t) \cdot dt = \delta_{\ell n}$$

and

$$(B\text{-}9) \qquad R(t-z) = \sum_{\ell=1}^{\infty} (\lambda_\ell - h_w) \cdot \phi_\ell(t)\phi_\ell(z)$$

The second term of Eq. (B-7) is equal to

(B-10)

$$-2m \cdot \sum_{j,\ell=1}^{m} R(t-x) f_\ell(x_\ell) g_j(z_j) \cdot \Psi(t,z) \cdot dx\, dt\, dz$$

$$= -2m \sum_{i,j=1}^{m} \iint_{-T}^{T} f_i(t_i) g_j(z_j) \cdot \sum_{\ell=1}^{\infty} \frac{\lambda_\ell - h_w}{m + \frac{h_w}{\lambda_\ell - h_w}} \phi_\ell(t)\phi_\ell(z) \cdot dt\, dz$$

The third term of Eq. (B-8) equals

(B-11)

$$m^2 \sum_{i,j=1}^{m} \iint_{-T}^{T} g_i(t_i) f_j(z_j) \cdot \sum_{\ell=1}^{\infty} \frac{\lambda_\ell - h_w}{\left(m + \frac{h_w}{\lambda_\ell - h_w}\right)^2} \phi_\ell(t)\phi_\ell(z) \cdot dt\, dz$$

The fifth term of Eq. (B-8) equals

$$(B\text{-}12) \qquad -2\, h_w \cdot \sum_{i,j=1}^{m} \iint_{-T}^{T} f_i(t_i)\, g_j(z_j) \cdot \Psi(t,z) \cdot dt\, dz$$

The sixth term of Eq. (B-8) is equal to

$$(B\text{-}13) \qquad m \cdot h_w \sum_{i,j=1}^{m} \iint_{-T}^{T} g_i(t_i) f_j(z_j) \cdot \sum_{\ell=1}^{\infty} \frac{\phi_\ell(t)\phi_\ell(z)}{\left(m + \frac{h_w}{\lambda_\ell - h_w}\right)^2} dt\, dz$$

Substituting Eqs. (B-10), (B-11), (B-12), and (B-13) into Eq. (B-7) and simplifying the resultant expression, yields

(B-14)

$$E\{L_f L_g | \Gamma, H_b\}$$

$$= h_w \left\{ \sum_{i=1}^{m} \int_{-T}^{T} f_i(t_i)\, g_i(t_i) dt - \sum_{i,j=1}^{m} \iint_{-T}^{T} f_i(t_i) g_j(z_j) \cdot \right.$$

$$\left. \cdot \Psi(t,z) \cdot dt\, dz \right\}$$

$$+ \varepsilon^2 \sum_{i,j=1}^{m} \iint_{-T}^{T} b_i(t_i) b_j(z_j) \cdot f_i(t_i)\, g_j(z_j) \cdot dt\, dz$$

$$-\varepsilon^2 \cdot \sum_{\ell,i,j=1}^{m} \iiint_{-T}^{T} b_i(t_i) b_\ell(x_\ell) \cdot [f_\ell(x_\ell) g_j(z_j) + g_\ell(x_\ell) f_j(z_j)] \cdot$$

$$\cdot \Psi(t,z) \cdot dx\, dt\, dz$$

$$+ \varepsilon^2 \sum_{\ell,n,i,j=1}^{m} \iiiint_{-T}^{T} b_i(t_i)\, b_\ell(x_\ell) \cdot f_n(y_n)\, g_j(z_j) \cdot$$

$$\cdot \Psi(x,y) \cdot \Psi(t,z) \cdot dx\, dy\, dt\, dz$$

The sum of the last three terms in Eq. (B-14) are equal to Eq. (B-4).

Case 1

We next determine the variance of L(R). L_f and L_g are equal to L(R) if f(t) = g(t) = s(t). Since the signal b(t) does not contain random parameters, the conditional mean is just the mean. Hence the variance of L(R) under H_b is

(B-15)

$$\text{var}\{L(R)|H_b\} = E\{L^2(R)|H_b\} - E^2\{L(R)|H_b\}$$

$$= \{\text{Eq. (B-14)}\}_{f(t)=g(t)=s(t)} - \{\text{Eq. (B-4)}\}_{f(t)=g(t)=s(t)}$$

$$= h_w \left\{ \sum_{i=1}^{m} \int_{-T}^{T} s_i^2(t_i) dt - \sum_{i,j=1}^{m} \iint_{-T}^{T} s_i(t_i) s_j(z_j) \cdot \Psi(t,z) \cdot dt\, dz \right\}$$

The variance of L(R) under H_a may be derived in the same manner. We have found that the variance under H_a has the same expression.

Case 2

When $b(t) = x\, u_b(t) - y\, v_b(t)$, where x, y, $u_b(t)$ and $v_b(t)$ are defined in Chapter V, then

(B-16)

$$E\{b_i(t_i)\, b_j(z_j)\} = \sigma_\Gamma^2[u_{bi}(t_i)\, u_{bj}(z_j) + v_{bi}(t_i)\, v_{bj}(z_j)]$$

and

$$E\{b_i(t_i)\} = 0$$

From Eq. (B-3), we obtain

$$E\{L_f|H_b\} = E\{E\{L_f|\Gamma, H_b\}\} = 0$$

Similarly,

$$E\{L_g|H_b\} = 0$$

For the sake of simplicity, we define that

$$\langle u,f\rangle \triangleq \sum_{i=1}^{m} \int_{-T}^{T} u_i(t_i)f_i(t_i)dt - \sum_{i,j=1}^{m} \iint_{-T}^{T} u_i(t_i)f_j(z_j)\psi(t,z)\cdot dt\, dz$$

$$\langle v,g\rangle \triangleq \sum_{i=1}^{m} \int_{-T}^{T} v_i(t_i)g_i(t_i)dt - \sum_{i,j=1}^{m} \iint_{-T}^{T} v_i(t_i)g_j(z_j)\psi(t,z)\cdot dt\, dz,$$

etc. From Eq. (B-14) and Eq. (B-16), we obtain

(B-17)

$$E\{L_f\, L_g|H_b\} = E\{E\{L_f\, L_g|\Gamma, H_b\}\}$$

$$= h_w \cdot \langle f,g\rangle + \varepsilon^2\sigma_\Gamma^2 \langle u_b,f\rangle \cdot \langle u_b,g\rangle$$

$$+ \varepsilon^2\sigma_\Gamma^2 \langle v_b,f\rangle \cdot \langle v_b,g\rangle$$

$E\{L_f \cdot L_g | H_a\}$ is readily obtained when the subscript b in Eq. (B-17) is changed to a. The parameters α_k, β_k and Γ_k, defined in Chapter V may be written as

$$\alpha_k = \frac{\sigma_\Gamma^2}{h_w} \langle u_k, u_k \rangle , \quad k = a \text{ and } b$$

$$\beta_k = \frac{\sigma_\Gamma^2}{h_w} \langle v_k, v_k \rangle$$

$$\gamma_k = \frac{\sigma_\Gamma^2}{h_w} \langle u_k, v_k \rangle = \frac{\sigma_\Gamma^2}{h_w} \langle v_k, u_k \rangle$$

We next formulate the variances. L_f and L_g are equal to $L_{ku}(\gamma)$, $k = a$ and b, if $f(t) = g(t) = h_w^{-1} u_k(t)$. Hence,

(B-18)

$$\text{var}\{L_{ku}(\gamma)|H_k\} = E\{L_{ku}^2(\gamma)|H_k\} - E^2\{L_{ku}(\gamma)|H_k\}$$

$$= k_w^{-1} \langle u_k, u_k \rangle + \varepsilon^2 \sigma_\Gamma^2 \cdot h_w^{-2} \langle u_k \cdot u_k \rangle^2 + \varepsilon^2 \sigma_\Gamma^2 h_w^{-2} \langle u_k, v_k \rangle^2$$

$$= \frac{1}{\sigma_\Gamma^2} \left\{ \alpha_k + \varepsilon^2 (\alpha_k^2 + \gamma_k^2) \right\}$$

$L_f(\gamma)$ and $L_g(\gamma)$ are equal to $L_{kv}(\gamma)$ if $f(t) = g(t) = -h_w^{-1} v_k(t)$. Hence

(B-19) $$\text{var}\{L_{kv}(\gamma)|H_k\} = \frac{1}{\sigma_\Gamma^2} \{\beta_k + \varepsilon^2 (\beta_k^2 + \gamma_k^2)\}$$

To examine if $L_{ku}(\gamma)$ and $L_{kv}(\gamma)$ are uncorrelated, we compute

(B-20)

$$E\{L_{ku}(\gamma) L_{kv}(\gamma)|H_k\} - E\{L_{ku}(\gamma)|H_k\} E\{L_{kv}(\gamma)|H_k\}$$

$$= -\frac{1}{\sigma_\Gamma^2} \{\gamma_k + \varepsilon^2 \gamma_k (\alpha_k + \beta_k)\}$$

Hence, in general, $L_{ku}(\gamma)$ and $L_{kv}(\gamma)$ under H_k are correlated. If an optimum-spaced array is used in the detection system, we have shown

in Chapter V that $\tilde{\gamma}_k = 0$. When the interference is a white noise process, we know that $\gamma_k \neq 0$. From Eq. (B-20), we conclude that $L_{ku}(\gamma)$ and $L_{kv}(\gamma)$ are uncorrelated for those two special cases. Other relations can also be obtained from the general formula Eq. (B-17). For example,

(B-21)

$$E\{L_{au}(\gamma)L_{bu}(\gamma)|H_b\}$$

$$= h_w^{-1}\langle u_b, u_a\rangle + \frac{\varepsilon^2\sigma_\Gamma^2}{h_w^2}\langle u_b, u_b\rangle\langle u_b, u_a\rangle + \frac{\varepsilon^2\sigma_\Gamma^2}{h_w^2}\langle v_b, u_b\rangle\langle v_a, u_a\rangle$$

$$= \frac{1}{h_w}\{\langle (u_a, u_b\rangle + \varepsilon^2\alpha_b \cdot \langle u_a, u_b\rangle + \varepsilon^2\gamma_b\langle u_a, v_a\rangle$$

Hence, $L_{au}(\gamma)$ and $L_{bu}(\gamma)$ are also correlated. In Section V.B, we need to know the variances of $L_{au}(\gamma)$ and $L_{av}(\gamma)$ when $\varepsilon = 0$. Letting $\varepsilon=0$ in Eq. (B-18) and Eq. (B-19), we obtain the variances:

(B-22) $$\text{var}\{L_{au}(\gamma)|H_k\} = \frac{\alpha_k}{\sigma_\Gamma^2}$$

and

(B-23) $$\text{var}\{L_{av}(\gamma)|H_k\} = \frac{\beta_k}{\sigma_\Gamma^2}$$

We can show from Eq. (B-17) that $L_{ku}(\gamma)$ and $L_{qv}(\gamma)$, where k, p=a and b, are uncorrelated if an optimum-spaced array is used in the detection system. The same results do not exist between $L_{au}(\gamma)$ and $L_{bu}(\gamma)$ or between $L_{av}(\gamma)$ and $L_{bv}(\gamma)$ if an optimum-spaced array is used.

BIBLIOGRAPHY

1. C.W. Helstrom, Statistical Theory of Signal Detection, New York: Pergamon Press, 1960.

2. D. Middleton, Introduction to Statistical Communication Theory, New York: McGraw-Hill, 1960.

3. H.L. Van Trees, Detection, Estimation, and Modulation Theory, Part I, New York: Wiley, 1968.

4. A. Papoulis, Probability, Random Variables, and Stochastic Processes, New York: McGraw-Hill, 1965.

5. W.B. Davenport, Jr., and W.L. Root, An Introduction to the Theory of Random Signals and Noise, New York: McGraw-Hill, 1958.

6. W.W. Peterson, T.G. Birdsall, and W.C. Fox, "The Theory of Signal Detectability," IRE Transactions, PGIT-4, pp. 171-211, September 1954.

7. P.L. Staklin, "Space-Time Sampling and Likelihood Ratio Processing in Acoustic Pressure Fields," J. Brit. IRE, vol. 26, pp. 79-91, July 1963.

8. F. Bryn, "Optimum Signal Processing of Three-Dimensional Arrays Operating on Gaussian Signals and Noise," J. Acoust. Soc. Am., vol. 34, pp. 289-297, March 1962.

9. N.T. Gaarder, "The Design of Point-Detector Arrays," Naval Research Contract (NR 373360), Stanford Research Institute, Menlo Park, Calif., May 1965.

10. J. Capon, R.J. Greenfield, R.J. Kolker, "Multidimensional Maximum-liklihood Processing of a Large Aperture Seismic Array," Proc. IEEE, vol. 55, February 1967.

11. G.O. Young, "Optimum Space-time Signal Processing and Parameter Estimation," IEEE Trans. Aerospace and Electronics Systems, vol. AES-4, pp. 334-341, May 1968.

12. G.O. Young and J.E. Howard, "Application of Space-Time Decision and Estimation Theory to Antenna Processing System Design," Proc. IEEE, vol. 58, pp. 771-778, May 1970.

13. G.O. Young and J.E. Howard, "Antenna Processing for Surface Target Detection," IEEE Trans. Antennas and Propagation, vol. AP-18, May 1970.

14. M.A. Gallop, "Adaptive Optimum Array Detectors," Ph.D. Dissertation, Duke University, Durham, N.C., May 1971.

15. H. Urkowitz, "On Detection and Estimation of Wave Fields for Surveillance," IEEE Trans. Military Electronics, vol. MIL-9, No. 1, pp. 44-56, January 1965.

16. F.S.K. Chen, "Optimum Array Processing for Detection of Signal in Interference," M.S. thesis, The Ohio State University, Columbus, Ohio, 1970.

17. Van Trees, op. cit., Chapter 3, p. 178.

18. Ibid, Chapter 3, p. 180.

19. Ibid, Chapter 3, p. 184.

20. Ibid, Chapter 2, p. 98.

21. Ibid, Chapter 2, p. 98.

22. Ibid, Chapter 4, p. 334.

23. Davenport and Root, op. cit., pp. 158-161.

24. R.L. Riegler and R.T. Compton, Jr., "An Adaptive Array for Interference Rejection,' Report 2552-4, 16 February 1970, ElectroScience Laboratory, Department of Electrical Engineering, The Ohio State University; prepared under Grant NGR-004-013 for National Aeronautics & Space Administration.

25. R.T. Compton, Jr., "Adaptive Antenna Arrays for Aircraft Communication Systems," Report 3098-1, July 1971, Electro-Science Laboratory, Department of Electrical Engineering, The Ohio State University; prepared under Contract N00014-67-A-0232-0009 for Office of Naval Research, Arlington, Virginia.

26. R.T. Compton, Jr., "Adaptive Arrays - On Power Equalization with Proportional Control," Report 3234-1, December 1971, ElectroScience Laboratory, Department of Electrical Engineering, The Ohio State University; prepared under Contract N00019-71-C-0219 for Naval Air Systems Command.

CONTRACT N00019-72-C-0184
DISTRIBUTION LIST

Technology Service Corporation
225 Santa Monica Boulevard
Santa Monica, California 90401
Attn: Dr. L. E. Brennan

Hughes Aircraft Company
Radar Microwave Laboratory
Centinela and Teale
Culver City, California 90230
Attn: Dr. W. Kummer

Commander
Naval Electronics Laboratory Center
San Diego, California 92152
Attn: Mr. J. Provencher, Code 2393 (1 copy)
Mr. Gustafson, Code 2100 (1 copy)

Director
Naval Research Laboratory
Washington, D. C. 20390
Attn: Mr. D. Townsend, Code 7435 (1 copy)
Code 5410 (1 copy)
Code 5420 (1 copy)

Commander
Naval Air Development Center
Warminster, Pennsylvania 18974
Attn: Mr. J. Guarini, Code AER-2 (1 copy)
Mr. H. Beyer, Code AETD (1 copy)

Commander
Naval Weapons Center
China Lake, California 93555
Attn: Mr. F. Essig, Code 604

Commander
Naval Air Systems Command
Department of the Navy
Washington, D.C. 20360
Attn: Mr. J. Willis, AIR-310B (2 copies)
Mr. F. Lueking, AIR-360F (1 copy)
Mr. R. Bauman, AIR-53343C (1 copy)

Dr. Norbert Bojarski
16 Circle Drive
Moorestown, N.J. 08057

UNCLASSIFIED
Security Classification

DOCUMENT CONTROL DATA - R&D

(Security classification of title, body of abstract and indexing annotation must be entered when the overall report is classified)

1. ORIGINATING ACTIVITY *(Corporate author)*
The Ohio State University ElectroScience Laboratory
Department of Electrical Engineering
Columbus, Ohio 43212

2a. REPORT SECURITY CLASSIFICATION
Unclassified

2b. GROUP

3. REPORT TITLE
OPTIMUM ARRAY PROCESSING FOR DETECTING BINARY SIGNALS CORRUPTED BY DIRECTIONAL INTERFERENCE

4. DESCRIPTIVE NOTES *(Type of report and inclusive dates)*
Technical Report

5. AUTHOR(S) *(Last name, first name, initial)*
Chiu, Chen-Shu

6. REPORT DATE	7a. TOTAL NO. OF PAGES	7b. NO. OF REFS
December 1972	124	26

8a. CONTRACT OR GRANT NO	9a. ORIGINATOR'S REPORT NUMBER(S)
Contract N00019-72-C-0184	ElectroScience Laboratory 3433-2
b. PROJECT NO.	
c. TASK	9b. OTHER REPORT NO(S) *(Any other numbers that may be assigned this report)*
d.	

10. AVAILABILITY/LIMITATION NOTICES
APPROVED FOR PUBLIC RELEASE;
DISTRIBUTION UNLIMITED

11. SUPPLEMENTARY NOTES	12. SPONSORING MILITARY ACTIVITY
	Department of the Navy Naval Air Systems Command Washington, D.C. 20360

13. ABSTRACT

This report examines optimum array processing for bit detection of a binary communication signal in the presence of a directional interfering signal. The binary communication signal is assumed to be either completely known or to have random parameters (Rayleigh amplitude and uniform phase). The interfering signal is a wide-sense stationary Gaussian process. The receiving antenna is a linear array of equally spaced isotropic point elements. Statistically independent white noise is added to the signal at each element.

An analytical expression for the inverse of the covariance matrix is obtained, and the general structure for the optimum detector is derived. The optimum processor is a correlation receiver whose detailed structure is dependent in general on the power spectrum of the interference, as well as the other antenna and signal parameters.

The detection error is calculated for several cases. It is found that the detection error is minimized if the array elements have an optimum spacing, determined by the array size and the incidence angles of the desired signal and the interference. When the optimum spacing is used, the structure of the detection system is not dependent on the power spectrum of the interfering signal

DD FORM 1 JAN 64 1473

UNCLASSIFIED
Security Classification

14. KEY WORDS	LINK A		LINK B		LINK C	
	ROLE	WT	ROLE	WT	ROLE	WT
Arrays Antennas Statistical detection theory Interference rejection Optimum array processing						

INSTRUCTIONS

1. ORIGINATING ACTIVITY: Enter the name and address of the contractor, subcontractor, grantee, Department of Defense activity or other organization *(corporate author)* issuing the report.

2a. REPORT SECURITY CLASSIFICATION: Enter the overall security classification of the report. Indicate whether "Restricted Data" is included. Marking is to be in accordance with appropriate security regulations.

2b. GROUP: Automatic downgrading is specified in DoD Directive 5200.10 and Armed Forces Industrial Manual. Enter the group number. Also, when applicable, show that optional markings have been used for Group 3 and Group 4 as authorized.

3. REPORT TITLE: Enter the complete report title in all capital letters. Titles in all cases should be unclassified. If a meaningful title cannot be selected without classification, show title classification in all capitals in parenthesis immediately following the title.

4. DESCRIPTIVE NOTES: If appropriate, enter the type of report, e.g., interim, progress, summary, annual, or final. Give the inclusive dates when a specific reporting period is covered.

5. AUTHOR(S): Enter the name(s) of author(s) as shown on or in the report. Enter last name, first name, middle initial. If military, show rank and branch of service. The name of the principal author is an absolute minimum requirement.

6. REPORT DATE: Enter the date of the report as day, month, year, or month, year. If more than one date appears on the report, use date of publication.

7a. TOTAL NUMBER OF PAGES: The total page count should follow normal pagination procedures, i.e., enter the number of pages containing information.

7b. NUMBER OF REFERENCES: Enter the total number of references cited in the report.

8a. CONTRACT OR GRANT NUMBER: If appropriate, enter the applicable number of the contract or grant under which the report was written.

8b, 8c, & 8d. PROJECT NUMBER: Enter the appropriate military department identification, such as project number, subproject number, system numbers, task number, etc.

9a. ORIGINATOR'S REPORT NUMBER(S): Enter the official report number by which the document will be identified and controlled by the originating activity. This number must be unique to this report.

9b. OTHER REPORT NUMBER(S): If the report has been assigned any other report numbers *(either by the originator or by the sponsor)*, also enter this number(s).

10. AVAILABILITY/LIMITATION NOTICES: Enter any limitations on further dissemination of the report, other than those imposed by security classification, using standard statements such as:

(1) "Qualified requesters may obtain copies of this report from DDC."

(2) "Foreign announcement and dissemination of this report by DDC is not authorized."

(3) "U. S. Government agencies may obtain copies of this report directly from DDC. Other qualified DDC users shall request through _____."

(4) "U. S. military agencies may obtain copies of this report directly from DDC. Other qualified users shall request through _____."

(5) "All distribution of this report is controlled. Qualified DDC users shall request through _____."

If the report has been furnished to the Office of Technical Services, Department of Commerce, for sale to the public, indicate this fact and enter the price, if known.

11. SUPPLEMENTARY NOTES: Use for additional explanatory notes.

12. SPONSORING MILITARY ACTIVITY: Enter the name of the departmental project office or laboratory sponsoring *(paying for)* the research and development. Include address.

13. ABSTRACT: Enter an abstract giving a brief and factual summary of the document indicative of the report, even though it may also appear elsewhere in the body of the technical report. If additional space is required, a continuation sheet shall be attached.

It is highly desirable that the abstract of classified reports be unclassified. Each paragraph of the abstract shall end with an indication of the military security classification of the information in the paragraph, represented as *(TS), (S), (C), or (U).*

There is no limitation on the length of the abstract. However, the suggested length is from 150 to 225 words.

14. KEY WORDS: Key words are technically meaningful terms or short phrases that characterize a report and may be used as index entries for cataloging the report. Key words must be selected so that no security classification is required. Identifiers, such as equipment model designation, trade name, military project code name, geographic location, may be used as key words but will be followed by an indication of technical context. The assignment of links, rules, and weights is optional.

END

FILMED